LEHRSTUHL FÜR EISEN- UND STAHLMETALLURGIE
MONTANUNIVERSITÄT LEOBEN

# Correlation of evaluation methods of iron ore pellets with their performance in a direct reduction plant

Masterarbeit

eingereicht von

**Gero Schwarz**

am Lehrstuhl für Eisen- und Stahlmetallurgie an der Montanuniversität Leoben
zur Erlangung des akademischen Grades

Diplomingenieur

in der Studienrichtung Eisen- und Stahlmetallurgie

MONTAN
UNIVERSITÄT

Lehrstuhl für Eisen-und Stahlmetallurgie – Montanuniversität Leoben
Franz-Josef-Straße 18 – 8700 Leoben, Österreich

# Acknowledgements

I want to thank my academic supervisors, Professor Johannes Schenk and Daniel Spreitzer from the Montanuniversität Leoben as well as Professor Emmanuel De Moor from the Colorado School of Mines, not only for all their support and expertise during the completion of this thesis, but also for making this thesis possible at all.

Furthermore, I want to thank everyone involved in this thesis at the industry partner, voestalpine Texas LLC, and the K1-MET project for giving me the opportunity to work with data from their state of the art reduction plant and for all their continuous support. I am especially grateful to Chris Harris. It was an honor to work with you and a pleasure to learn from you.

I am also thankful for the financial support provided by the Austrian Marshall Plan Foundation. This accomplishment may not have been possible without them.

A very special thank you also goes out to my family and friends for their unconditional emotional and financial support throughout my studies. Moreover I must express my gratitude to everyone who not only helped me with this thesis, but also motivated me when things were not going as great as expected.

# Abstract

This thesis analyzes the evaluation methods of iron ore pellets in the Midrex process and examines the performance of six different pellet types under industrial conditions.

The performance of the different pellet types in the furnace was based on industry data and a series of mass balances used to calculate process parameters reflecting pellet performance. Eleven different cases of different raw material mixes were analyzed, and the performance of six pellet types was calculated. These calculations were then compared to the available standardized test results (ISO 11257 and ISO 11258). While the ISO 11257 showed some correlation to the furnace performance, no correlation was observed regarding the ISO 11258.

A chemical and thermal profile of the furnace was calculated to relate the test parameters to industrial conditions. The incoming gas and iron oxide composition and flow was taken from industrial data and the reaction rate was calculated based on reduction tests performed at different gas compositions. The resulting profile was compared to six standardized reduction tests and both temperature and gas profiles show the highest similarities with the R180 test.

Based on the calculated reduction profile of the furnace, the R180 test is slightly modified to even closer resemble the furnace conditions. Apart from a temperature profile change, this includes adding water to the gas composition. The results show a correlation between the industrial furnace performance and the test, but also show potential for further improvement.

# Kurzfassung

Diese Arbeit analysiert die vorhandenen Methoden um Eisenerzpellets für den Midrex-Prozess zu beurteilen. Des Weiteren wird das Verhalten von sechs unterschiedlichen Pelletarten unter Industriebedingungen untersucht.

Um das Verhalten im Schacht zu beurteilen werden mittels einer Reihe von Massenbilanzen und Industriedaten verschiedene Leistungskennzahlen berechnet. Dafür werden unterschiedliche Rohstoffbeschickungen analysiert und die Leistungskennzahlen von den sechs verschiedenen Pelletarten berechnet. Diese Leistungskennzahlen werden mit den verfügbaren Ergebnissen der standardisierten Tests (ISO 11257 und ISO 11258) verglichen. Während beim ISO 11257 Test eine Korrelation zwischen den Testergebnissen und dem Verhalten im Schacht festgestellt werden konnte, war dies beim ISO 11258 Test nicht der Fall.

Um die standardisierten Testparameter mit den Betriebsbedingungen zu vergleichen, wird das chemische und thermische Profil der Anlage berechnet. Dafür werden die Gas- sowie Eisenerzzusammensetzung und Menge, welche dem Prozess zugeführt werden, den Betriebsdaten entnommen. Die Reaktionsgeschwindigkeit der Pellets wird experimentell aus Reduktionstests bei unterschiedlichen Gaszusammensetzungen ermittelt. Die resultierenden Profile zeigen mit dem R180 Test die größten Übereinstimmungen.

Basierend auf den berechneten Profilen wird der R180 Test leicht verändert, um ihn noch weiter an die Bedingungen im Ofen anzupassen. Abgesehen vom Ändern der Temperatur, wird auch Wasserdampf dem reduzierenden Gas beigemischt. Die Ergebnisse dieses Tests korrelieren zum Teil mit den Industriedaten, zeigen aber noch weiteres Optimierungspotential auf.

# Affidavit

I declare in lieu of oath, that I wrote this thesis and performed the associated research work myself, using only literature cited in this volume.

# Eidesstattliche Erklärung

Ich erkläre an Eides statt, dass ich diese Arbeit selbstständig verfasst, andere als die angegebenen Quellen und Hilfsmittel nicht benutzt und mich auch sonst keiner unerlaubten Hilfsmittel bedient habe.

Gero Schwarz

August 15, 2018

# Index

# Image Index

# Table Index

# Acronyms

| | |
|---|---|
| BF | Blast Furnace |
| BG | Bustle Gas |
| BOF | Basic Oxygen Furnace |
| DRI | Directly Reduced Iron |
| EAF | Electric Arc Furnace |
| GQ | Gas Quality |
| HBI | Hot Briquetted Iron |
| KPI | Key Process Indicator |
| LOI | Loss on Ignition |
| RD | Reduction Degree |
| TG | Top Gas |
| wt | Weight |

Acronyms representing chemical elements are appreciated according to the International Union of Pure and Applied Chemistry [1]

# 1 Introduction and Objectives

In recent decades, the direct reduction of iron ore has gained importance, mostly due to the high $CO_2$ savings compared to conventional iron and steel production technologies. [2, 3] The rising popularity of electric arc furnace steelmaking route compared to the integrated blast furnace route, combined with high quality scrap becoming more scarce makes the direct reduction process an important strategic investment for steelmakers around the world. Additionally, pressure is being exerted by politics, particular in Europe by the Paris agreement, that makes iron and steel producers strive to lower their $CO_2$ emissions. [4] Producing steel via the electric arc furnace, using direct reduced iron as a partial input material lowers the total $CO_2$ emissions by 30 percent compared to the otherwise dominant integrated blast furnace route. [3]

Austria's largest steel producer, voestalpine, went into production with its first, and currently the world's largest, Midrex plant producing hot briquetted iron (HBI) in Corpus Christi, Texas, in October 2016. This direct reduction plant is unique due to its brand-new technology and its size. As this plant has just gone into production, there is still great potential for optimizing this direct reduction plant.

One of these optimization potentials concerns the feed material i.e. the iron ore pellets which account for about 70 percent of the operating costs. Due to their physical and chemical properties, these iron ore pellets show a different behavior in the direct reduction plant. Since these iron ore pellets originate from various suppliers, their quality must be recorded in order to guarantee a stable and predictable process. It is of high importance to understand and record the behavior of the iron ore pellets for this particular direct reduction plant and, subsequently, be able to predict the behavior. To date there are multiple different pellet laboratory tests and methods used which try to determine the behavior of iron ore in blast furnaces, as well as fewer tests which do this for direct reduction plants.

## 1.1 Objectives of the thesis

From the startup of the Midrex reduction plant it received six different brands of pellets. The correlation between the performance of the plant and the iron ore used is of particular interest to the plant operators. For this work, two different questions arise. The first question is: Which pellet material used in the direct reduction plant of the voestalpine Texas LLC leads to which reduction behavior? The second question is: What tests are currently available to predict the operating behavior of iron ore pellets? And which of these tests has the potential to predict accurately the behavior of the direct reduction plant? In particular the following key questions are investigated in the course of this thesis:

- What differences does the industrial data show concerning the reduction behavior of six different pellet types?
- What is the expected chemical and thermal profile these pellets experience under industrial conditions?
- Which pellet tests are available to date and how do their specified conditions compare to the industrial conditions in the shaft?
- Do any of the available test results correlate with the performance of the pellets in the shaft, and if so, to what degree?

Finally, based on the information gained by investigating these questions, one or more reduction tests are to be suggested to evaluate the reducing characteristics of different iron ores. Additionally, this thesis should also introduce a new test based on the expected chemical and thermal profile in furnace.

# 2 Direct Reduction of Iron

Direct reduction of iron ores are processes in which metallic iron is produced by removing oxygen from iron ore below the melting temperature of any material involved. Carbon monoxide and, depending on the type of process, hydrogen gases are commonly used to reduce the iron ore to metallic iron. **Figure 1** shows the different steps in the reduction from a hematite iron ore to pure iron in a DRI process. The resulting product of such a process is called direct reduced iron (DRI). Iron ore can be processed in the form of fines, pellets or lump ores and the resulting products are mechanically compacted into dense briquettes. The briquetting process can either be performed as hot-briquetting or with the help of binders through cold-briquetting. [5, 6]

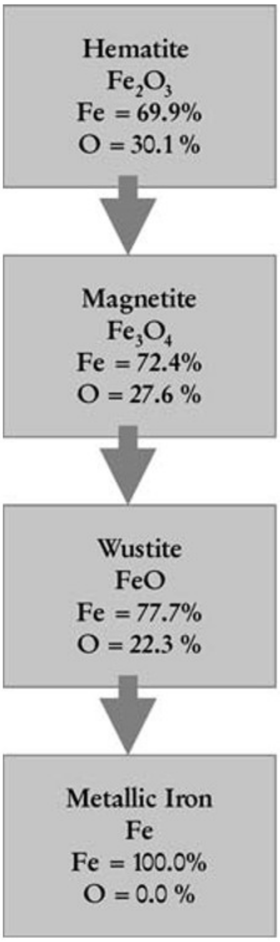

**Figure 1:** Reduction steps and weight percentages of phases in a DRI processes [6]

The first ironmaking methods used by mankind have been direct reduction processes and have been used for thousands of years. However, it was not until the 1950s that economic conditions made commercial DRI production possible and the first DRI plant went into production. [7] DRI plants are typically built in regions where natural gas is inexpensive. Before 1990 nearly all plants were built to serve an adjacent steel mill, today DRI is also exported, usually as HBI, to be used as a raw material mainly in electric arc furnaces (EAF) for steel production. [5, 7]

## 2.1 Use of DRI in Iron- and Steelmaking

In 2017 about 87.1 million tons of DRI were produced, which is modest compared to an overall steel production of 1,689 Million tons in the same year. Although DRI accounts only for a fraction of the overall steel production its growth since 1970 is impressive. While the overall steel production today has not quite tripled compared to 1970, the DRI production has increased by a factor of 100, as can be seen in **Figure 2**. [8, 9]

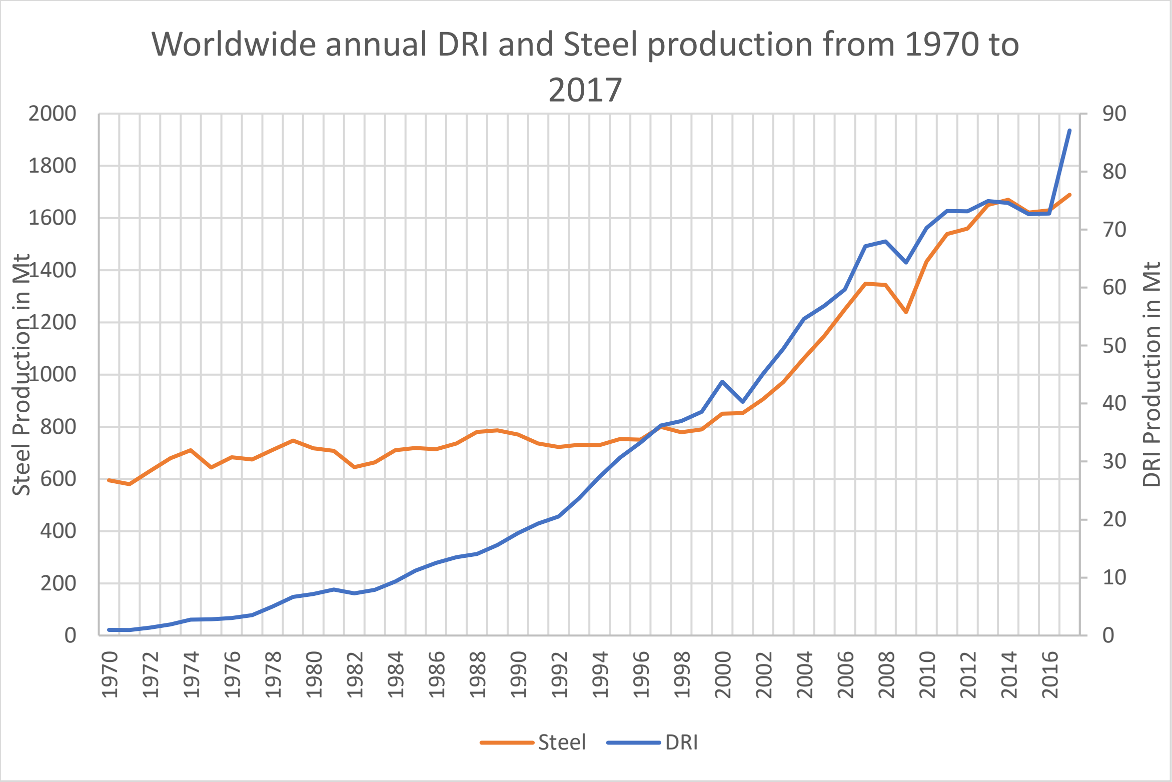

**Figure 2:** World steel and DRI production from 1970 to 2016 in Mt [8, 9]

This large growth is based on the success of the EAF route, accounting for about 25 % of the world steel production and 70 % of the US steel production. [8] Because it is less capital and labor intensive, cleaner and has lower economies of scale, the EAF route will continue to grow significantly faster than the BF production. However, as the EAF grows not only in capacity but also into new segments, producing higher quality products, the availability and quality of raw materials, mainly scrap, play an increasingly important role. Due to manufacturing efficiencies, the supply of prime scrap worldwide is only growing slowly. At the same time steel makers increasingly face the challenge of nonferrous metallic impurities such as copper, chromium, nickel, molybdenum and tin in the scrap they purchase and in the subsequent melt. HBI therefore is not only being used as a substitute for scrap, but also seen as a necessity for producing “clean” steels via the EAF route. [7, 9]

Because of its high metallization, DRI is also used in BF/BOF steelmaking. In the BF it can increase production in case of bottlenecks such as repairs on other blast furnaces. HBI also increases the hot metal production while lowering the coke consumption at the same time. When looking at decreasing $CO_2$ production, using HBI as a raw material in the BF is the only option to utilize existing production facilities while reducing $CO_2$ emissions at the same time. Overall the applications for DRI in steelmaking can be summed up to the following points: [7, 9, 5]

1. A low impurity feed for EAFs looking to make high quality products
2. An iron source for EAFs in areas where scrap supply is limited
3. An alternative to scrap as a cold charge in the BOF
4. BF feed to increase production in a bottleneck situation
5. BF feed to increase production while decreasing coke consumption and with that $CO_2$ emissions.

## 2.2 Direct Reduction Processes

In the past century more than one hundred different DRI processes or process concepts have been developed. Due to either economical or technical reasons most of them were unsuccessful or were abandoned. The ones that have been successful to date can be classified into coal and gas based processes as well as by the types of furnaces they use. The most common processes are summarized in the following **Table 1** and **Table 2**. [7, 6]

**Table 1:** Coal Based Processes [7]

| Coal Based Processes | |
|---|---|
| **Types** | **Processes** |
| Rotary kiln processes | • SL/RN<br>• Krupp-CODIR<br>• DRC<br>• ACCAR/OSIL |
| Retort process | • Kinglor Metor |
| Rotary hearth processes | • Inmetco<br>• Fastmet |

**Table 2:** Gas Based Processes [7]

| **Gas Based Processes** | |
|---|---|
| **Types** | **Processes** |
| Shaft processes | - Midrex<br>- HYL<br>- Purofer |
| Fluidized bed processes | - FIOR/FINMET<br>- Iron Carbide<br>- Circored |

As illustrated in **Figure 3** about 18 percent of today's DRI production comes from coal-based rotary kiln processes most commonly the SL/RN or the DRC process. Over 80 % of the total production comes from gas-based processes. While fluidized bed processes make up a small fraction of the gas-based processes, the majority is produced by shaft furnace processes, which are dominated by the HYL and Midrex processes, accounting for 17.4 and 64.8 percent of the total DRI production in 2016, respectively.

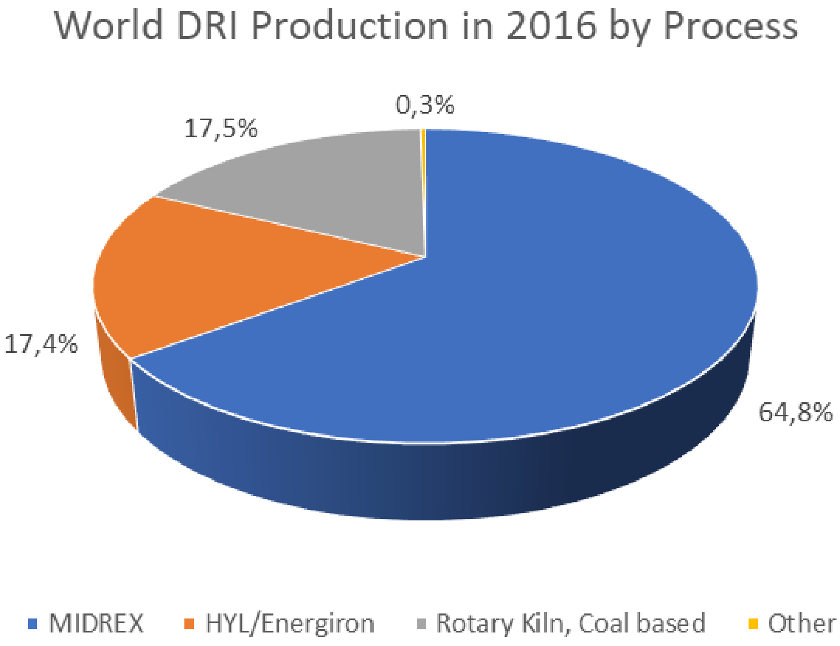

**Figure 3**: World DRI Production by Process [9]

# 3 Midrex Process

The Midrex process was developed in the 1960’s by the Midland-Ross Corporation and the first commercial plant went into production in 1969.

## 3.1 Process Scheme

The process, as shown in **Figure 4**, is based on the principle of counter current flow in which iron-oxide material descends through a shaft furnace where it is heated and reduced by a rising stream of hot reducing gas. On the top of the furnace there is a conical hopper that distributes the feed material through multiple feed pipes. The furnace itself consists of a cylindrical refractory lined section and a reversed conical, uninsulated lower cooling section. Burden feeders below the reduction zone ensure that the burden descends uniformly throughout the cross section of the furnace. Below the furnace is a vertical discharge pipe which, in case of HBI plants, leads to briquetting machines. The feed pipe is sealed with the help of inert gas to prevent reduction gas from escaping and air from entering the furnace. [7, 5, 10]

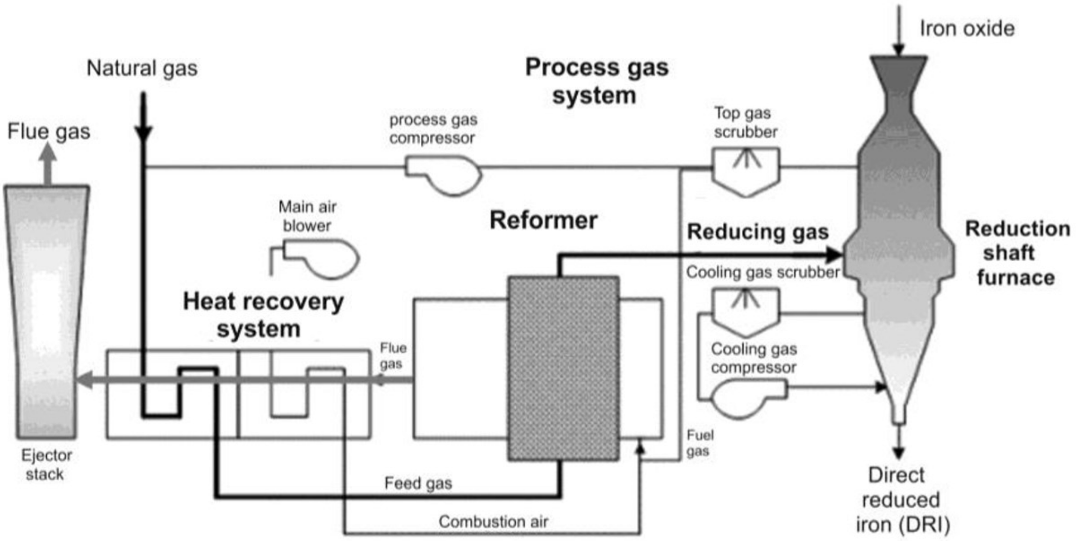

**Figure 4**: Typical Midrex process flow sheet [10]

The reducing gas is fed into the reduction zone from entry points around the shaft at about one third of the height of the furnace. Temperatures will typically range from 750 to 850 °C in the reduction zone. Below the reduction zone, in the transition zone, natural gas is added to the furnace. Because of the high temperatures in the furnace, iron acts as a catalyst and the natural gas can react to form hydrogen and carbon monoxide. This endothermic reforming reaction helps to cool down the DRI. In the reduction zone itself hydrogen and carbon monoxide react with the iron ore to form metallic iron as the gas flows upward. It takes the charge about 6 hours to pass through the reduction zone after which the metallic iron is then either cooled with inert gas and discharged or directly discharged to the briquetting machine. [5, 7]

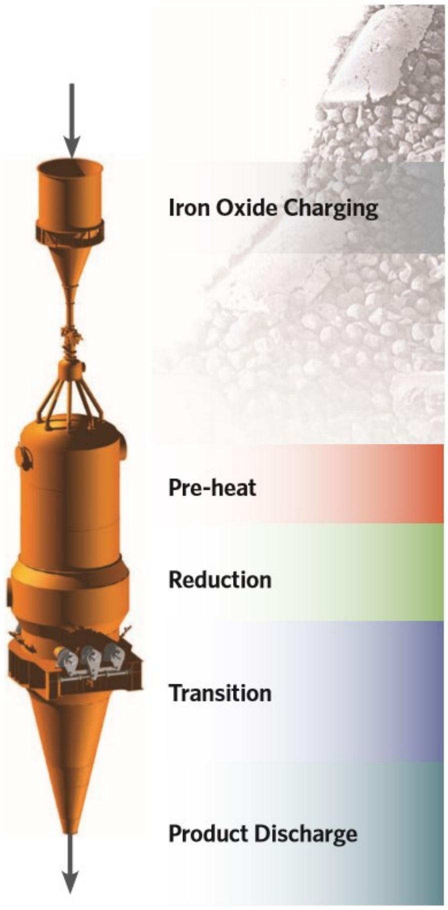

**Figure 5:** The Midrex Shaft and Reaction Zones [9]

The reducing gas is produced using natural gas and is done with a Midrex reformer. If the plant is operated with coal including high sulfur coals or coke oven gas, then a gasifier or a thermal reactor system can be used to produce reducing gas.

A typical gas system for a plant operated on natural gas would be the following:

At the top of the reduction zone the top gas, the partially oxidized reduction gas, exits the furnace and is scrubbed in the top gas scrubber. While a part of the top gas is used as top gas fuel to provide heat for the reformer, most of it is mixed with natural gas to form process gas. This process gas then passes through the reformer in which the reforming reactions take place. After that a small part of the gas is taken and injected at the bottom of the furnace as reheat gas, while the rest of the gas is enriched with natural gas and injected in the reduction zone.

Inside the reformer the following reactions take place:

$$CH_4 + CO_2 \longrightarrow 2\,CO + 2\,H_2 \tag{3-1}$$

$$CH_4 + H_2O \longrightarrow CO + 3\,H_2 \tag{3-2}$$

$$2\,CO \longrightarrow C + CO_2 \tag{3-3}$$

$$CO + H_2O \longrightarrow CO_2 + H_2 \tag{3-4}$$

$$CH_4 \longrightarrow C(S) + 2\,H_2 \tag{3-5}$$

The gas quality, reductant / oxidant ratio, is an important property of the reducing gas to measure the potential for the gas to reduce iron oxide. The higher the gas quality, the less gas has to be used, which has a positive effect on the efficiency of the process.

$$Gas\ Quality = \frac{\%\,H_2 + \%\,CO}{\%\,H_2O + \%\,CO_2} \tag{3-6}$$

## 3.2 Physical Chemistry under Process Conditions

To better understand various modelling approaches in section 3.4 and the importance of raw material composition in section 3.3, the following chapters 3.2.1 and 3.2.2 will outline the thermodynamics and kinetics of the direct reduction of iron, with special regard to the conditions present in the Midrex process.

### 3.2.1 Thermodynamics of Iron-Oxide Reduction

All direct reduction processes are designed to extract metallic iron from its oxides with the common reducing agents carbon monoxide and hydrogen. **Figure 6** shows the system Fe-O-C (dashed green line) as well as Fe-O-$H_2$ (dashed blue line). The solid black line shows the equilibrium lines for a typical Midrex gas composition. The two red points indicate the start and end points of the reduction, the starting point being the top gas composition and temperature and the end point being the bustle gas composition and temperature. [11]

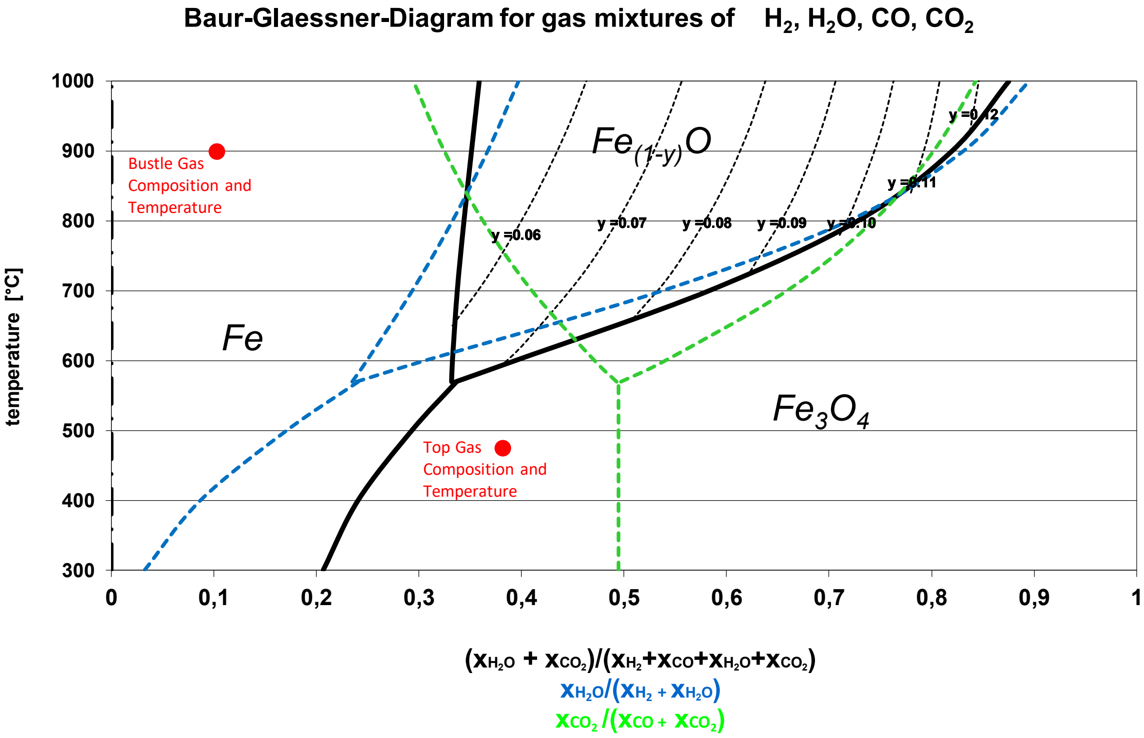

**Figure 6:** Baur-Glaessner-Diagram of a typical Midrex gas mixture [11]

By definition, the iron and its oxides are solid at all times during a direct reduction process. This expression is historically used for the conversion of iron ore directly to metallic iron. The definition of direct reduction process is not to be confused with indirect reduction reaction of iron oxides. The following three different solid oxide phases of iron occur during the process: [7, 5]

- **Hematite** ($Fe_2O_3$): is the most common and therefore most important mineral form of iron ore. The iron in $Fe_2O_3$ is trivalent ($Fe^{3+}$) [7]
- **Wüstite** ($Fe_xO$): as seen in the Baur-Glaessner Diagram, wüstite is an intermediate reduction product which is thermodynamically unstable below the eutectoid temperature of 570 °C. The “x” in the Formula $Fe_xO$ shows that the composition of wüstite is variable. Wüstite has a cubic crystal structure in which anion sites are occupied by $O^{2-}$ and most cation sites are occupied by divalent $Fe^{2+}$ ions. Some other cation sites are occupied by $Fe^{3+}$ ions, with one half of this number being vacant to make the overall charge neutral. “Stoichiometric” wüstite is written as FeO (x=1). In indirect reduction most wüstite is in equilibrium with Fe. Fe saturated wüstite contains 51.26 % oxygen at 1371 °C and 51.38 % at 570 °C. Therefore, wüstite in indirect reduction has an average composition of $Fe_{0,95}O$. [7]

- **Magnetite** ($Fe_3O_4$ or FeO* $Fe_2O_3$): contains both divalent and trivalent iron. Below 1000 °C, in the temperature range of the Midrex process, magnetite is nearly stoichiometric. [7]

The degree of reduction in DR-processes is defined as zero if 100% $Fe_2O_3$ is present with all iron being trivalent. The weight ration of this ore (wt% O/wt% Fe) is 0.4297. Metallic Fe is defined as having a degree of reduction of 100 percent. Hence the reduction degree of partially reduced DRI can be calculated as follows: [7]

$$\% \, reduction = \left( \frac{\left( 0.4297 - \left( \frac{wt\%O}{wt\%Fe} \right) \right)}{0.4297} \right) * 100 \tag{3-7}$$

At given feed streams and process conditions, based on the assumption of equilibrium the reaction products and heat losses can be calculated by applying a mass balance as well as an enthalpy or heat balance. These calculations can be performed by hand or by means of simple thermodynamic models. To calculate whether and in which direction a reaction proceeds it is necessary to calculate the Gibbs free energy. The effect of partial pressures can best be summed up by the equilibrium constant K. Details on the calculation of mass-, heat balances, Gibbs free energy and equilibrium constant can be taken from various books or online databases on thermodynamics. Mass and heat balances are important to get an overview of the process, but they cannot tell if and to what extent the reactions really occur, for this the kinetics of each reaction need to be taken into account as described in chapter 3.2.2. [7]

#### 3.2.1.1 Reactions in Direct Reduction Processes

Above 570 °C the following indirect reduction reactions reduce iron oxide to iron: [7]

**Indirect reduction reactions with carbon monoxide gas:**

$$3\,Fe_2O_3 + CO = 2\,Fe_3O_4 + CO_2 \tag{3-8}$$

$$Fe_3O_4 + CO = 3\,FeO + CO_2 \tag{3-9}$$

$$FeO + CO = Fe + CO_2 \tag{3-10}$$

**Indirect reduction reactions with hydrogen gas:**

$$3\ Fe_2O_3 + H_2 = 2\ Fe_3O_4 + H_2O \tag{3-11}$$

$$Fe_3O_4 + H_2 = 3\ FeO + H_2O \tag{3-12}$$

$$FeO + H_2 = Fe + H_2O \tag{3-13}$$

The Midrex Process uses hydrogen as well as carbon monoxide to reduce iron ore. Both can be formed in the furnace from methane in the presence of metallic iron. Their relative ratios are coupled by the following equations:

**Water-gas shift reaction:**

$$CO + H_2O = CO_2 + H_2 \tag{3-14}$$

**Reforming reactions:**

$$CH_4 + CO_2 = 2\ CO + 2\ H_2 \tag{3-15}$$

$$CH_4 + H_2O = CO + 3\ H_2 \tag{3-16}$$

For the methane reformation the presence of a catalyst is needed to achieve near equilibrium, in the Midrex process, reduced iron functions as a catalyst in the transition zone of the furnace.

To calculate the carbon deposition and the carbon content in solution in α and γ iron the equilibrium constant of the Boudouard reaction has to be calculated:

**Boudouard reaction:**

$$C + CO_2 = 2\ CO \tag{3-17}$$

The carbon deposition reaction (from right to left) occurs quite slow at temperatures below 900 °C, therefore, thermodynamic equilibrium of this reaction does not occur in the Midrex process.

## Reaction Kinetics and Rate Controlling Factors

Since thermodynamics give no information on how fast certain reactions occur in direct reduction processe, it is necessary to look at the reaction kinetics for this information. Because rates of chemical reactions generally increase with higher temperature, kinetics do not play as important a role in blast furnaces as they do in the Midrex process. While some of the rate controlling steps are determined by the reaction system and the contact between the reacting phases, others are controlled by the nature of the iron ore. [12, 7, 5]

For the reduction reactions the reducing gas, carbon monoxide and hydrogen, must be in contact with the oxide surfaces inside in the particles. Therefore, the reducing gas is required to diffuse inward and to react with the oxide, whereas the product gas is required to diffuse outward. When looking at the cross section of a partially reduced pellet from macroscopic point of view, the concentration of hematite is highest in the center, and the concentration of metallic iron is highest at the edge of the pellet. On a microscopic scale the individual particles inside the pellet show a similar picture. At the core there is hematite ore, with a small layer of magnetite around it, which is again surrounded by a wüstite layer and a metallic iron layer on the edge of the particle. [7]

When the reducing gas enters the pellet through its pores, it has to diffuse through these layers. When the reducing gas is unable to contact the magnetite and hematite core, the reduction mechanism is based on the solid-state diffusion of ferrous ions. When Oxygen is removed from the surface of the wüstite layer, the concentration of ferrous ions ($Fe^{++}$) increases. Some of these ferrous ions do not precipitate as metallic iron, but rather diffuse through the wüstite crystal lattice. They then react with magnetite and hematite to produce wüstite and magnetite respectively. [7, 12]

The solid-state diffusion rate of these ferrous ions is higher than the one of carbon monoxide and also hydrogen gas through the pores of the pellet, therefore it is usually not the rate determining step. [12, 7]

When hematite reacts to metallic iron, the overall volume increase is about 25 to 27 %. This effect opens the structure and increases the rate of the gas diffusion. However, when natural magnetite is reduced to metal there is about a 4-5 % shrinkage of the final product. [7] The lack of expansion in the reduction of magnetite causes the formation of dense metallic iron layers surrounding the remaining wüstite and prevent the removal of oxygen. For this reason, magnetite ores are oxidized to hematite first to increase the reducibility. Experiments have shown, that when reducing pure magnetite with hydrogen and carbon monoxide, hydrogen leads to much better results in the early stages due to its faster diffusion rate. In the final stages of the reduction, carbon monoxide was significantly faster. The ore reduced with hydrogen stagnated in the final stages and the microscopy showed grains of wüstite completely enveloped by dense metallic iron layers. When reduced with carbon monoxide, the metallic phase consisted of almost pure pearlite. At reducing temperatures, the iron was therefore pure austenite with a large amount of carbon in solution. Due to the high diffusion rates of carbon in austenite there was enough carbon present at the wüstite – austenite interface to complete the reduction. The resulting formation of carbon monoxide and carbon dioxide was then able to burst the iron layer and thereby separate it from wüstite to let the gaseous reduction continue. [12, 7]

## 3.3 Raw Material

As seen in **Figure 7** the raw material makes up about 70 % of the FOB (Free on Board) cash costs of a DRI Plant. [13]

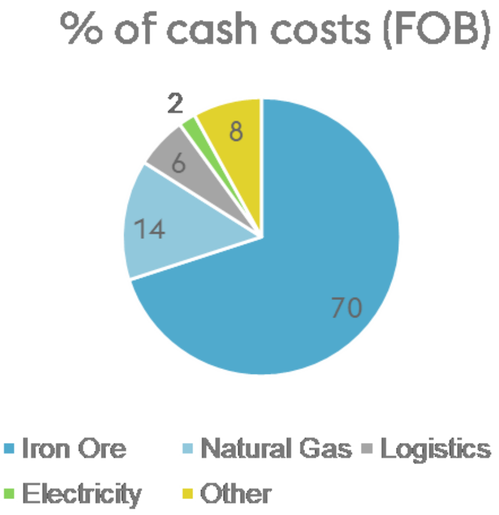

**Figure 7**: Cash costs of operating a DRI plant [13]

Under these circumstances, selecting the right raw material plays a very important role. When selecting the feed of materials for DRI production not only the economic requirements but also the requirements of the process need to be taken into consideration. The general requirements for raw material can be summed up by the following:

1. Have an acceptable chemistry in the natural state or be upgraded by concentration processes
2. Be of specified size for the reduction process
3. Be metallurgically reducible
4. Do not contain undesirable elements in the reduced product that would later negatively impact steel quality
5. Not show sticking or clustering tendencies in the furnace

Given the operating parameters of the Midrex process, iron oxide can be charged in the form of lump ore as well as pellets. The following chapters describe the requirements to raw materials specifically for the Midrex process, give an overview of the typical production paths of pellets as well as lump ores and describe the most current testing methods to ensure the quality of the raw materials today. [7, 5]

### 3.3.1 Required characteristics of raw materials

In the Midrex furnace the efficiency of the reduction is highly favored by a high amount of solid – gas contact and therefore a high permeability.

#### 3.3.1.1 Physical Properties

To ensure a maximum in productivity the feed material should be wear resistant, highly reducible, nonsticking and nonswelling. At a given chemical composition reducibility is associated with a high porous structure. Factors affecting the permeability play an important role in determining the suitability of raw materials in the Midrex process. To maintain a high permeability, it is necessary to ensure the proper size distribution (low amount of fines), porosity of the feed material itself, ability of the material to resist degradation due to impact and abrasion (low generation of fines) and the physical as well as chemical behavior of the feed material at elevated temperatures. High fine content in the raw material is undesirable because fines will promote channeling of the gas which in turn leads to a poor fuel economy and a variability in the reduction degree of the product. Fines screened out before the process can be briquetted and fed into the furnace or shipped to sinter plants, but in both cases the value lost exceeds 50 percent of the pellet cost. The low porosity of over fired pellets and hard dense lump ores lead to a far lower reducibility due to the resulting lower permeability. For the same reason the size of the feed material needs to be limited to ensure a good reduction rate.

The following **Table 3** shows typical physical property requirements for raw materials in the Midrex process: [7, 9]

**Table 3:** Physical Property Specifications for the Midrex Process [7]

| | ***Pellets*** | | ***Lump Ore*** | |
|---|---|---|---|---|
| ***Size Range*** | 9 – 16 mm | | 5 – 50 mm | |
| *minimum* | 85 % | | 70 % | |
| *preferred* | 95 % | | 10 – 30 mm, 85 % | |
| ***Fines*** | < 5 mm | | < 5 mm | |
| *maximum* | 5 % | | 8 % | |
| *preferred* | < 3 % | | < 5 % | |
| ***Strength - Tumbler*** | + 6.3 mm | - 0.5 mm | + 6.3 mm | - 0.5 mm |
| *minimum* | 92 % | | 85 % | |
| *maximum* | | 6 % | | 10 % |
| *preferred* | 95 % | < 4 % | 90 % | < 5 % |
| ***Strength - Compression*** | | | | |
| *minimum* | 150 kg | | | |
| *preferred* | 250 kg | | | |

Other factors, which adversely affect the process are degradation, fragmentation, swelling and sticking during reduction. While all pellets swell during reduction, a swelling of more than 25 to 30 percent is considered undesirable. Some materials even show tendencies to disintegrate during the reduction of hematite to magnetite. The presence of alkali oxides promotes excessive swelling and degradation. Sticking of pellets is minimized by the use of additives such as limestone, lime or dolomite during the pelletizing process as described in section 3.3.2.

#### 3.3.1.2 Chemical Properties

The chemical compositional quality requirements of the product are mainly derived from their use in EAF steelmaking. These requirements of the product directly translate back to the requirements of the raw material, since almost all impurities and gangue of the feed material are also present in the product. In summary the requirements to the most common elements present are the following: [7, 12, 5]

- Iron: To optimize the operating cost the iron content should be at least 66 to 67 percent
- $SiO_2$, $Al_2O_3$, $TiO_2$: A high silica content is unfavorable since it leads to a high slag volume in EAF steelmaking and requires additional power consumption. However, if the silica content is very low this will induce excessive swelling and sticking during the reduction. The $Al_2O_3$ and $TiO_2$ contents do not seem to be critical during the reduction process but show the same characteristics in steelmaking as silica. Therefore, the cumulative content of $SiO_2$, $Al_2O_3$ and $TiO_2$ should be held to under 2-3 percent.
- CaO, MgO: Both lime and magnesia are desirable components in both direct reduction and steelmaking. In pig iron production lime and magnesia act as a fluxing agent and decrease the requirements for added flux. During reduction they reduce sticking tendency and have shown to lower reducibility. The cumulative content of CaO and MgO is desirable up to 3 percent.
- Na, K oxides: Alkali oxides promote swelling and degradation during the reduction process. Their content should be held as low as possible.
- P: While phosphorus has no influence during reduction, it has to be removed during steelmaking. Its content should therefore be held to under 0.03 percent.
- S: Undesirable in the steelmaking process and the Midrex process. If released during reduction in the Midrex process, sulphur will be introduced into the reformer and poison the catalyst. Therefore, sulphur needs to be held to below 0.008 percent.
- Zn: Is normally not present in ores. Recycled materials including Zn are unsuitable for the Midrex process, since they would lead to a Zn circulation in the furnace.
- Cr, Pb, Cu, Sn, Ni, Mo, As, Sb, V, Li and other minor elements: Since the DRI competes with primary scrap in EAF steelmaking, these contents should be lower than those of prime scrap available on the market.

- Free Moisture and Loss on ignition (LOI): Lead to undesirable heat and energy loss and should therefore be held as low as possible.

#### 3.3.1.3 Metallurgical Properties

The metallurgical properties are the properties upon which raw material is evaluated for use in the reduction plant. These properties result from the chemical as well as the physical properties and directly indicate the suitability for direct reduction. Apart from the materials ability to reduce oxygen, its reducibility index, metallurgical properties also include the degradation tendency, the swelling behavior and the sticking tendency. Specific minimum values for reduction parameters and metallization cannot be given, because of the different ways to measure these values. Depending on which testing parameters are used, the results may vary.

Generally, the material should be able to reach a high reduction degree in a short amount of time.

The reduction degree can be measured by a variety of different testing methods, but it is usually given as the percentage of the ratio of mass of oxygen ($m_{os}$) in the sample before the test over the mass of oxygen removed from the sample during the test ($m_{of}$) as seen in the following equation: [14, 7]

$$R[\%] = \frac{m_{os}}{m_{of}} * 100\% \tag{3-18}$$

The reduction degree R is the total reduction after a certain time. Also relevant for assessing the metallurgical properties are the rates at different reduction degrees, also called reducibility index. Their calculation is explained in chapter 3.3.3. [7, 14] The metallization degree (M) is the ratio of metallic iron ($m_{met}$) in the sample after reduction to the amount of total iron ($m_{tot}$) in the sample after the reduction as expressed in the following equation: [14, 7]

$$M = \frac{m_{met}}{m_{tot}} \tag{3-19}$$

The tendency of the material to disintegrate during reduction is often quantified by the disintegration tendency (RDI). At elevated temperatures the material is tumbled and then sieved. The disintegration tendency is given by the ratio of the mass of material larger than a 6.3 mm mesh over the total mass. The abrasion tendency is given by the ratio of the mass of material smaller than 0.5 mm mesh over the total mass. For the Midrex process, the disintegration tendency should be at least 88 % and the abrasion tendency should not be larger than 10 %. Both are expressed in percent and calculated as follows: [14, 7]

$$RDI_{+6.3} = \frac{m_{+6.3}}{m_{tot}} * 100\% \qquad (3\text{-}20)$$

$$RDI_{-0.5} = \frac{m_{-0.5}}{m_{tot}} * 100\% \qquad (3\text{-}21)$$

Swelling describes the volumetric expansion during the heating process and is favorable from 10 to 20 %.

To quantify sticking, there has been no parameter found fully applicable to the Midrex process, however the HYL sticking test procedure quantifies the sticking tendency of raw materials at a slightly higher temperature. The HYL sticking test procedure is conducted as follows: "1,200 g of pellet sample consisting of 50 % 10–12.5 mm and 50 % 12.5–16 mm; reduction temperature of 950 °C; 55 % $H_2$, 21 % CO, 14 % $CO_2$ and 10 % $N_2$ reduction gas composition; heating and cooling in $N_2$ atmosphere; and applying a load of 1.5 $kg/cm^2$ in $N_2$ atmosphere at 950 °C for 30 min after reaching 90 % reduction. The percentage of clusters is determined on the cooled sample. The clustered pellets consisting of more than two pellets are dropped 20 times from a height of 1 m against a hard surface. After each drop, the percentage of remaining clusters are calculated. In the end, number of drops versus percentage of clusters is plotted. The area under the curve is calculated as the sticking index (SI). SI is zero when no clusters of more than two pellets form, and 100 when all pellets are clustered and do not disintegrate during drop tests." [15]

### 3.3.2 Production of Iron Ore Pellets

The term iron ore refers to any iron contained in the earth's crust which is economically as well as spatially available to industry. Every iron ore deposit carries various iron ore minerals as well as other compounds (gangue).

After discovering suitable iron ore deposits, the ore is mined either open pit or underground. In the Midrex process lump ores and pellets are the only suitable iron containing raw materials. For both materials certain restrictions apply, generally a high iron content and certain size restrictions are necessary as mentioned in the previous chapter. For this reason, the ores have to undergo certain treatments before being used in DR processes. [16–18]

On a high level, ores can be classified into three categories:

1. High grade ores with an iron content of > 67 % (for DR)

2. Associated low grade ores with an iron content of 35 – 67 %
3. Underlying iron formations with an iron content of 25 – 35 %

High grade ores with iron contents of at least 67 percent qualify to be processed as lump ores for direct reduction. Ores as mined on site can be over one meter in size. For very high-grade ores it is only necessary for them to be crushed and screened in several steps until they have the desired size. Since a single crusher cannot reduce the dimensions of a lump by more than a factor of about eight, multi stage crushing is usually necessary. Each crushing process is followed by a screening process in which the coarse material is separated from its fines. [14, 5, 16, 14]

For associated low grade ores, in some cases minor upgrading by washing or gravity separation can prove to be sufficient to upgrade them to high grade ores.

Associated low grade ores, not able to be upgraded by simple separation steps, and underlying iron formation ores call for pelletizing in order to be used in the Midrex process. Prior to pelletizing certain concentration steps (e.g.: magnetic separation, gravity separation, flotation, electrostatic separation) need to be performed. Which processing steps are used depend of course on the specific situation, since every ore has different characteristics and therefore leads to different processing requirements. [14, 5, 19]

#### 3.3.2.1 Pelletizing

Pelletizing is the process of agglomeration very fine iron bearing material. Usually the grain size of the fines is < 0.2 mm with a content of ultra fines < 0.04 mm of 70-80 percent. This fine grain material is then formed to spherical shapes by means of a rotating pelletizer plate, balling drums and disc pelletizers. Moisturing fluid (9-12 % $H_2O$) and binding additives (bentonite, clay or hydrated lime) are added to influence the ballability and the characteristics of the final pellet. The most common used additive is bentonite. When preparing the feed, about 0.5 to 1 percent bentonite is added to produce the following effects. [16] [20]

The hydrocolloidal property allows it to absorb water and to expand and spread between the iron oxide particles to agglomerate them. In the firing process the calcium and sodium cations act as fluxing agents fusing the iron oxide particles together. Unfortunately bentonite contains 45 – 65 percent silica which has a negative effect in the refining of the direct reduced iron product downstream. [20]

Since the resulting green balls are not mechanically stable for use in any reduction aggregate they undergo drying, pre-heating, firing and cooling in an induration furnace. The induration process itself takes place at high temperatures of 1000 – 1350 °C and can be devided into two stages: [14, 16]

1. Pre-heating stage
    a. partial oxidation of magnetite to hematite
    b. calcination
    c. solid oxide bonding and grain growth

2. Firing stage
    a. Completion of magnetite oxidation and grain growth
    b. Chemical reactions between the natural and/or added gangue of the pellet, which may involve reactions with the iron constituent

After the induration process ideally, all magnetite gets fully oxidized to hematite, the hematite crystals have recrystallized, and the fluxes have melted, effectively joining the ore grains together. **Figure 8** shows the typical structure of a fully recrystallized pellet and an incompletely recrystallized pellet, g indicates the slag phases and $h_1$ shows the hematite phase. [14]

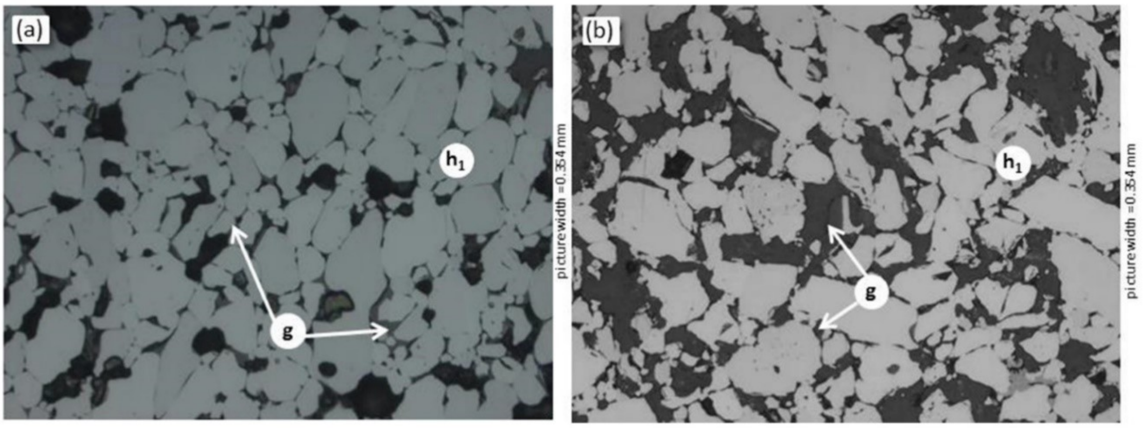

**Figure 8:** Light optical micro graph of a typical pellet structure (a) fully recrystallized, low slag amount; (b) not fully recrystallized, higher slag amount. [14]

The available products for the Midrex process are two different pellet types. Pellets designed for use in the blast furnace, BF pellets, and ones designed specifically for direct reduction, DR pellets. While the requirements for BF pellets are generally similar to the ones of DR pellets, the sticking qualities for BF pellets are not nearly as relevant. This is because the iron in the BF is mixed with different species (coke and limestone) and will eventually melt. Also reducing with $H_2$ is a lot more prone to sticking than CO. To reduce sticking DR pellets can be coated with a thin layer of refractory minerals. **Table 4** shows the findings of Basdag and Arol, that with the right coating the sticking index can be reduced from 92.1 (very high) to zero. [15]

**Table 4:** Effect of coating on sticking index of Midrex pellets reduced at 950 °C [15]

| *Coating Material* | *Dosage, [Kg/t]* | *TFe, %* | *Sticking Index, (SI)* |
|---|---|---|---|
| ***None*** | - | 67.31 | 92.1 |
| ***Limestone + Bentonite*** | 4.9 | 67.13 | 0.0 |
| ***Bauxite*** | 4.9 | 67.26 | 4.2 |
| ***Serpentine*** | 4.2 | 67.16 | 6.1 |

### 3.3.3 Testing Procedures

Midrex plant operators rely on the following tests to make sure that raw material properties meet their requirements and in order to compare different raw materials to each other. While the exact instructions to the testing procedures can be found elsewhere [21, 22], this section focuses on most important parameters of the tests, mainly temperature, time and reducing gas composition. [21–23]

#### 3.3.3.1 ISO 11258

The test according to ISO 11258 is used to determine the reducibility index, final degree of reduction and the degree of metallization after 90 minutes of reduction.

At 800 °C a test portion (approximately 500 grams) is isothermally reduced in a fixed bed. The reducing gas has the following composition: [22]

**Table 5:** Gas composition in the ISO 11258 test [22]

| Gas | Volume Fraction |
|---|---|
| CO | 30 % |
| $CO_2$ | 15 % |
| $H_2$ | 45 % |
| $N_2$ | 10 % |

The overall flow rate of the gas should be maintained at 50 Nl/min. The sample is weighed continuously until 90 minutes of reduction time is reached. **Figure 9** shows the schematic setup of the testing procedure.

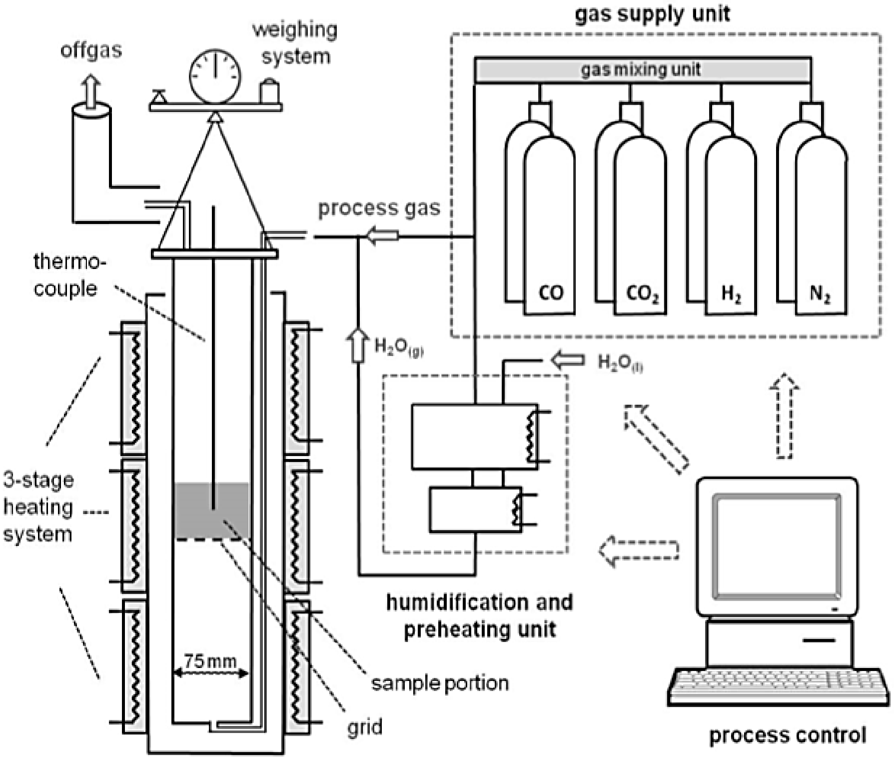

**Figure 9:** Schematic diagram of ISO 11258 test apparatus [14]

The final degree of reduction, reducibility indices and degree of metallization are calculated as follows:

Final degree of Reduction (R90):

$$R_{90} = \left(\frac{0{,}111 * w_1}{0{,}430 * w_2} + \frac{m_1 - m_2}{m_0 * 0{,}430 * w_2} * 100\right) * 100 \qquad (3\text{-}22)$$

Reducibility index for 40 % reduction:

$$\frac{dR}{dt_{R=40}} = \frac{33{,}6}{t_{60} - t_{30}} \qquad (3\text{-}23)$$

Reducibility index for 90 % reduction:

$$\frac{dR}{dt_{R=90}} = \frac{13{,}9}{t_{95} - t_{80}} \qquad (3\text{-}24)$$

Final degree of metallization (M):

$$M = \frac{w_0}{w_t} * 100 \qquad (3\text{-}25)$$

Where:

$m_0$ = mass of test portion [g]

$m_1$ = mass of test portion immediately before ignition [g]

$m_2$ = mass of test portion after 90 min of reduction [g]

$w_0$ = metallic iron content of the reduced test portion [mass %]

$w_t$ = total iron content of the reduced test portion [mass %]

$w_1$ = iron(II) oxide content prior to the test [mass %]

$w_2$ = total iron content prior to the test [mass %]

$t_x$ = time to attain a degree of reduction of x % [min]

#### 3.3.3.2 ISO 11257

The ISO 11257 test provides information on the degree of size degradation and the degree of metallization of the iron ores under conditions resembling those in a direct-reduction process. [21, 23]

A test sample of approximately 500 g is reduced isothermally at 760 °C for 300 minutes. The reduction takes place in a rotating chamber, rotating at 10 rpm, in which the reducing gas passes over the charge. The rotating chambers internal diameter is 130 mm and its length is 200 mm. The reducing gas used has the following composition: [21]

**Table 6:** Gas composition in the ISO 11257 test [21]

| Gas | Volume Fraction |
|---|---|
| CO | 36 % |
| $CO_2$ | 5 % |
| $H_2$ | 55 % |
| $CH_4$ | 4 % |

The overall flow rate of the gas is 13 Nl/min.

The reduced product is first sieved through a mesh with 10 mm openings and then again through a mesh with 3.15 mm openings, the reduction-disintegration index is then given by the mass percentage of the material smaller than 3.15 mm. [21]

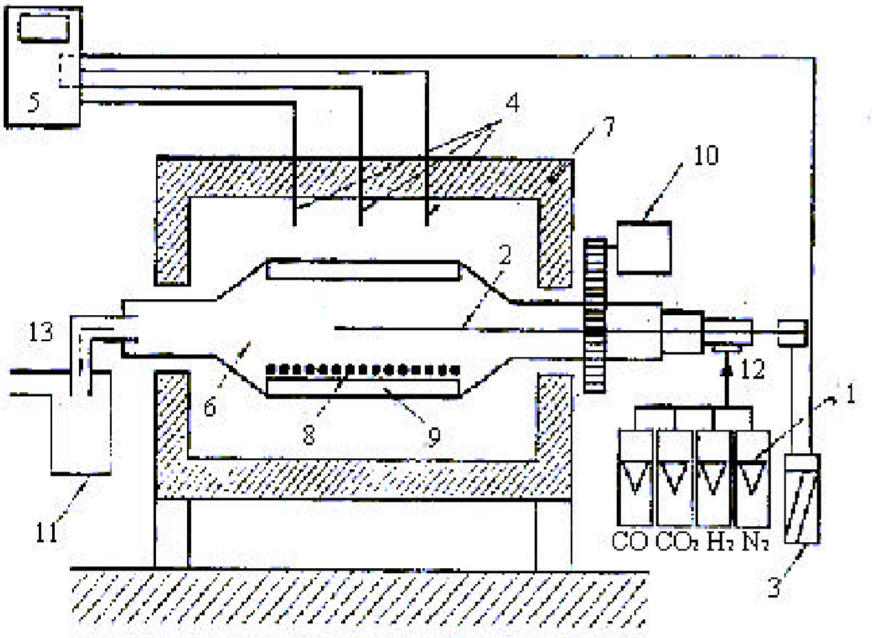

**Key**

1) Gas flowmeters
2) Thermocouple for measuring reduction tube temperature
3) Temperature recorder
4) Thermocouple for measuring furnace temperature
5) Temperature control unit
6) Reduction tube, 540 mm * 150 mm, four lifters
7) Furnace
8) Test portion
9) Lifter
10) Electric motor
11) Dust collector
12) Gas in
13) Gas out

**Figure 10:** Schematic diagram of ISO 11257 test apparatus [24]

The reduction disintegration index and metallization are calculated as follows:

Reduction-Disintegration Index ($RDI_{DR}$):

$$RDI_{DR} = \frac{m_0 - (m_1 + m_2)}{m_0} * 100 \tag{3-26}$$

Metallization (M):

$$M = \frac{w_0}{w_t} * 100 \tag{3-27}$$

Where:

$m_0$ = mass of test portion before sieving and including the dust from the dust collector [g]

$m_1$ = mass of the fraction of the test portion retained in the 10 mm sieve [g]

$m_2$ = mass of the fraction of the test portion retained in the 3.15 mm sieve [g]

$w_0$ = metallic iron content of the reduced test portion [mass %]

$w_1$ = iron(II) oxide content prior to the test [mass %]

#### 3.3.3.3 Midrex “Linder” Test

The Midrex test is very similar to the ISO 11257 test. It uses the same test setup, reducing temperature, reducing gas composition and sample size, however the overall gas flow and sieving meshes are slightly different.

The overall gas flow for the Linder test is specified as 15 Nl/min, compared to 13 Nl/min as specified in the ISO 11257. The mesh used for sieving the mass fraction relevant to the reduction-disintegration index is 3.36 mm, compared to 3.15 mm for the ISO 11257 test. [23]

#### 3.3.3.4 Midrex Hot Load Test

The Midrex Hot Load Test gives information on the physical durability and clustering tendency of the feedstock material during reduction and under load. The test simulates the increasing load experienced by the material descending in the furnace. The test takes place at a temperature of 816 °C, but no detailed information is available in the literature about this test. [23]

A test sample is chosen to form a bed-height of 38-46 cm (approximately 15-18 kg). The pressure drop is measured after loading, after heating and after the reduced product has cooled. The reducing time is 360 min and the gas composition for the reducing gas is as follows: [25]

**Table 7:** Gas composition for the Midrex Hot Load Test [25]

| Gas | Volume Fraction |
|---|---|
| CO | 19.5 % |
| $CO_2$ | 1 % |
| $H_2$ | 38.5 % |
| $CH_4$ | 0.6 % |
| $N_2$ | 40.4 % |

During reduction the load on the material is increased according to the following table:

**Table 8:** Applied load over time of the Midrex Hot Load Test [25]

| Reduction time [h] | Applied load [kg] |
|---|---|
| 0 | 0 |
| 1 | 16 |
| 2 | 114 |
| 3 | 114 |
| 4 | 227 |
| 5 | 227 |
| 6 | End |

After this the furnace is unloaded and the sample is analyzed for size, clustering, chemical analysis and strength. A sketch of the apparatus used can be seen in the following **Figure 11**: [25]

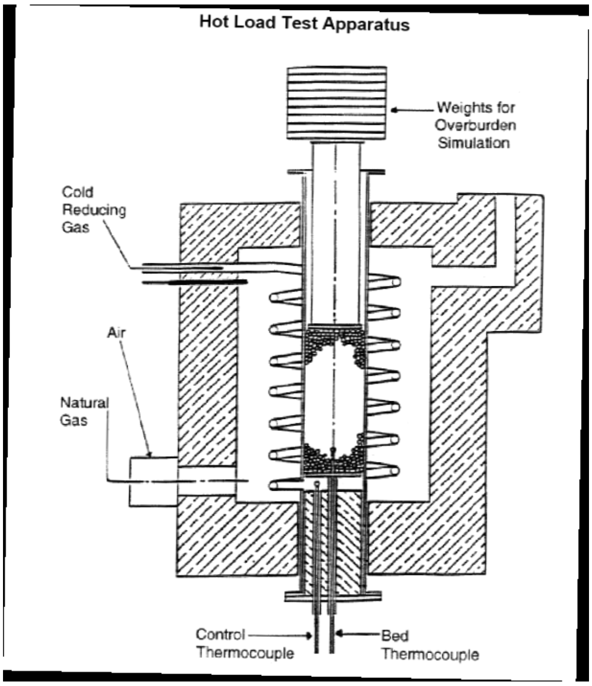

**Figure 11:** Hot load apparatus [25]

#### 3.3.3.5 ISO 11256

The ISO 11256 standardized test was developed to access the clustering tendency of the feedstock material in direct reduction. A sample of 2000 g is isothermally reduced at 850 °C in a fixed bed until a reduction degree of 95 % is reached. After 60 min of reduction a constant load of 147 kPa is applied to the sample. [23] The gas composition during reduction is as follows:

**Table 9:** Gas composition of the ISO 11256 test [25]

| Gas | Volume Fraction |
|---|---|
| CO | 30 % |
| $CO_2$ | 15 % |
| $H_2$ | 45 % |
| $N_2$ | 10 % |

After reduction, the clustered material is tumbled seven times, each time for 5 revolutions (at 25 rpm) in a 1 m diameter tumble drum. The clustering index is then calculated from the mass percentage of the clustered material accumulated after each disintegration operation. [23]

#### 3.3.3.6 R180 test

All previously mentioned tests use isothermal conditions as well as constant gas compositions which do not resemble the conditions experienced by the feedstock material in the Midrex furnace. Therefore, the R180 test was developed to better resemble the conditions present in the Midrex furnace. The test uses three temperature steps with three different gas compositions over a total time of 180 minutes to create a more realistic temperature and gas profile. For the R180 test the same setup is used as in the ISO 11258 standard, also known as the R90 test. While the sample weight is also 500 g, the temperature, gas flow rate, gas composition and reduction time differ from the ISO 11258 standardized test. [26]

The R180 test utilizes three different reduction gas compositions at temperatures ranging from 400 to 850 °C. The total reduction time is 180 minutes.

The first step starts with a temperature of 400 °C and continuously increases the temperature to 750 °C at a rate of 9 K/min. The second step isothermally reduces the sample at 750 °C until 70 % reduction degree is reached. The third step increases the temperature from 750 to 850 °C at 8 K/min then holds the temperature at 850 °C until the total time elapsed from the start of step one is 180 minutes. The gas compositions of the three steps are as follows:

**Table 10:** Gas composition of the three gas mixtures in the R180 test [27]

| Gas | Volume Fraction Mix 1 | Volume Fraction Mix 2 | Volume Fraction Mix 3 |
|---|---|---|---|
| CO | 5.5 % | 14% | 26% |
| $CO_2$ | 28.5 % | 20 % | 8 % |
| $H_2$ | 61 % | 61 % | 61 % |
| $N_2$ | 5 % | 5 % | 5 % |

The following figure shows the temperature profile of the R180 Test: [27]

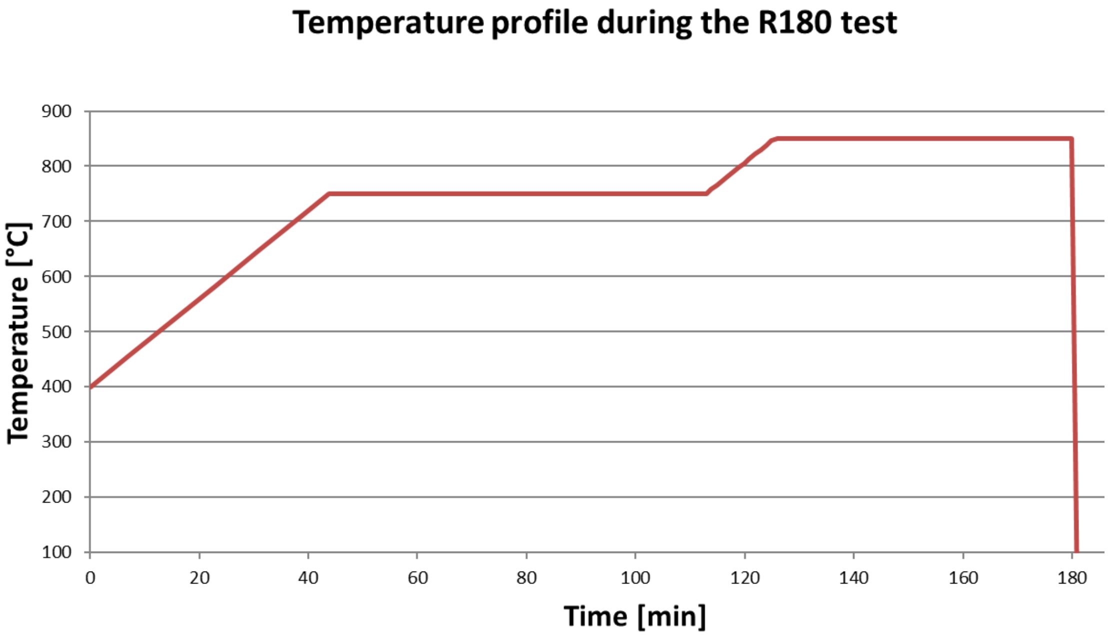

**Figure 12:** Temperature profile of the R180 test [27]

Compared to the ISO 11258 standard, with which this test shares the same setup, this test should be more representative of the industrial Midrex reduction process. The longer time period and different gas compositions lead to a greater sensitivity of the final reduction range. [27]

## 3.4 Modelling and Simulation approaches for the Midrex Process

This part of the thesis gives an overview of the various approaches to model and simulate the reactions occurring in the Midrex process.

### 3.4.1 Pellet Model - Unreacted Shrinking Core Models

The unreacted shrinking core model is most commonly used when it comes to describing the kinetics and mechanisms of iron oxide reduction, especially in the form of pellets, with $H_2$ and CO as in a Midrex furnace. [28, 29, 7, 11, 30, 12] While most simulations make use of the shrinking core model, the models still differ from each other depending on the assumptions which have been made.

A very general approach is laid out in detail by Feinman [7]. The reaction interface of the hematite pellet is assumed to be spherical and moves towards the center of the pellet as the reaction progresses. Thus, the reaction interface decreases over the course of the reduction.

To model the overall reaction of the pellet, five kinetic steps are modeled individually, namely:

1. Mass transfer of the reductant across the boundary layer outside the spherical specimen
2. Diffusion of reductant across the porous product layer
3. Interfacial reaction
4. Diffusion of gaseous product across the solid product layer
5. Mass transfer of gaseous product across the boundary layer

To solve the resulting equations a number of assumptions are made depending on which model is used. The most common assumptions being: [7, 28, 11]

- The system is isobaric
- The system is isothermal
- The interfaces are assumed to be sharp
- The gas diffusivities are independent of the gas composition
- There is no volume change during the reduction

The resulting equation is usually dependent on mass transfer coefficients, effective diffusivities and interfacial rate constants.

As an example of a rather complex approach the model used by Alhumanaizi et al. [28] relies on a shrinking core model with three sharp interfaces in which the reactions of hematite to magnetite, magnetite to wüstite and wüstite to iron take place. **Figure 13** shows the interfaces between the phases and the concentrations of the reducing gas ($C_j$) as well as the product gas ($C_{jP}$). Unlike many other models the reactions are also assumed to be reversible.

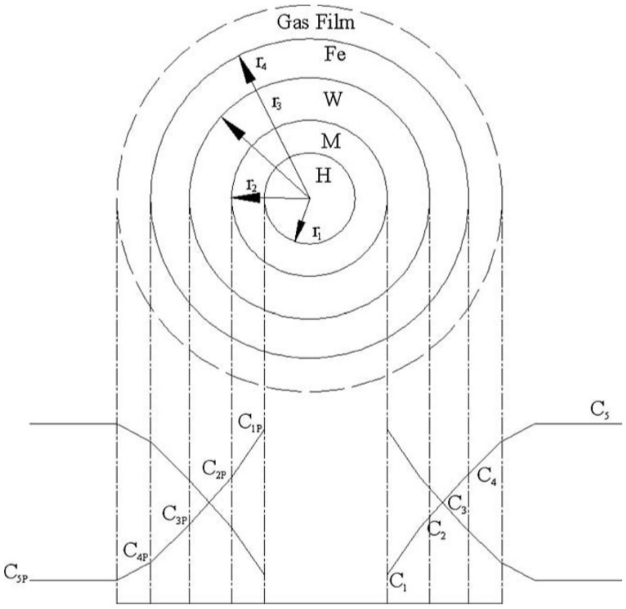

**Figure 13:** Three-interface shrinking core iron oxide pellet model [28]

Other approaches use a somewhat simplified shrinking core model with only a single interface, the wüstite – iron interface. The reason for being that, as Zuo et al. argue, the reduction from wüstite to iron is the most difficult step as well as the step with the maximum level of deoxygenation, therefore it is valid to assume that the rate determining reaction occurs at this interface. [29]

The resulting models are often relatively complicated, and adjustable parameters also lead to the model only being applicable for a finite amount of data it has been adjusted for. While such models are useful for the development of better agglomerates, they have limited use to furnace operators in predicting pellet quality. Further weaknesses concerning the practicality of this model to commercial DRI plants result from the following: [7]

- Real interfaces are diffuse and not sharp
- The porosity and diffusivity are usually unknown
- Gas flow conditions in the furnace vary
- Effects of impurities are neglected (e.g.: swelling)
- Reactivity of iron oxides can vary widely

### 3.4.2 Reduction Zone (Furnace) Model

A moving bed model is the basis for most simulations of the reduction zone. The pellet model just described lays the basis for further calculations. With the help of mass and energy balances, chemical and thermal profiles of the solid and gaseous phases can be calculated.

Since the boundaries around the reduction zone are very difficult to draw, and the formation of free carbon does not occur in the reduction zone, most simulations of the reduction zone include simulations of the transition and cooling zones as well, making it a simulation of the entire shaft. This is done by adding two sets of mass and energy balances. Most models of the entire shaft assume that the carburization and cracking reactions occur in the transition and cooling zone only. [7, 11]

### 3.4.3 Plant Model

To fully simulate the Midrex process, it is also necessary to consider its interactions with other parts of the plant, mainly the reformer.

The work of Alhumaizi et al. [28] is a good example of how the pellet model is used as the basis for simulating the reduction furnace. This simulation also takes into account the interactions between the furnace and all other components of the plant, mainly the reformer and the scrubbers. [28]

Most simulations found in literature are able to calculate results that are quite close to the results produced by industrial data [31, 30, 11, 28]. However, it has to be kept in mind that some parameters used in the calculation are fitted towards one specific plant. Especially in the reformer the quality of the results depends strongly on the fitted parameters. [32, 28] But also for the reduction zone a number of parameters are usually fitted, these may include kinetic parameters for side reactions and heat transfer coefficients. [28, 11]

# 4 Process Conditions at the Plant

The industry partner of this thesis, voestalpine Texas LLC, operates a Midrex HBI plant in Corpus Christi, Texas. The following chapter focuses on deriving the process conditions of the plant from plant data and theory. The resulting profiles are later compared to the conditions in the standardized tests.

In order to be able to identify or even design a suitable test for assessing the reducibility of raw materials, knowing and understanding the process conditions is the key. The relevant profiles which have to be determined are:

- The temperature profile
- The gas composition profile
- Reduction degree and metallization profile (= pellet composition)

## 4.1 Temperature Profile

The temperature profile is developed from 15 sensors inside the furnace, from the top gas temperature and from the geometry of the furnace.

The 15 temperature sensors are installed at three different heights inside the furnace. At each of these heights there is one sensor mounted in the center of the furnace and four sensors evenly distributed at 90-degree angles, at a radius ($R_s$) around the center of the furnace. These outer temperature sensors constantly show higher temperature measurements than the temperature sensors in the center of the furnace. This effect is mainly caused by the hot bustle gas being injected from the outside edge of the furnace. To take this into account a linear temperature increase was assumed from the center to the outer temperature sensors ($R_s$). From the outer temperature sensors ($R_s$) to the furnace wall ($R_f$) the temperature was assumed to be constant. **Figure 14** schematically shows the temperature sensor placements and the assumed temperature profile from the center (dashed black line) to the wall (solid black line) of the furnace. The resulting average temperature for the three specific heights in the furnace, where the temperature sensors are placed, are calculated as follows:

$$T_{Ri} = \frac{(T_{R1i} + T_{R2i} + T_{R3i} + T_{R4i})}{4} \tag{4-1}$$

$$T_{avg\,i} = \frac{\left(T_{ci} + \frac{2}{3} * (T_{Ri} - T_{ci})\right) * R_s^2 + T_{Ri} * \left(R_f^2 - R_s^2\right)}{R_f^2} \tag{4-2}$$

$T_{avg\,i} = Average\ temperature\ at\ sensor\ height\ i;\ i \ldots Top, Middle, Bottom$

$T_{ci} = Temperature\ of\ center\ sensor\ at\ height\ i$

$T_{Rji} = Temperature\ of\ outer\ sensor\ j\ at\ height\ i; j \ldots 1,2,3,4$

$T_{Ri} = Average\ Temperature\ of\ outer\ sensors\ at\ height\ i$

$R_s = Radius\ from\ center\ of\ furnace\ to\ outer\ sensors$

$R_f = Radius\ from\ center\ of\ furnace\ to\ wall\ of\ furnace$

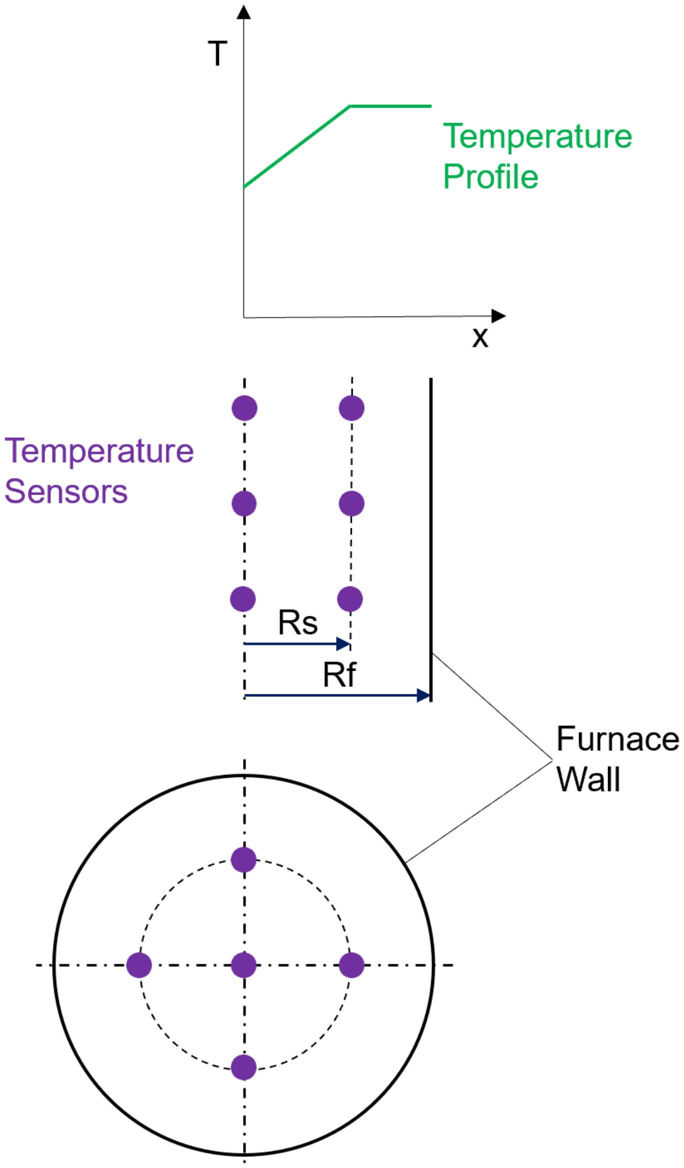

**Figure 14:** Temperature profile from center to wall of furnace

After calculating the average temperatures for each of the three sensor heights, the next step is to come up with a temperature profile from the top to the bottom of the furnace. By fitting a logarithmic function to match the observed profile, as seen in **Figure 15**, the following equation for the average furnace temperature as a function of the distance from the top of the reduction zone is obtained. In the following formula and figure the temperatures are displayed as dimensionless. The dimensionless temperature is obtained by dividing the calculated temperature through the temperature of the Bustle Gas.

$$T(h) = 0.0409 * \ln(h) + 0.9971 \qquad (4\text{-}3)$$

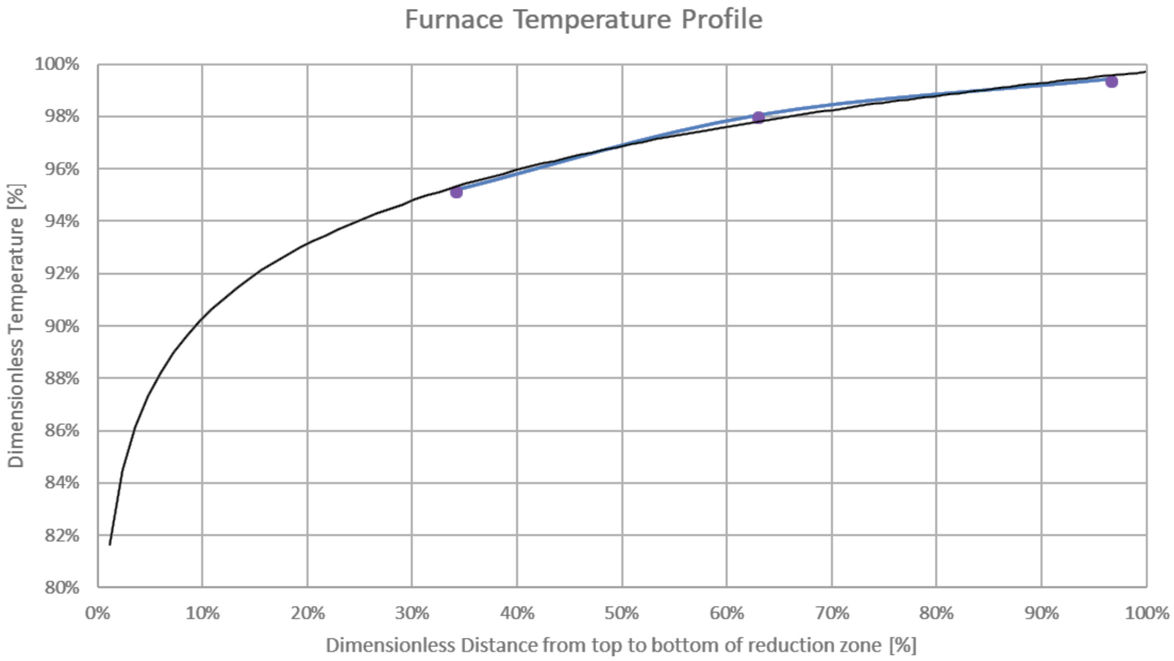

**Figure 15:** Temperature profile from top sensors to bustle gas inlet

While the obtained equation closely resembles what is expected for most part of the reduction zone, different assumptions are made for the top part of the reduction zone. It is assumed that the raw material enters the furnace at room temperature and is then heated up to the temperature of the top gas exiting the furnace. This heating process is further assumed to be linear and to occur in the first 5 % of the reduction zone height. From there, again a linear temperature increase to the average temperature of the top temperature sensors is assumed. These assumptions give us the final temperature profile over the total height of the furnace, as seen in **Figure 16**. This calculated temperature profile will be used for calculating the chemical profiles of the gas and pellet composition through the furnace.

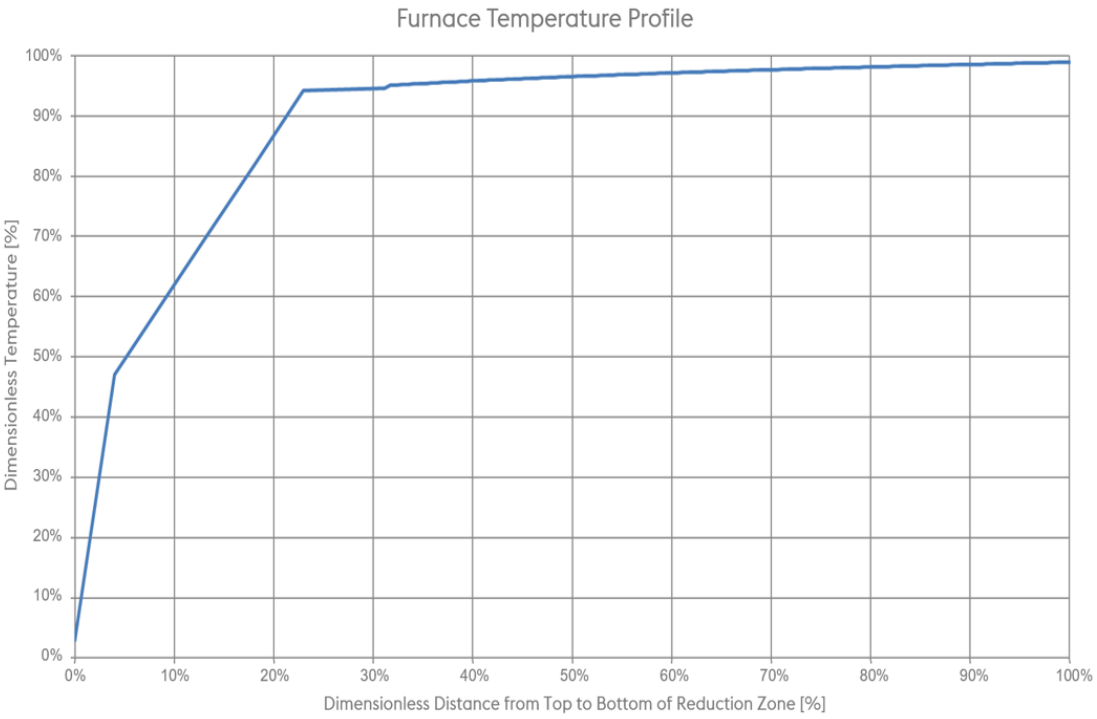

**Figure 16:** Furnace temperature profile of reduction zone

## 4.2 Chemical Profile

The chemical profile over the height of the furnace can be split into two interdependent profiles:

- The chemical composition of the solids (pellets)
- The chemical composition of the gaseous components

As a first step the relation between the solid profile and the gaseous profile is established by determining the reduction rate of the oxides.

### 4.2.1 Reduction Rate Determination

To gain insight into how the chemical profile of the pellet changes based on the different gaseous environments when it passes through the furnace, experimental data is needed. For this reason, the ISO 11258 test is modified and run a specific pellet. While the test setup remains the same as for the ISO 11258 tests, the reduction time, overall gas flow and also the gas composition are modified.

#### 4.2.1.1 Rate Determining Reduction Test Parameters

Based on the volume of the reduction zone and the production of HBI, the time it takes for a pellet to pass through the reduction zone of the furnace is calculated to be about 180 minutes. Hence, the time used in the rate determining tests is also set to 180 minutes and therefore doubled in comparison to the 90 minutes of the ISO 11258 test.

Regarding the gas composition, it was decided that three tests at three different gas compositions were to be performed. In defining the gas compositions, the aim was to choose a composition as closely as possible resembling the gas composition in a Midrex furnace. For this reason, it is decided to add $H_2O$ to the gas mix. To design the gas composition, typical Midrex plant data [33] regarding the composition and flow of the top gas as well as of the bustle, transition and reheat gases was used. The top gas composition is defined as the composition of the gas at the top of the reduction zone. To calculate the composition at the bottom of the reduction zone, the bustle, transition and reheat gases are summed up. The resulting gas composition is then modified by subtracting the amount of carbon in the product from the $CH_4$ composition and adding 2 mole $H_2$ to the $H_2$ composition for every mole $CH_4$ subtracted. In addition, the difference between the remaining $CH_4$ and the $CH_4$ in the top gas is assumed to also go to $H_2$ and CO immediately.

At this point the compositions at the top and the bottom of the furnace are known, however no information on how the composition changes during the reduction exists. The closest data available was the existing ISO 11258 test result of this pellet. This reduction profile gives information on how much oxygen is removed as a function of the reduction time and can therefore be used to calculate the change of gas composition according to this profile. Because production data indicates that the total residence time of the pellet in the reduction furnace is approximately three hours, the reduction profiles are stretched from 90 minutes to 180 minutes before calculating the furnace gas profiles. The resulting gas composition and gas quality profiles can be seen in **Figure 17** and **Figure 18**. These profiles are used to decide at which gas compositions to perform further tests in order to develop a more exact profile of the furnace.

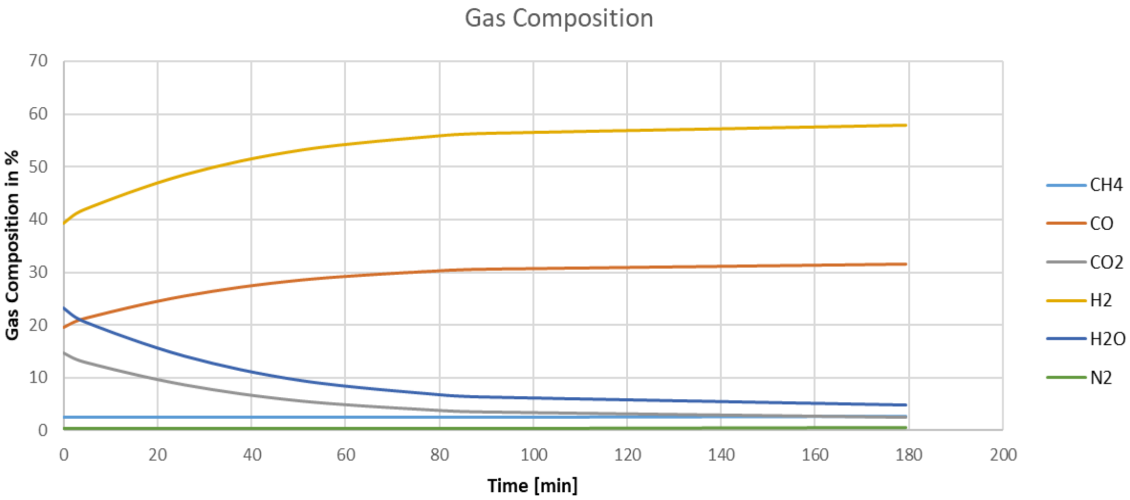

**Figure 17:** Gas composition profile of the furnace based on the ISO 11258 test

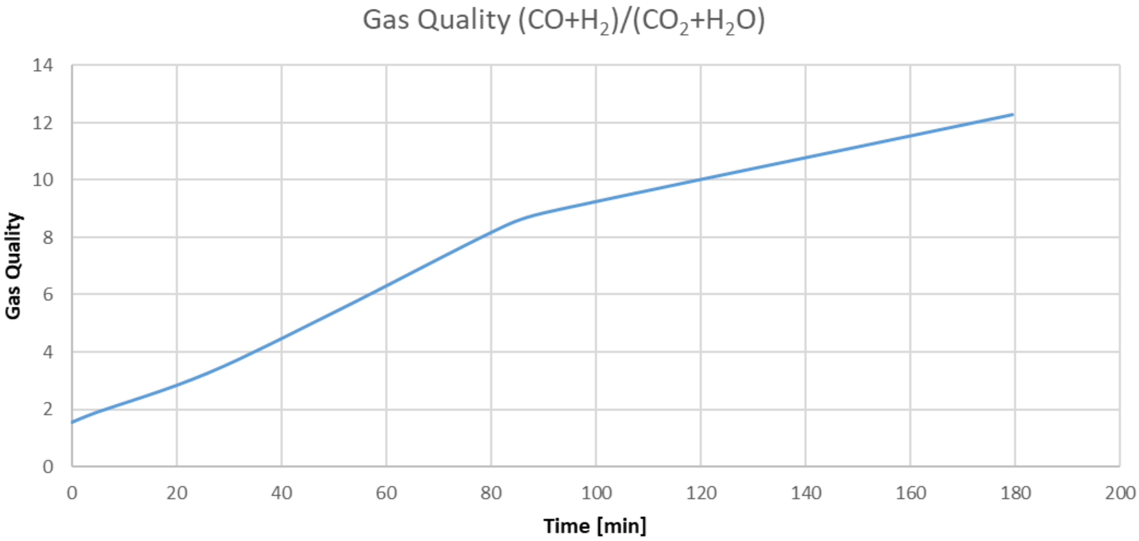

**Figure 18:** Gas quality profile of the furnace based on the ISO 11258 test

Based on these profiles it was decided that the tests would be performed at gas qualities of 10.25, 5 and 2 with their corresponding composition of $CO_2$, CO, $H_2$ and $H_2O$. The gas quality 10 and 2 are chosen to resemble the conditions close to the bottom and top of the reduction zone. The gas quality 5 is chosen, to be able to compare the test result (which would include $H_2O$ in the mixture) to the result of the previously mentioned ISO 11258 test (which also reduces at a gas quality of 5 but does not include $H_2O$ in the mixture).

Regarding the lower gas quality of 2 a restriction of the testing equipment has to be taken into account. The maximum throughput of $H_2O$ is limited by the evaporator to 250 g/h or 5.2 Nl/min, meaning at a total gas flow of 50 Nl/min the maximum $H_2O$ concentration cannot exceed 10.4 %. Therefore, the overall gas flow during the tests is reduced to 28 Nl/min, which at a nitrogen flow of 10 % allows for the gas composition corresponding to a gas quality of 2 to be realized.

The temperature during the test was 800 °C as in the ISO 11258 test. The parameters, different from the ISO 11258 test, are summarized below in **Table 11**.

**Table 11:** Reduction rate test parameters different from ISO 11258

| Reduction rate tests | $N_2$ | CO | $CO_2$ | $H_2$ | $H_2O$ | Gas Quality | Total Flow [Nl/min] | Total Time [min] |
|---|---|---|---|---|---|---|---|---|
| Test 1 | 10 % | 29 % | 2.8 % | 53 % | 5.2 % | 10,3 | 28 | 180 |
| Test 2 | 10 % | 26 % | 5.3 % | 49 % | 9.7 % | 5 | 28 | 180 |
| Test 3 | 10 % | 22 % | 11 % | 39 % | 18 % | 2,1 | 28 | 180 |

### 4.2.1.2 Rate Determining Reduction Test Results

Three different reduction curves are measured in the three tests performed. The resulting reduction curves are shown in **Figure 19**.

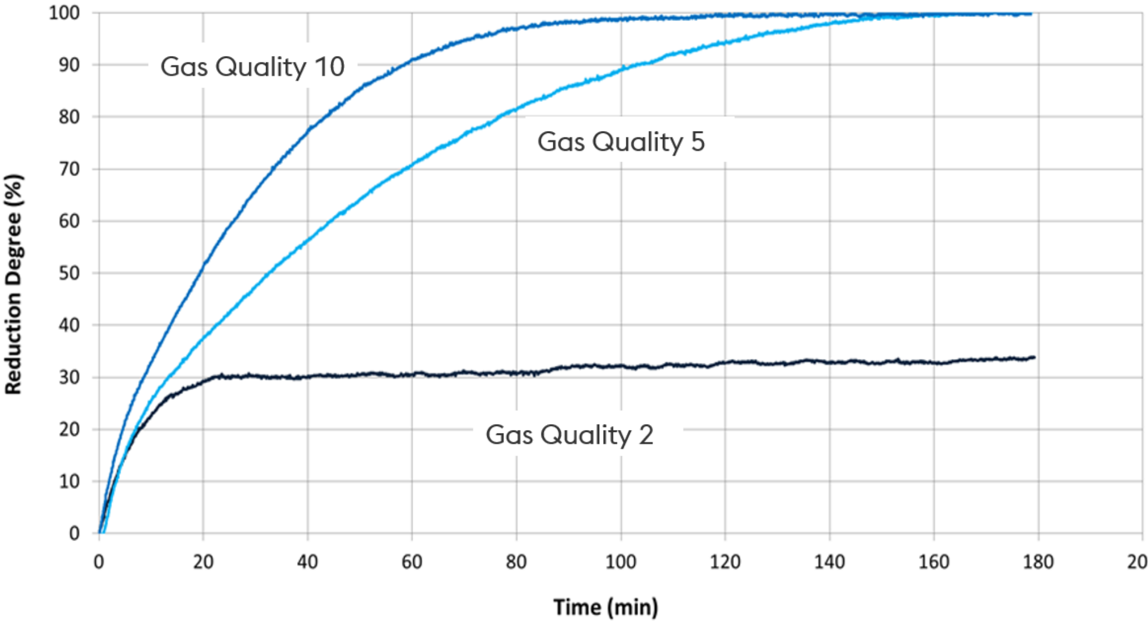

**Figure 19:** Reduction profile of rate determining reduction tests at gas qualities 2, 5 and 10.3

From these reduction profiles two conclusions about the reduction from $Fe_2O_3$ to Fe can be drawn.

Firstly, the reduction from $Fe_2O_3$ to FeO, which occurs in the top part of the reduction zone, and is equivalent to about 33 % reduction degree, can be achieved even with the lowest gas quality used in the tests. At this lowest gas quality of two it takes about 20 minutes to reach 90 % reduction of $Fe_2O_3$ to FeO. For the plant it therefore can be assumed, that since the gas quality increases as the pellet progresses through the furnace that it takes no more than 30 minutes for the reduction of $Fe_2O_3$ to FeO to be completed at sufficiently high temperatures.

Secondly, the reduction rate of FeO to Fe, which only occurs at the tests with Gas Qualities of 5 and 10 because Fe is not stable at a Gas Quality of 2, is strongly dependent on the gas quality. If assumed that the $Fe_2O_3$ to FeO reduction is completed before any Fe is formed, then the rate of the metallization is equal to the rate at which the reactions FeO to Fe take place. According to Bogdandy and Engell [12], the rate limiting factors for this reaction are diffusion as well as the phase boundary reaction itself. The reaction rate for the reduction of FeO to Fe is therefore given by: [12]

$$\dot{\mathfrak{R}} = \frac{\left(3 * D^P * k_3 * (1-\mathfrak{R})^{\frac{2}{3}} * (p^0 - p^*)\right)}{d_0 * r_0 * D^P + d_0 * r_0^2 * k_3 * \left((1-\mathfrak{R})^{\frac{1}{3}} - (1-\mathfrak{R})^{\frac{2}{3}}\right) * R * T} \tag{4-4}$$

$$\dot{\mathfrak{R}} = \ rate\ of\ reduction$$

$$\mathfrak{R} = degree\ of\ reduction = Metallization$$

$$D^P = diffusion\ coefficient\ through\ the\ product\ layer\ (Fe)\ \left[\frac{cm^2}{s}\right]$$

$$k_3 = rate\ constant\ of\ the\ phase\ boundry\ reaction\ \left[\frac{mole}{cm^2 * s * atm}\right]$$

$$d_0 = oxygen\ content\ of\ the\ ore\ \left[\frac{mole}{cm^3}\right]$$

$$r_0 = radius\ of\ the\ ore\ [cm]$$

$$p_0 = partial\ pressure\ of\ reducing\ agents\ (H_2 + CO)\ [atm]$$

$$p_* = equilibrium\ pressure\ of\ reducing\ agents\ (H_2 + CO)\ [atm]$$

$$T = temperature\ [K]$$

$$R = univeral\ gas\ constant = 0{,}082057\ \left[\frac{cm^3 * atm}{K * mole}\right]$$

For the pellets used in the test constants $d_0$ and $r_0$ are assumed to be:

$$d_0 = \frac{\left(5.2\ \left(Hematite\ density\ \left[\frac{g}{cm^3}\right]\right) * 0.3\ (\%\ O\ in\ Hematite) * 0.95\ (\%\ Hematite\ in\ ore)\right)}{16\ \left(\left[\frac{g}{mole}\right]\right)}$$

( 4-5)

$$d_0 = 0{,}0926\ \ \left[\frac{mole}{cm^3}\right] \qquad (4\text{-}6)$$

$$r_0 = 0.5\ [cm] \qquad (4\text{-}7)$$

The gas composition, the temperature and therefore also the equilibrium gas pressures are constant for each of the tests:

$$T = 1073\ \ [K] \qquad (4\text{-}8)$$

$$(p^0 - p^*)_{Test1} = 0.219\ [atm] \qquad (4\text{-}9)$$

$$(p^0 - p^*)_{Test2} = 0.148\ [atm] \qquad (4\text{-}10)$$

The two remaining constants are calculated by first calculating two reduction curves based on the formula above and then fitting the calculated curves to the metallization curves of the reduction test. The metallization curves as well as the calculated curves can be seen in **Figure 20**.

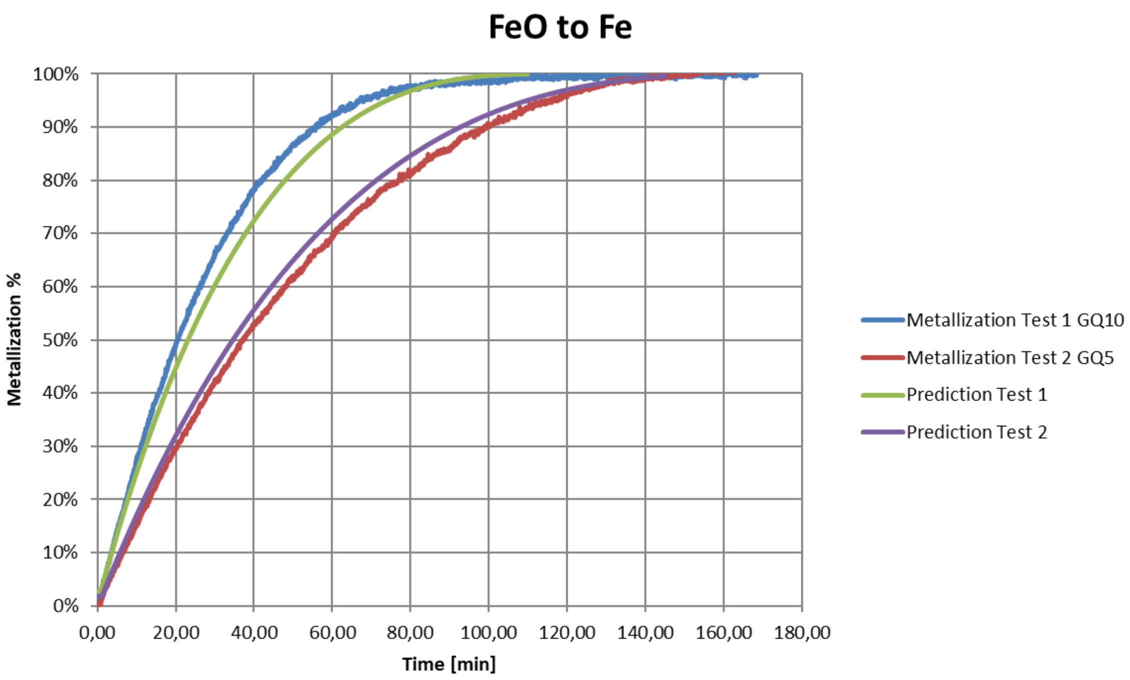

**Figure 20:** Calculated reduction curves fitted to reduction curves from experimental data

By changing the diffusion constant (Dp) and the rate constant ($k_3$), the two predicted reduction curves can be fitted to the reduction curves of the test. Since these constants should be the same for both tests, they are fitted by minimizing the overall difference between Test 1 and prediction 1 as well as Test 2 and prediction 2. The diffusion coefficient and rate constant are thereby calculated to be:

$$D^P = 3.27 * 10^{-3} \left[\frac{cm^2}{s}\right] \tag{4-11}$$

$$k_3 = 3.25 * 10^{-5} \left[\frac{mole}{cm^2 * s * atm}\right] \tag{4-12}$$

As a result, all constants in the reduction rate formula are known and the rate of reduction is dependent on the temperature, partial pressure of CO and $H_2$ and the reduction degree. All other factors are either known constants or, as in the case of the equilibrium pressure, functions of the temperature.

### 4.2.2 Chemical Profile Determination

The chemical profiles inside the furnace are calculated by using the temperature profile, the incoming gaseous stream and the incoming solid stream. The following assumptions apply for the calculation:

- The temperature profile as calculated in chapter 4.1 is constant and not influenced by any chemical reactions
- The incoming gaseous stream consists of bustle, transition and reheat gas streams and its composition is calculated as an average from plant data during stable production.
- The quantity of incoming gas is given by the specific gas flow, again an average value from plant data is used.
- The incoming gaseous stream is defined by the average production of HBI from plant data, and an oxide to HBI ration of 1.4.
- The dry composition of the incoming pellets is assumed to be 5 % gangue and 95 % $Fe_2O_3$. The moisture content is assumed to be 2%.
- The volumetric flow of the pellets and with it the total time in the furnace is calculated from the production rate, the area of the reduction zone, which are plant parameters, and the bulk density of DRI, which is assumed to be 1.5 t/m³.
- The incoming $CH_4$ reacts as soon as the gas enters the furnace as follows:
  - 55 % exits the furnace in top gas, it is treated as an inert gas
  - Based on the production rate and the assumption of 1.5 % carbon in the product, a certain amount of C goes into the HBI. The remaining hydrogen goes into the gas stream as $H_2$
  - The rest of the $CH_4$, which is not used as carbon in the product and does not exit the top gas, is assumed to react to CO and $H_2$. The oxygen which is needed to create CO is assumed to be the first oxygen to react, before any CO reacts to $CO_2$ or any $H_2$ reacts to $H_2O$.
- The moisture in the pellets evaporates before the pellets reach the top gas temperature
- The $Fe_2O_3$ to FeO reduction starts at 600 °C and takes 30 min to complete, independently of gas composition, based on the findings in section 4.2.1.2.
- The rate of the reaction FeO to Fe is given by the fitted rate equation as in section 4.2.1.2
- The water gas shift reaction happens instantly and at any time in the furnace
- The equilibrium constants for the reduction of FeO with CO and $H_2$ are assumed to be linear for the relevant temperatures between 750 °C and 850 °C

Based on these assumptions, the reaction rate and with it the metallization (= chemical composition of the pellets) is calculated on a 60 second basis from the top of the furnace to the bottom using the gas composition and the temperature profile as a variable. The gas composition in turn is calculated from the bottom up and as a first step uses a variable cell with a constant reduction degree for each step. By minimizing the sum of errors over all steps between the calculated reduction degree and the variable used to calculate the gas composition, the overall chemical profile is calculated.

## 4.3 Results and Validation of Chemical Profile Calculation

**Figure 21** shows the chemical profile of the pellet in the furnace. **Figure 22** and **Figure 23** show the gas quality and the gas composition profile over the time a pellet spends in the furnace.

The profiles of metallization as well as reduction degree show a close to linear behavior for large parts of the furnace. In reality parts of the $Fe_2O_3$ to FeO and FeO to Fe reduction are likely to occur simultaneously, and not consecutively as modelled.

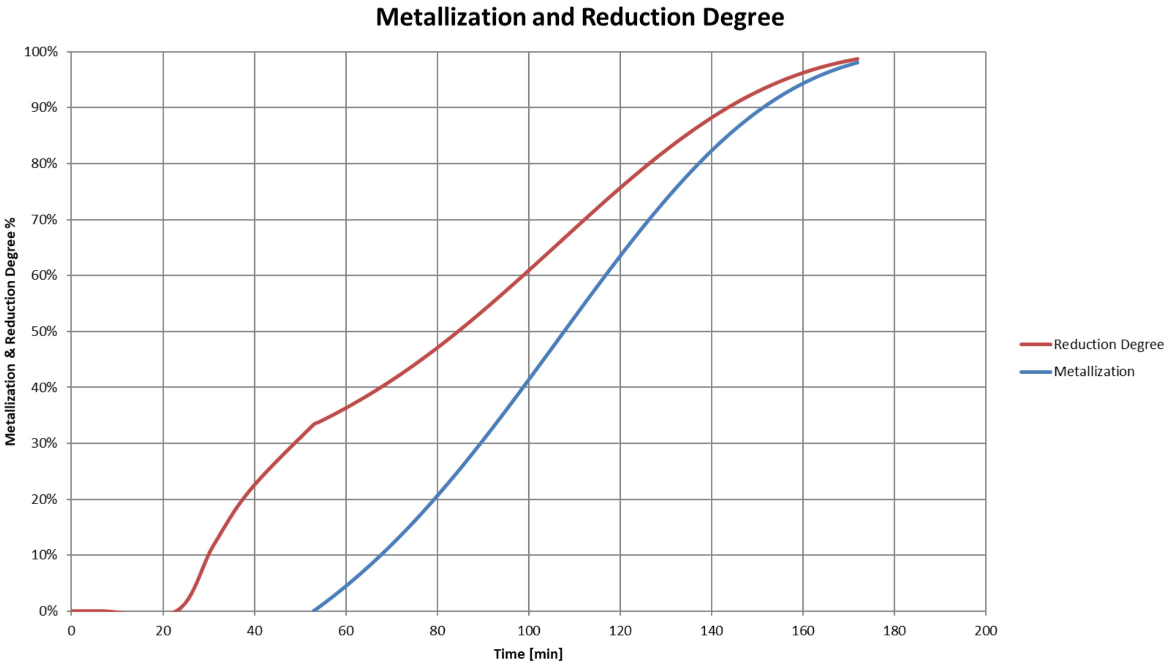

**Figure 21:** Reduction degree and metallization profile of the pellet in the furnace

Regarding the gas quality it can be observed, that the gas quality is quite low over most of the time in the furnace. Starting at a gas quality below 2, the first half of the time the pellet spends in the furnace, the gas quality is lower than 3.5. During the half of the time in the furnace the gas quality increases to above 10. Under the assumption that the reduction from $Fe_2O_3$ to FeO and FeO to Fe do not occur simultaneously, it can be seen that the FeO to Fe reduction starts at a gas quality of 2.5. The flat gas quality period towards the end of the reduction zone is an effect of parts of the $CH_4$ reacting to CO and $H_2$. The oxygen needed for this is used before oxidizing any of the reducing agents $H_2$ or CO.

The chemical profiles of the various gas components show a linear profile for most part of the FeO to Fe reaction. With the help of this profile, conclusions on the composition in the furnace can be drawn for any specific gas quality above 2.5. Since the $Fe_2O_3$ to FeO reduction is not modeled in detail, no detailed conclusion can be drawn about the change in chemical composition during this period.

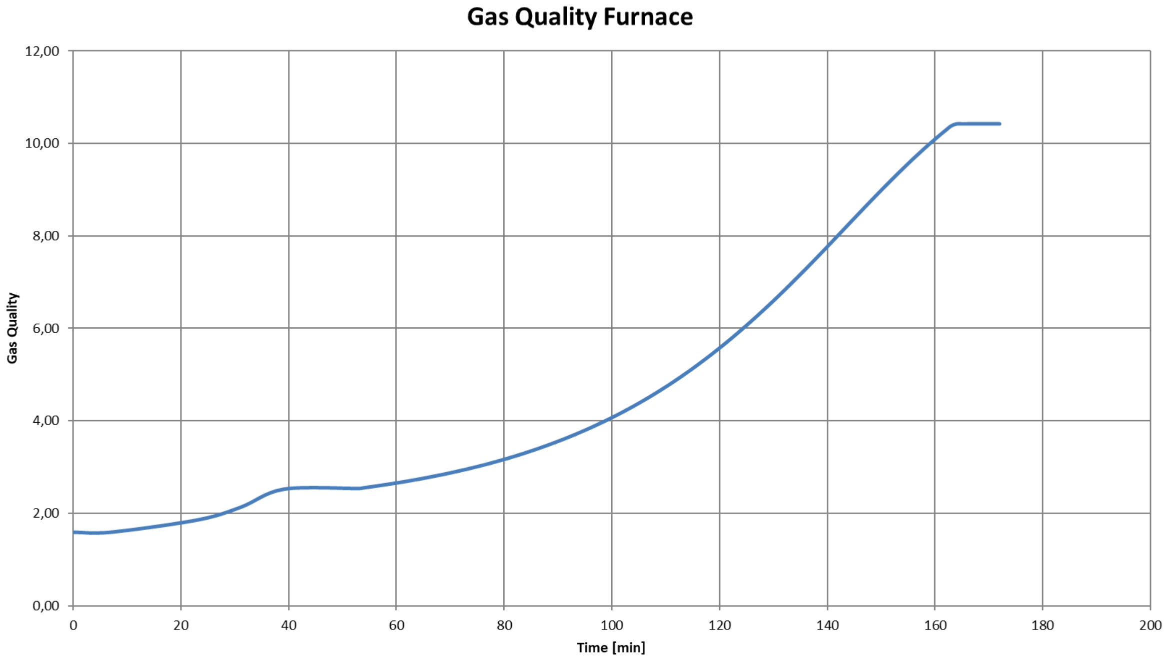

**Figure 22:** Gas quality profile in the furnace

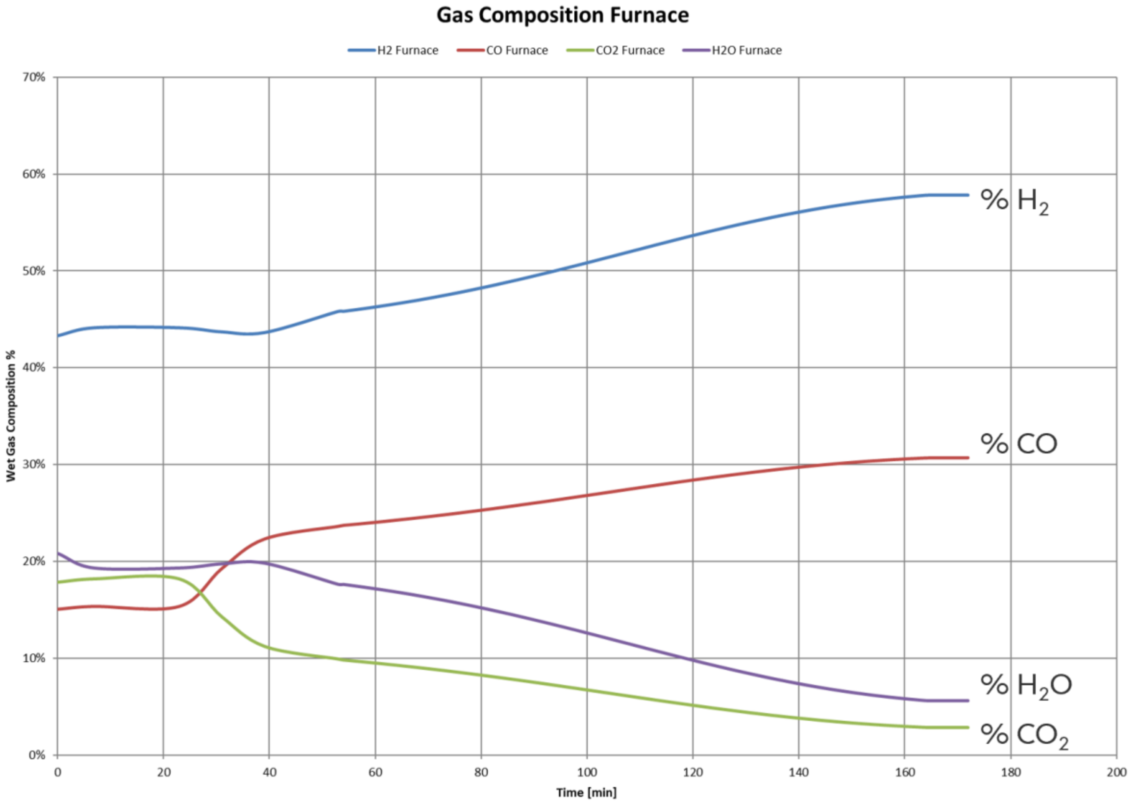

**Figure 23:** Gas composition profile in the furnace

In order to trust these results, they have been verified with the help of plant data. Different scenarios of the calculation are run with 19 different specific bustle gas flows. The relative specific bustle gas flows in these scenarios ranged from 0.9 to 1.1, with 1.0 being the average specific bustle gas flow for a stable production period of the analyzed pellet type B. These calculations are then compared with hourly averages of plant data from the same pellet. Since the plant data however is based on the chemical analysis of the HBI and the calculation is designed to determine the metallization of DRI, some extent of reoxidation has to be taken into account to be able to compare the results. The amount of reoxidation is difficult to determine for the data points used from the plant. Considering the high temperatures of the briquette and contact with air and water after the briquetting process a reoxidation of 2 % in metallization is assumed. These 2 % were subtracted from the resulting metallization of the calculation. The plotted results of the calculation as well as the plant data points can be seen in **Figure 24**. The blue dots in the plot represent the calculated DRI metallization for different specific bustle gas flow scenarios, while the red dots show the same results with 2 % of a reoxidation, representing the HBI. The green dots represent hourly averages of specific bustle gas flows from plant data and the metallization measured from the corresponding HBI. It can be seen, that where plant data is available, between 92 and 95 percent metallization, the calculations match the plant data very closely.

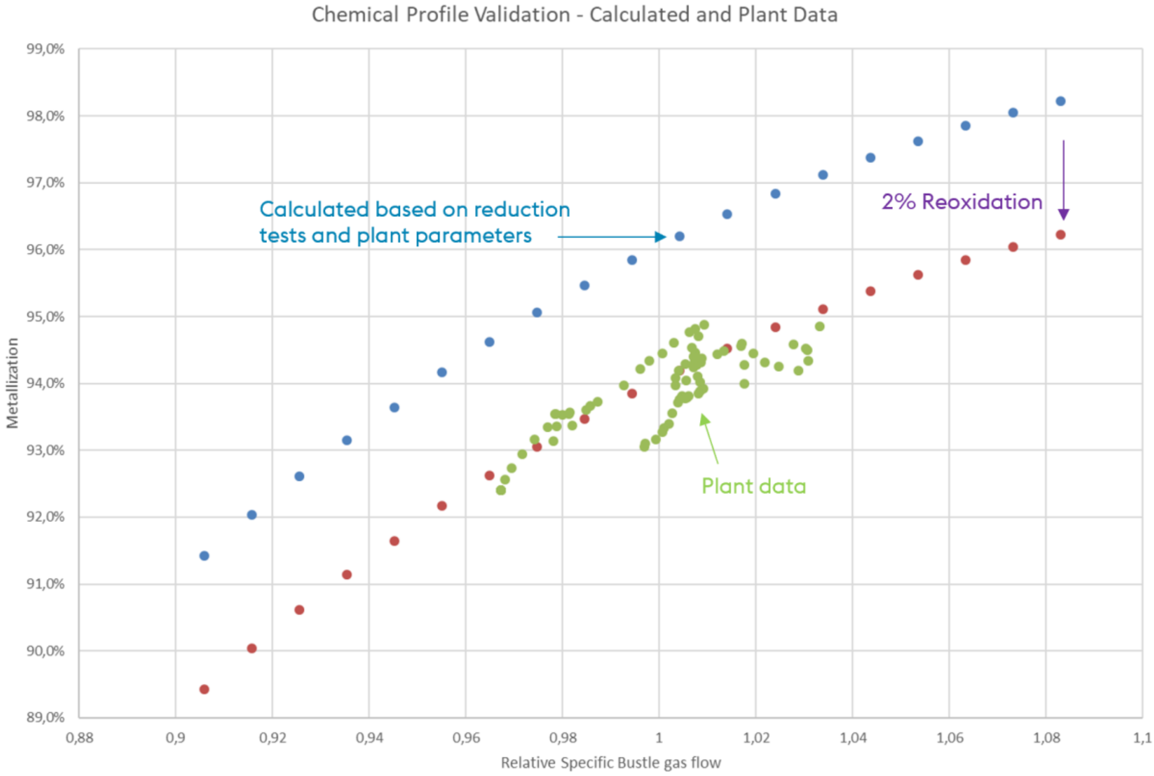

**Figure 24:** Metallization over specific bustle gas flow of calculated and plant data

## 4.4 Comparison of Process Conditions to Reduction Tests

The calculated furnace profile conditions are compared to the standardized tests introduced in chapter 3.3.3. **Table 12** compares the approximate process conditions to the different tests. The ISO 11257, ISO 11258 and R180 tests specifically aim at determining the reducibility of the pellets. All tests except for the ISO 11257 use a fixed bed, which resembles the conditions in the furnace. Regarding the temperature, most tests are relatively close to furnace conditions, since the temperatures in the furnace are above 800 °C for most part of the reducing time. The R180 is the only test changing the temperature profile over time. None of the tests with reducibility as their prime objective include an applied load on the pellets. With a test time of 90 minutes the ISO 11258 is a lot shorter than the reduction time in the furnace and the R180 seems to be very close to the furnace reduction time. All other tests reduce for a significantly longer time.

Regarding the gas composition, the biggest difference all tests have compared to plant conditions is the absence of water in the gas mix. Regarding the gas quality, an indicator of the reducing strength of a gas, the ISO 11257 and the Hot Load test are a lot higher than in the process, all other tests use a gas quality which is present in the furnace at some point. Another big difference between the tests and the furnace is that, except for the R180, the gas composition is constant for the entire test duration.

**Table 12:** Standardized test conditions compared to process conditions

| Parameters | Tests | | | | | Process Conditions |
|---|---|---|---|---|---|---|
| | ISO 11256 | ISO 11257 | ISO 11258 | Hot Load | R180 | |
| Bed type | fixed | rotating | fixed | fixed | fixed | moving bed (fixed) |
| Reduction Curve | No | No | Yes | No | Yes | |
| Maximum Load [kPa] | 147 | | | 283 | | 0 - 230 |
| Temperature [°C] | 850 | 760 | 800 | 816 | 400<br>750<br>850 | 400 - 840 |
| Reduction Time [min] | to 95% RD | 300 | 90 | 360 | 180 | 170 |
| CO % | 30 | 36 | 30 | 19,5 | 5.5<br>14<br>26 | 19,6 - 32,2 |
| $CO_2$ % | 15 | 5 | 15 | 1 | 28.5<br>20<br>8 | 14,6 - 2,5 |
| $CH_4$ % | | 4 | | 0.6 | | 5 - 2,7 |
| $H_2$ % | 45 | 55 | 45 | 38.5 | 61 | 39.3 – 54.7 |
| $H_2O$ % | | | | | | 23.3 – 4.9 |
| $N_2$ % | 10 | | 10 | 40.4 | 5 | 0.6 |
| Gas Quality | 5 | 18.2 | 5 | 58 | 2.3<br>3.75<br>10.8 | 1.8 - 11 |
| $H_2/CO$ | 1.5 | 1.5 | 1.5 | 2.0 | 2.3<br>4.4<br>11.1 | 2 – 1.7 |
| H/C | 2.00 | 2.80 | 2.00 | 3.76 | 3.59 | 3.7 |
| Aim of the Test | Clustering Index, time to RD=95% | Metallization, Disintegration | RD90, Metallization, reducibility index (40, 90) | Clustering, Durability | RD180, Metallization | |

The gas composition and temperature profile of the R180 test and the furnace are not constant. Therefore, it is difficult to compare these two to each other based on the table above.

**Figure 25** and **Figure 26** show the temperature and gas composition profile of both, the R180 test and the furnace. The temperature profiles are very similar to each other, however for the first two hours the temperature is substantially lower compared to the furnace. In the final hour, the temperature is then increased and slightly higher than expected in the furnace. The gas quality is higher in the test than it is in the furnace for most of the time. Only from approximately minute 100 to 120 the expected gas quality in the furnace is higher than in the test. Overall the steps do follow the trend of the furnace, but because of the limited number of steps the accuracy is also limited.

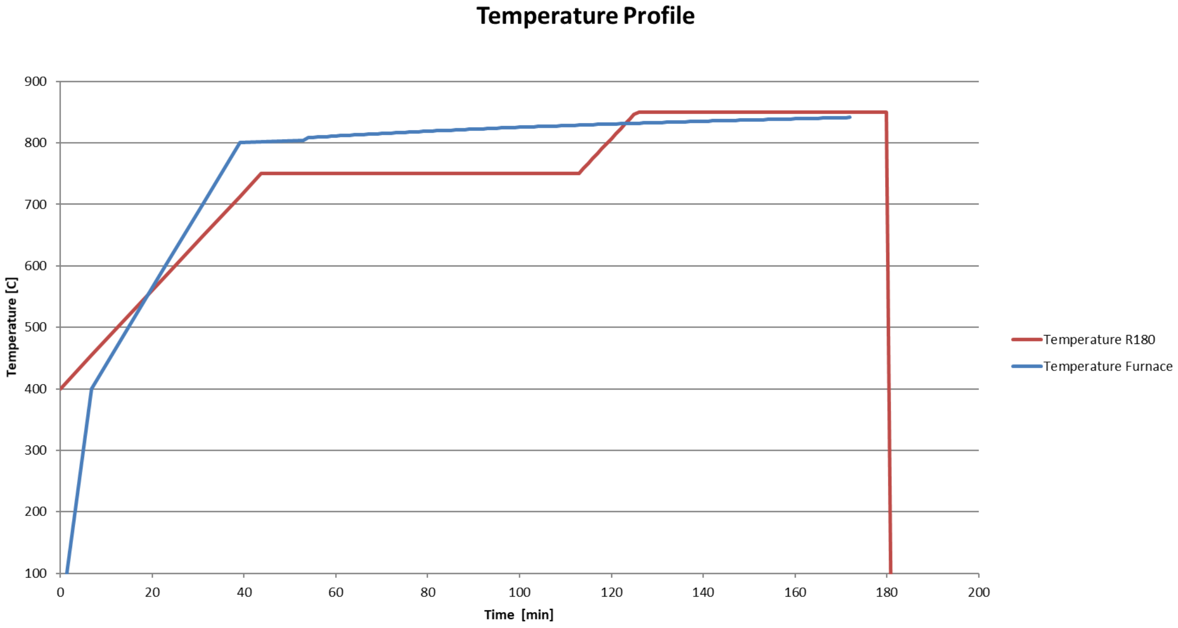

**Figure 25:** Temperature profile of R180 and furnace

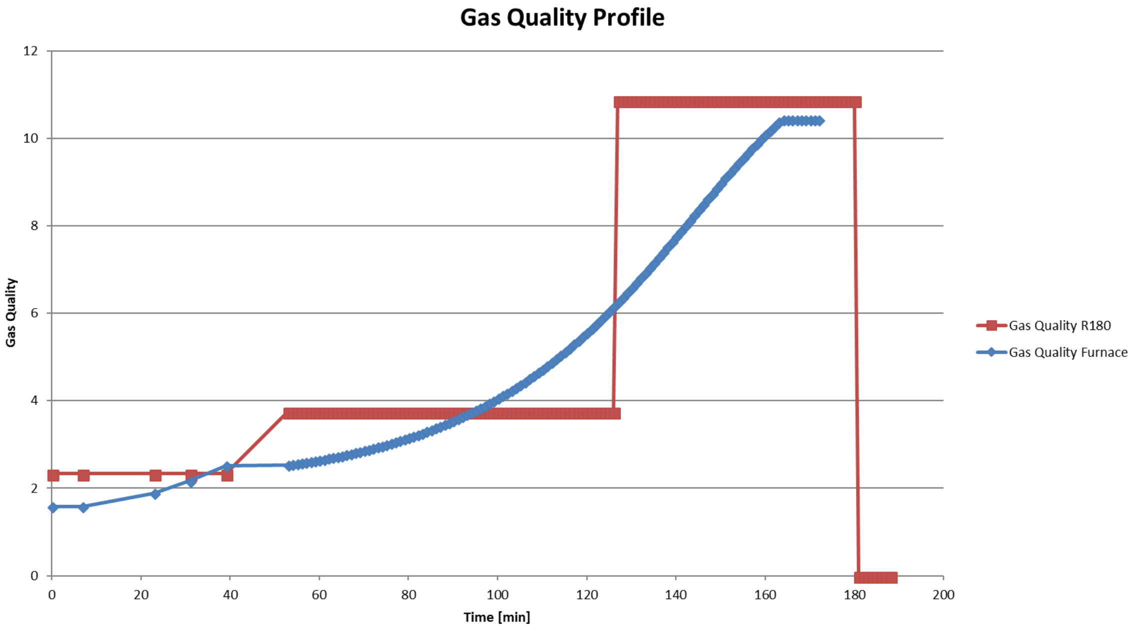

**Figure 26:** Gas quality profile of R180 and furnace

# 5 Pellet Performance

The following chapters show how the pellet performance is evaluated and calculated by analyzing operating data. The operating data is taken from the Midrex plant operated by voestalpine Texas LLC in Corpus Christi.

## 5.1 Pellets investigated

In this thesis six different pellet types are investigated. The pellet types analyzed will be named A through F. **Table 13** shows the typical chemical composition of the six pellets. The total iron content of the different pellet types is as low as 66.6 percent for pellet D and as high as 68 percent for pellet C.

**Table 13:** Chemical composition of pellets analyzed

| Chemical Composition in wt. % | A | B | C | D | E | F |
|---|---|---|---|---|---|---|
| Fe tot | 67.2 | 67.7 | 68 | 66.6 | 67.8 | 67.6 |
| FeO | 1.29 | 0.5 | 0.06 | 1.2 | 0.06 | - |

Additionally, so called “remet” is also charged to the furnace in some cases. Remet is partially reduced DRI which is produced when ramping up or shutting down the plant. Its chemical composition is not measured frequently and can vary anywhere from iron oxide to HBI quality.

## 5.2 Plant Performance Calculation

The performance of different pellet types under industry conditions is calculated with the help of the plant data from the industry partner.

### 5.2.1 Raw Data

The raw data from the plant is obtained through the so called “Level 2 System” which is a Manufacturing Execution System (MES). The data is pulled from the system, most of it as hourly average, of the various data-points. The data used for calculating the plant performance can be divided into the following categories:

- Temperature measurements in the furnace and the gas system
- Pressure sensors in the gas system
- Dry chemical analysis of the gas composition at various points in the system
- Gas flows at various points in the system
- Moisture content measurement of the gas
- Chemical analysis of the HBI (every 2 hours)
- Chemical analysis of the DRI (every 12 hours)
- Chemical analysis of the raw material x (per shipment)
- Belt scale measurements of raw materials, fines, and product
- Calculated production based on briquetting machine parameters

These data-points are pulled for different time periods which are to be analyzed. Before using the data for further calculations, it had to be reformatted. Especially different data formatting systems depending on which category of data it is and time the data is created called for detailed attention.

### 5.2.1 Calculation Method

A series of mass balances around the various components of the plant is used to first calculate the flows and compositions of the gases and then the flows and compositions of the solids entering and exiting the furnace.

#### 5.2.1.1 Calculation of Gas Flows and Compositions

In order to calculate how much a pellet is being reduced it is necessary to know exactly what gas composition and flow enters and exits the furnace. The gas system is basically an open loop in which natural gas is fed into the system at different points and top gas fuel as well as moisture is removed from the system at the scrubber. The following diagram in **Figure 27** shows the available measurements in the gas system at the plant. Reheat and transition zone (TZG) gas streams are meant to ensure the carbon content of the final product. [34] A gas flow measurement is indicated by “Q”, a dry composition measurement by “xi” and “$x_{H2O}$” indicates that the moisture can be calculated through pressure and temperature measurements according to the Antoine equation.

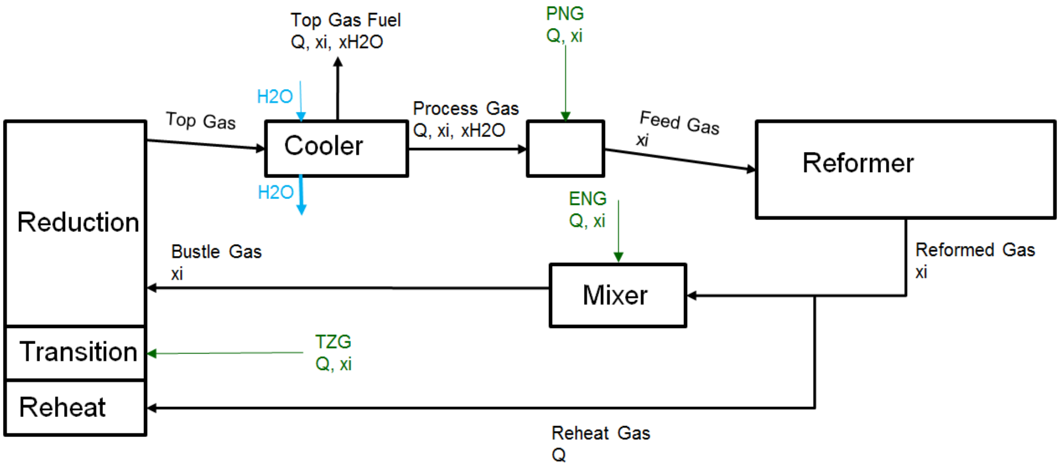

**Figure 27:** Diagram of the plants gas system and its composition and flow measurements

When starting to examine the loop where the top gas exits the furnace, it becomes clear that neither flow nor composition or water content of the gas is known at this point.

This unknown gas continues into the top gas scrubber (or cooler) where it is cooled with water and thereby an unknown amount of water (blue arrow) is also removed from the gas.

The top gas fuel and the process gas both exit the scrubber. For both gases the dry composition and flow is measured and, since it is safe to assume that at this point the gas is saturated with water, the water content is calculated from the temperature and pressure measurements. The top gas fuel is the only gas removed from the system and is later burned in order to heat the reformer.

The process gas, of which all relevant flow and composition data are known, is mixed with the Process Natural Gas (PNG) of which composition and amount is known. It also is assumed that this natural gas is free of any moisture. By simply adding the two gas streams the composition, gas flow and moisture of the feed gas is calculated. The calculated composition can be compared to the measured composition to makes sure the calculation is correct.

The feed gas then enters the reformer, where the $CH_4$ and other hydrocarbons react with $H_2O$ and $CO_2$ to form $H_2$ and CO. The extent and efficiency of the reforming reactions are unknown. Therefore, the wet composition and flow of the reformed gas is calculated with the help of the measured dry composition of the reformed gas. A carbon and nitrogen mass balance is used to first calculate the amount of carbon and nitrogen containing components as well as the total dry flow of the gas. Using the total dry flow and the dry composition, the amount of $H_2$ can also be calculated. This leaves the amount of $H_2O$ as the last unknown, which can now be calculate in two ways: by closing the hydrogen or the oxygen balance.

After the reformer, a part of the reformed gas, the reheat gas, is injected directly into the reheat zone of the furnace. The flow of this gas is measured, and the chemical composition is identical to the reformed gas.

The rest of the reformed gas not used as reheat gas goes on into another mixer, where it is enriched with natural gas, so called Enrichment Natural Gas (ENG). Since the composition and flow of the ENG is known, all parameters of the bustle gas exiting the mixer can be calculated by simply adding the components of the reformed gas and the ENG together. The resulting dry composition can be compared to the measured dry composition of the bustle gas to check for any errors.

In addition to the bustle and reheat gas, the transition zone natural gas also is injected into the furnace. As with the other natural gases in the process, the transition zone natural gas is assumed to be free of water and the dry composition and flow is measured.

At this point the exact (wet) composition and flow of all gases entering the furnace is known. To calculate the (wet) composition and flow of top gas exiting the furnace, first the water removed from the top gas in the scrubber is needed to be determined.

A hydrogen mass balance, taking into account all gas streams, around the system of furnace and scrubber the amount of $H_2O$ removed from the top gas in the scrubber is determined. Any $H_2O$ introduced to the furnace as moisture of feed material, has to be added to the calculated amount and in further consequence also to the top gas composition.

To calculate the top gas composition and flow, a final mass balance around the scrubber is needed. Since no chemical reactions occur in the scrubber, the two gas streams exiting the scrubber (top gas fuel and process gas) and the $H_2O$ removed from the top gas in the scrubber simply are added together to obtain the top gas composition and flow. The moisture of the pellets is assumed to go directly into the scrubber and thereby adding to the $H_2O$ removed.

#### 5.2.1.2 Calculation of Solid Flows and Compositions

The solid flows of the process consist of the iron oxide entering the furnace, on the top and the briquettes exiting the furnace on the bottom.

Concerning the iron ore, the composition of the different pellet and lump ore types is known from chemical analysis. Additionally, to pellets and iron ore, remet is also fed into the furnace in small amounts. The composition of remet varies strongly since it consists of partially reduced DRI. Unfortunately, it cannot be determined which remet composition is fed into the furnace, therefore an average composition of remet is assumed for all remet fed into the furnace. Belt scales measuring the weight of the different oxide types and remet fed into the furnace make it possible to calculate the ratios of the individual components in the mix and thereby determine the dry chemical composition of the feed at any given time. The total amount of ore fed into the furnace is also measured by means of a belt scale.

The weight and with that the flow of the HBI leaving the furnace is determined by a belt scale as well as calculated based on the operating data of the briquetting machines. The chemical composition of the HBI is measured every two hours by taking a sample from the cooling conveyor and analyzing it in the laboratory.

Since for both the oxide feed and HBI composition and flow information is available, in theory no additional calculation is necessary. However, comparing the oxygen removed from the pellets to the oxygen added to the gas streams frequent and non-neglectable deviations are observed. These differences seem to stem from, at times, unreliable measurements from the belt scales as well as the briquetting machines.

To calculate the quantities of oxides feed and HBI produced, an oxygen and iron mass balance over the furnace is used. Depending on the production rate measured by the briquetting machines, the HBI and oxide compositions are shifted in time to match the reaction taking place in the bottom of the reduction zone of the furnace. The flow and composition of the gas streams in the furnace are known from calculations in chapter 5.2.1.1 and the composition of both the solid streams are also known. To account for the reoxidation from the moment the briquettes leave the furnace to the time they are analyzed in the lab, a constant reoxidation rate is assumed. **Figure 28** shows a schematic diagram of the furnace with the known variables in green and the unknown variables in red. By using the oxygen and iron mass balance the amount of oxide pellets fed to and the amount of HBI removed from the furnace are calculated.

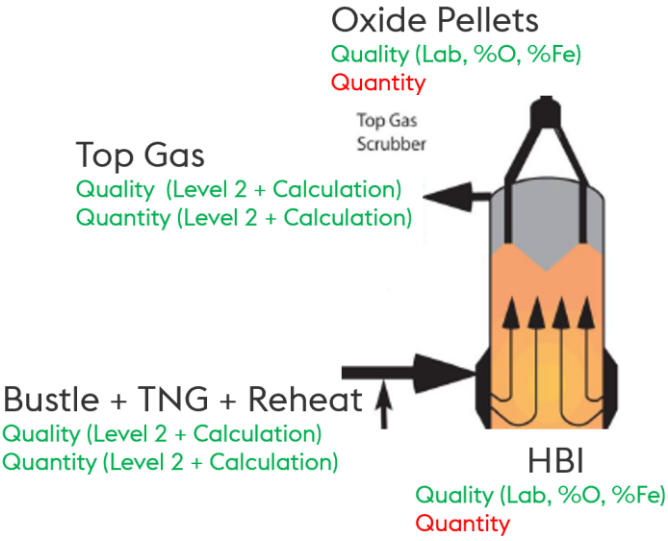

**Figure 28:** Schematic diagram of the furnace and the incoming and outgoing gas and solid streams

### 5.2.2 Process Parameters

To identify stable operation periods and as a next step to be able to quantify the performance of different pellets in the furnace, different process parameters are calculated on an hourly basis and plotted over time.

#### 5.2.2.1 Key Process and Reduction Indicators

In order to define the performance of pellets in the furnace first the key process indicators (KPI), which relate to the reducibility of pellets, of good pellet performance were defined:

Firstly, the metallization [%] is needed to define the quality of the product. It is defined as the amount of metallic iron over the amount of total iron present. This value is a direct measurement which is taken every two hours. As mentioned previously however not the DRI is measured, but the HBI. Nevertheless, this value gives information if the product itself meets the minimum specifications. Generally, the metallization level of the HBI should be above 93 % to ensure product specification and below 94 % to avoid inefficiency. All the following process indicators can only be seen as valuable information if the metallization fulfills the minimum specification.

The most relevant process indicator for the plant operator from an economical point of view is the maximum production rate [t/h]. For this thesis the maximum production rate will be discussed as the relative maximum production rate, which is simply the reduction rate of any given pellet type divided by the maximum production rate of pellet type B. As explained in chapter 5.2.1.2 the relevant production rate is calculated from the gas composition and flow and the composition of the HBI and oxides.

Since the maximum production rate is influenced by many factors, for example the amount of remet added to the oxide, the oxygen removal rate is also selected as a KPI. The oxygen removal rate is the amount of oxygen the gas is enriched with per hour. Again, when comparing oxygen removal rates to each other, these will be relative to the oxygen removal rate of pellet type B.

Specific Gas flows [(scfm)/(t/h)], are calculated as the gas flow needed to produce one ton of product per hour. When multiplying this value by 60 the unit reduces to the amount of gas necessary to produce one ton of product. The specific gas flows calculated are the specific bustle gas flow, specific natural gas flow (into the furnace) and the specific process gas flow. The specific natural gas flow is the amount of $CH_4$ entering the furnace, the amount of $CH_4$ reformed is not taken into account. When comparing these values, they will also be calculated relative to the corresponding value of pellet type B.

The last KPI, Gas Utilization, relates the plant performance to the theoretical optimum. The gas utilization is calculated by dividing the minimum amount of gas needed to reduce the pellet by the amount of gas that is actually consumed by the pellet. The theoretical amount of molar flow $M_t$ needed is calculated from the following three formulas. The activities for all solid reactants and products are set to 1 and the activities for any gaseous reactants and products are equal to their partial pressure. The partial pressures of the gases are proportional to their molar ratios, and therefore the equilibrium constants can be calculated as follows:

$$K_I = \frac{M_t * \%_{CO_2} + y}{M_t * \%_{CO} - y} \tag{5-1}$$

$$K_{II} = \frac{M_t * \%_{H_2O} \ + z}{M_t * \%_{H_2} \ - z} \tag{ 5-2}$$

$$x = y + z \tag{ 5-3}$$

$$K_I = equilibrium\ constant\ of\ the\ reaction\ FeO + CO \rightarrow Fe + CO_2$$

$$y = moles\ of\ FeO\ reacted\ with\ CO$$

$$K_{II} = equilibrium\ constant\ of\ the\ reaction\ FeO + H_2 \rightarrow Fe + H_2O$$

$$z = moles\ of\ FeO\ reacted\ with\ H_2$$

$$\%_i = mole\ \%\ of\ component\ i\ in\ the\ incomming\ gas$$

$$M_t = minimum\ molar\ flow\ of\ of\ the\ incomming\ gas$$

$$x = total\ amount\ of\ FeO\ reduced$$

These three equations give us three unknowns: y, z and $M_t$. The variable x is known from the subtracting the amount of metallic from the amount of total iron in the product. $M_t$, the theoretical amount of molar flow is thus calculated to be:

$$M_t = \frac{x}{\frac{K_{II} * H_2 - H_{2O}}{K_{II} + 1} - \frac{CO_2 - K_I * CO}{K_I + 1}} \tag{5-4}$$

From the molar flow the flow in standard cubic meters per minute can easily be calculated. This flow is then divided by the actual flow of gas into the furnace, which results in the gas utilization.

### 5.2.2.2 Process Stability Indicators

The process indicators introduced in this chapter are calculated to aid in achieving at least one of the following goals:

- Identifying stable operation periods
- Identifying operation periods in which the reducibility of the ore is likely to be the limiting factor to production rate
- Confirming that the mass balance calculations are correct

Just like the KPIs, the following process stability indicators are calculated on an hourly basis and plotted over the time period being analyzed. When selecting stable operation periods, these indicators, together with the KPIs mentioned above are inspected in detail. If irregularities were detected in any of these indicators, the process is identified as not stable and the time period analyzed is shortened to focus only on the process data identified as stable.

The furnace pressure drop [psi] is calculated by subtracting the pressure measured in the top gas from the pressure measured in the bustle gas. A high or strongly fluctuating pressure drop indicates a high fines content which leads to channeling of the gas stream in the furnace. Under these circumstances most likely the mechanical properties and not the reduction rate of the ore are the limiting factors to the production rate. The furnace pressure drop is dependent on the bustle gas flow and temperature. Therefore, also the normalized furnace pressure drop [psi] is calculated which cancels out pressure drop changes due to flow and temperature fluctuations.

Stable average bed temperatures [°F] are a good indication for stable production. The average temperatures for different heights in the furnace are calculated according to the formulas in chapter 4.1. The standard deviations of bed temperatures are also calculated for the three levels equipped with temperature sensors. They indicate if one side of the furnace is hotter than the rest and therefore the reduction occurs unequally.

Bustle and top gas temperatures [°C] give information on how much thermal energy is fed or removed from the furnace. As mentioned for bed temperatures, unstable gas temperatures indicate that the reduction process itself is also unstable.

The HBI carbon content [%] can be obtained in two ways. Either via the measured value of the chemical analysis or via closing the carbon mass balance over the furnace. These values give a very good indication of how well the assumptions made for the calculation of the production are.

The carbon utilization [%] gives an overview of how the carbon from $CH_4$ in the bustle gas is used in the process. The carbon can either slip to the top gas, form carbon in the HBI or be used as a reducing agent.

Similarly, to the carbon content the oxide head grade [wt%] gives a good indication if the calculations work properly. The oxide head grade is the amount of iron in the oxide feed. It can either be calculated by looking at the ore analysis and mix of the feed material. Or it can be calculated from the chemical content in the HBI and the oxygen removed by the gas. These values should match up very closely as long as the remet content is low. If higher amounts of remet are fed into the furnace and the oxide head grades do not match up, this indicates that the assumption made for the remet composition is incorrect.

The iron oxide feed [t/h] can either be calculated as described in chapter 5.2.1.2, or can simply be taken from the belt scale measurements. Under the assumption that the belt scale produces accurate values and the calculations are correct, the belt scales calculation should be slightly higher than the calculated feed. The difference is most likely oxide fines and moisture. High fluctuations in the calculated oxide feed indicate that the limiting production factor is not the reducibility of the oxides.

To be able to identify which pellets are fed for which period of time, the feed material mix [%] visualizes this information. This makes it easier to select time periods of nearly constant oxide feed mixes.

The $H_2$/CO ratio and the process gas $CO_2$ [%] are indicators for how stable not only the reduction in the furnace, but the whole plant is operating. When the furnace or the reformer is not operating at a steady state, these indicators fluctuate.

In case of any issues with the gas reforming system, bustle gas quality would be low. Also, when comparing final degrees of metallization of different pellets to each other it is important to keep an eye on comparing similar bustle gas qualities.

## 5.3 Plant Performance Results

Sixteen months of production data were thoroughly examined and eleven different stable production periods containing a total of 6 different pellet types, pellets A through F, were analyzed. Of these eleven cases only four cases were fed with exclusively one pellet type, not counting remet. In the other seven cases always two different pellet types were fed into the furnace, with one pellet type being pellet type B in all the cases. For pellets A, B and F at least one case was analyzed with only this pellet being fed. A pure feed of pellet B was even analyzed twice, once with and once without remet being added to the mix. In total, pellet B was fed in nine of the eleven cases analyzed. For this reason, all KPIs except for metallization were presented relative to the KPIs of pellet B (without remet in the feed). **Table 14** gives an overview of the eleven cases and their oxide mixes, as well as the time period of stable data for these cases.

**Table 14:** Overview of cases analyzed for plant pellet performance

| Case # | Pellet type analyzed | % of Pellet type analyzed | % of Pellet type B | % of Remet | Time period [days] |
|---|---|---|---|---|---|
| 1 | A | 100% | 0% | 0% | 3.00 |
| 2 | B | 100% | | 0% | 3.17 |
| 3 | B | 97% | | 3% | 2.29 |
| 4 | C | 45% | 52% | 3% | 1.00 |
| 5 | C | 65% | 33% | 2% | 2.00 |
| 6 | C | 32% | 67% | 1% | 1.75 |
| 7 | D | 17% | 83% | 0% | 1.00 |
| 8 | E | 50% | 50% | 0% | 0.92 |
| 9 | E | 43% | 55% | 2% | 1.25 |
| 10 | E | 19% | 77% | 4% | 1.50 |
| 11 | F | 97% | 0% | 3% | 0.71 |

Because case 2 is the reference case and the basis for calculating the relative KPIs, the following results are always compared to the results of case 2. The cases with only one pellet in the mix can be compared to each other fairly simply. For pellet mixes the assumption is made, that the influence one pellet has on the reducibility KPIs of the mix is linear. An overview of the resulting KPIs of the cases can be seen in **Table 15**.

**Table 15:** Overview of KPI results of the analyzed pellet cases

| Case # | Pellet type analysed | Average Metallization | rel. Production rate | rel. O-removal rate | rel. Specific BG flow | rel. Gas Utilization |
|---|---|---|---|---|---|---|
| 1 | A | 92.0% | 86% | 84% | 103% | 94% |
| 2 | B | 93.9% | 100% | 100% | 100% | 100% |
| 3 | B | 93.8% | 104% | 100% | 96% | 103% |
| 4 | C | 93.7% | 92% | 88% | 105% | 93% |
| 5 | C | 93.9% | 88% | 85% | 108% | 92% |
| 6 | C | 93.8% | 92% | 91% | 108% | 94% |
| 7 | D | 93.8% | 102% | 101% | 100% | 100% |
| 8 | E | 93.8% | 94% | 94% | 103% | 98% |
| 9 | E | 94.6% | 86% | 84% | 108% | 94% |
| 10 | E | 93.7% | 105% | 100% | 98% | 101% |
| 11 | F | 93.5% | 98% | 93% | 100% | 97% |

### 5.3.1 Pellet B (Cases 2 and 3)

Pellet B is the exclusive pellet fed in two cases. In case 2 a stable production period of over 3 days is analyzed with only pellet B being fed to the furnace. The big difference regarding the oxide input between these two cases is that in Case 3 apart from pellet B also 3 % of the feed material is remet. Also, the stable production period analyzed in Case 3 is a bit shorter with 2.3 days.

The average metallization over the time periods examined is 93.9 % for Case 2 and 93.8 % for Case 3. The average oxygen removal rates are also nearly identical. Per definition Case 2 has a relative oxygen removal rate of exactly 100 %, for Case 3 a relative oxygen removal rate of 100.1 % is calculated. Because of this, it is concluded that the remet does not have a notable influence on the oxygen removal rate. The relative gas utilization of 103 percent (Case 3, with remet) to the value of 100 percent (Case 2, without remet) shows that either the remet is reduced very efficiently, or that the remet is of higher quality than assumed for the calculation. A similar conclusion can be drawn from comparing specific bustle gas flows. The bustle gas flows also show the high impact remet has on the gas consumption. Trusting this data, a 3 % remet feed leads to a 4 % reduction in the specific bustle gas flow, which would indicate that very high quality remet is fed during this period. The following **Figure 29** shows the difference in relative specific bustle gas flow and metallization for a 6-hour moving average of the hourly calculated values. The same metallization can clearly be achieved with a lower specific bustle gas flow if remet is fed to the furnace. The degree to which the specific bustle gas flow influences the metallization appears to be very similar, as can be seen by the two almost parallel trendlines.

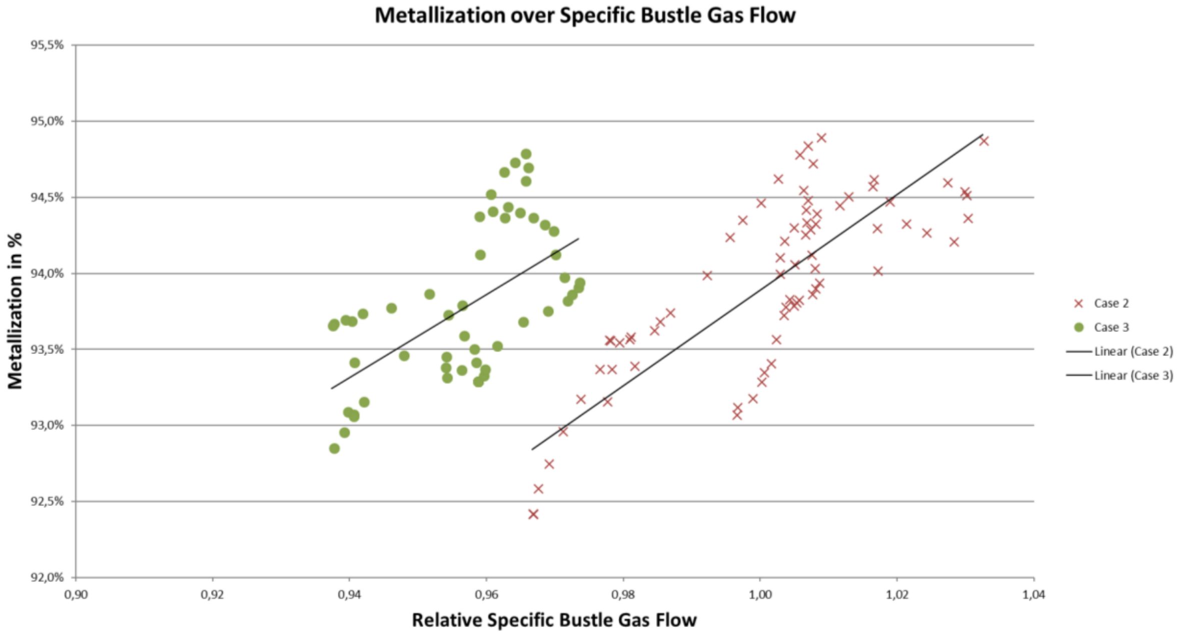

**Figure 29:** Metallization over the relative specific BG-flow for Case 2 and 3

The remet feed in Case 3 also leads to a production rate increase of 4 %. In order to better compare cases including remet to other cases not including remet, a production rate correction for small amounts of remet is derived from this information. Concerning the remet composition it is assumed, that it is constant for all cases. Furthermore, the influence of remet on the KPIs calculated is assumed to be linear, from this the following formulas are derived.

$$P_{no\ Remet} = P_{Remet} - 1.2338 * \%Remet \tag{5-5}$$

$$P_i = relative\ production\ rate\ containing\ component\ i; i = no\ remet, remet$$

The same can be done for all other KPIs as well:

$$OR_{no\ Remet} = OR_{Remet} - 0.0439 * \%\ Remet \tag{5-6}$$

$$OR_i = relative\ Oxygen\ removal\ rate\ containing\ component\ i; i = no\ remet, remet$$

$$SBG_{no\ Remet} = SBG_{Remet} + 1.4271 * \%Remet \tag{5-7}$$

$$SBG_i = relative\ specific\ BG\ flow\ containing\ component\ i; i = no\ remet, remet$$

$$GU_{no\ Remet} = GU_{Remet} - 0.9391 * \%Remet \tag{5-8}$$

$$GU_i = relative\ gas\ utilization\ containing\ component\ i; i = no\ remet, remet$$

### 5.3.2 Pellet A (Case 1)

A three-day long time period is identified during which pellet A is fed exclusively and the production rate is stable. The metallization achieved is very low at only 92 %, nevertheless this is the most stable production period identified for pellet A. All other KPIs of pellet A also range at the bottom of the scale when compared to pellet B. The limited potential of this pellet becomes especially clear when comparing the hourly average values of production and metallization to the ones of pellet B, as can be seen in **Figure 30**. Despite the low metallization pellet A only averages a relative production rate of 86 %. The trend for both pellets clearly shows that with an increased production rate the metallization decreases. The data-points for pellet A indicate, that in order to reach an average metallization of 93 % or higher, the average production would most likely decrease further.

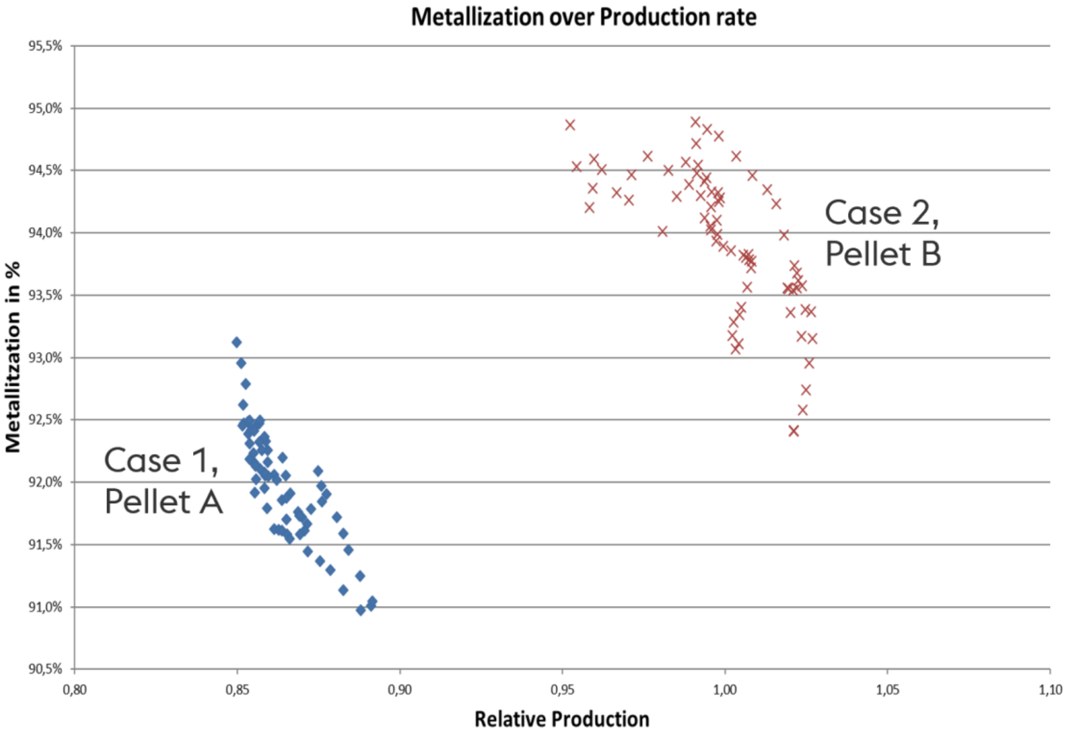

**Figure 30:** Metallization over production rate for Cases 1 and 2

**Table 16:** KPIs of pellet A

| Pellet type | Metallization | rel. Production rate | rel. O-removal rate | rel. Specific BG flow | rel. Gas Utilization |
|---|---|---|---|---|---|
| A | 0.92 | 0.86 | 0.84 | 1.03 | 0.94 |

### 5.3.3 Pellet F (Case 11)

A relatively short but stable production period of 17 hours is identified in which pellet F is the only pellet being fed into the furnace. Additionally, to pellet F an average of 3 % remet was also fed during this time. When comparing the KPIs of pellet F to pellet B, this can either be done by recalculating all KPIs of pellet F to account for the effect remet has on the mix, or by comparing it directly to Case 3, in which pellet B is fed with 3 % remet. The following **Figure 31** shows the metallization over the production for cases 2, 3 and 11. To compare the cases including remet, the blue squares (pellet F) need to be compared to the green circles (pellet B + remet). So it becomes obvious that at similar metallization and remet feed, pellet F cannot be processed at the same rate as pellet B. The relative average production rate for pellet F without remet is calculated according to the formula derived from pellet B in chapter 5.3.1. This results in a relative production rate of 93.5 %, placing pellet F between pellet A and B from a production rate point of view.

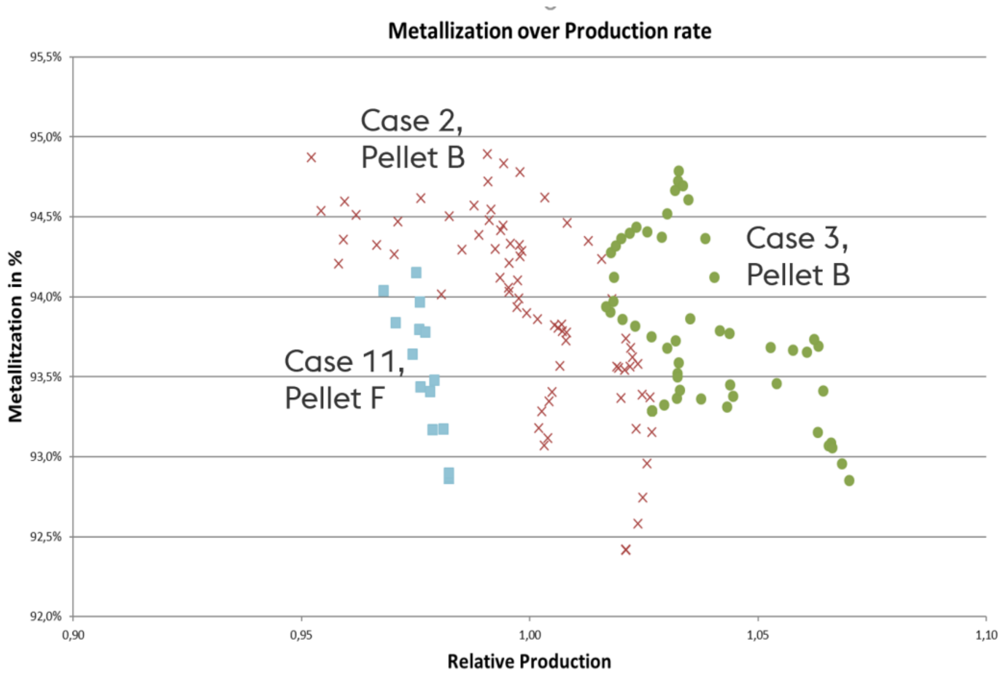

**Figure 31:** Metallization over production for Cases 2,3 and 11

For better comparison, the effect of remet on all other KPIs is also taken into account, thus creating the following values.

**Table 17:** KPIs of pellet F

| Pellet type | Metallization | rel. Production rate | rel. O-removal rate | rel. Specific BG flow | rel. Gas Utilization |
|---|---|---|---|---|---|
| F (3% Remet) | 0.93 | 0.975 | 0.934 | 0.998 | 0.965 |
| F (no Remet) | 0.93 | 0.935 | 0.933 | 1.045 | 0.934 |

Based on the new KPI values, the oxygen removal rate and gas utilization are about 7 % lower compared to pellet B and the specific bustle gas flow is about 4.5 % higher.

### 5.3.4 Pellet C (Case 4, 5 and 6)

Three different stable production periods are analyzed in which three different raw material mixes are fed. All mixes contain pellet B, C and remet in different ratios and are fed for at least 24 hours. The composition of feed material is as follows:

- Case 4: 45% pellet C, 52% pellet B, 3% remet
- Case 5: 65% pellet C, 33% pellet B, 2% remet

- Case 6: 32% pellet C, 67% pellet B, 1% remet

In **Figure 32** hourly average values of metallization and production of all pellet C cases are plotted and compared to pellet B (cases 2 and 3). From this, it is difficult to quantify how well the pellet performs, due to the varying remet content. It is obvious that the relative maximum production rate of pellet C is lower than pellet B.

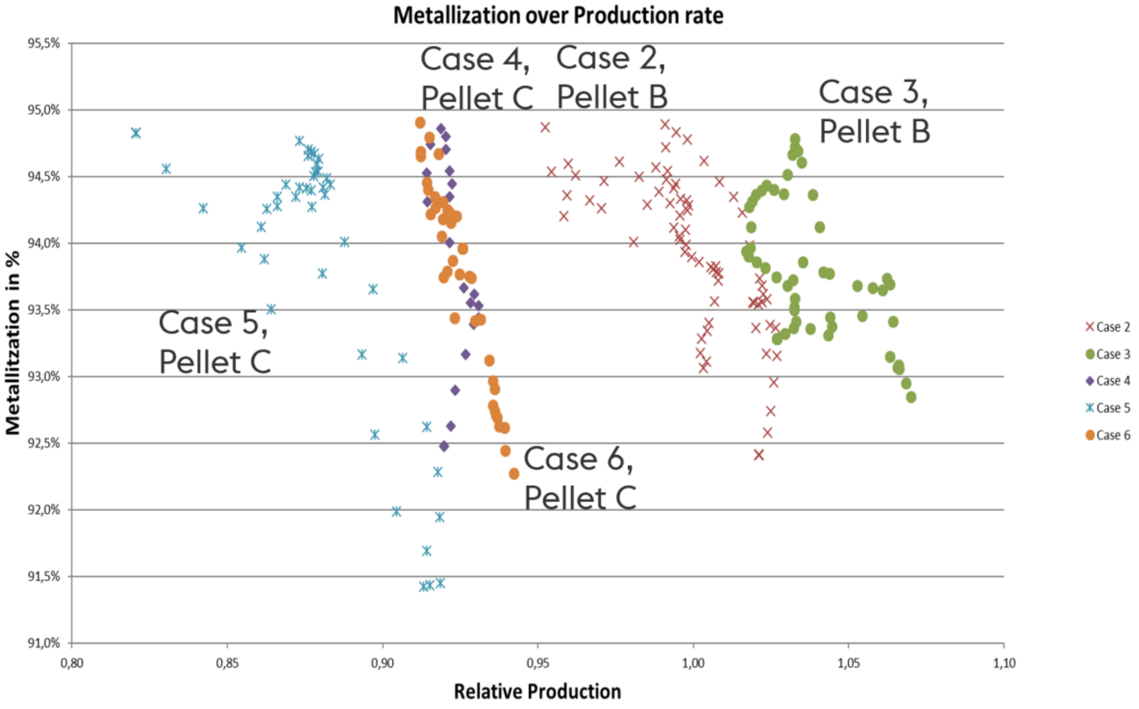

**Figure 32:** Metallization over production for Cases 2,3,4,5 and 6

To draw conclusions on how pellet C performs if fed to the furnace exclusively, the KPIs are calculated for the same mix without remet.

**Table 18:** KPIs of Cases 4,5,6 with and without remet

| % of Pellet type C | Metallization | rel. Production rate | rel. O-removal rate | rel. Specific BG flow | rel. Gas Utilization |
|---|---|---|---|---|---|
| 45% (3% Remet) | 0.94 | 0.921 | 0.884 | 1.049 | 0.934 |
| 45% (no Remet) | 0.94 | 0.885 | 0.883 | 1.091 | 0.906 |
| 65% (2% Remet) | 0.94 | 0.876 | 0.846 | 1.077 | 0.921 |
| 65% (no Remet) | 0.94 | 0.847 | 0.845 | 1.110 | 0.899 |
| 32% (1% Remet) | 0.94 | 0.925 | 0.910 | 1.076 | 0.937 |
| 32% (no Remet) | 0.94 | 0.910 | 0.909 | 1.093 | 0.926 |

From this table, some trends can be seen. With increasing pellet C content in the mix, the relative production rate, oxygen removal rate, and gas utilization decrease; at the same time the relative specific bustle gas flow increases. **Figure 33** shows the average relative production of the three cases as calculated for no remet in the mix. According to this graph the predicted relative production rate of 100 % pellet C is calculated based on a linear function of the three cases without remet. The predicted relative production of pellet C is 75 % of pellet B.

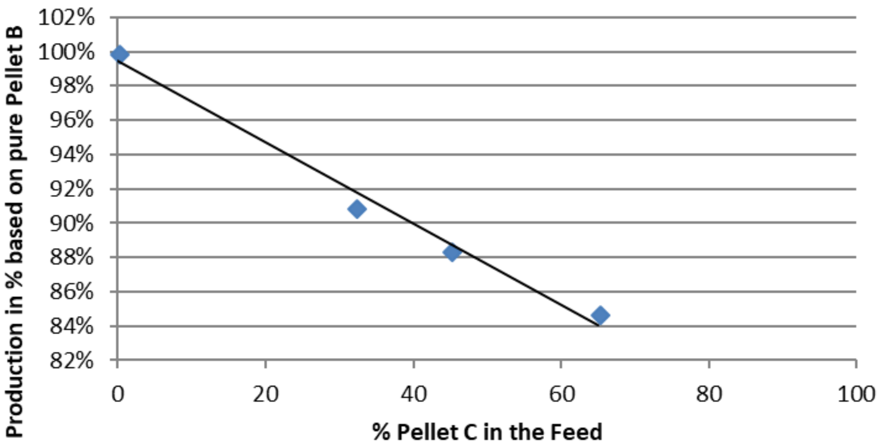

**Figure 33:** Relative production rate over pellet C content

The same calculations can be performed for oxygen removal rate, specific gas flow and gas utilization. The results can be seen in **Table 19**. The relative production and oxygen removal rates show relatively clear linear trends, as seen in **Figure 33**. The relative specific bustle gas flows and gas utilizations do not show such clear trends, which is why linear extrapolations for these two KPIs are difficult to compare to other pellets KPIs.

**Table 19:** KPIs of pellet type C prediction

| Pellet type | Metallization | rel. Production rate | rel. O-removal rate | rel. Specific BG flow | rel. Gas Utilization |
|---|---|---|---|---|---|
| C (Prediction) | 0.94 | 0.75 | 0.75 | 1.18 | 0.83 |

### 5.3.5 Pellet D (Case 7)

One case is analyzed containing pellet D (17 % pellet D, 83 % pellet B) over a time period of 24 hours. The calculated KPIs hardly differ from the ones of 100 % pellet B feed, as can be seen when comparing the relative production rate in **Figure 32**.

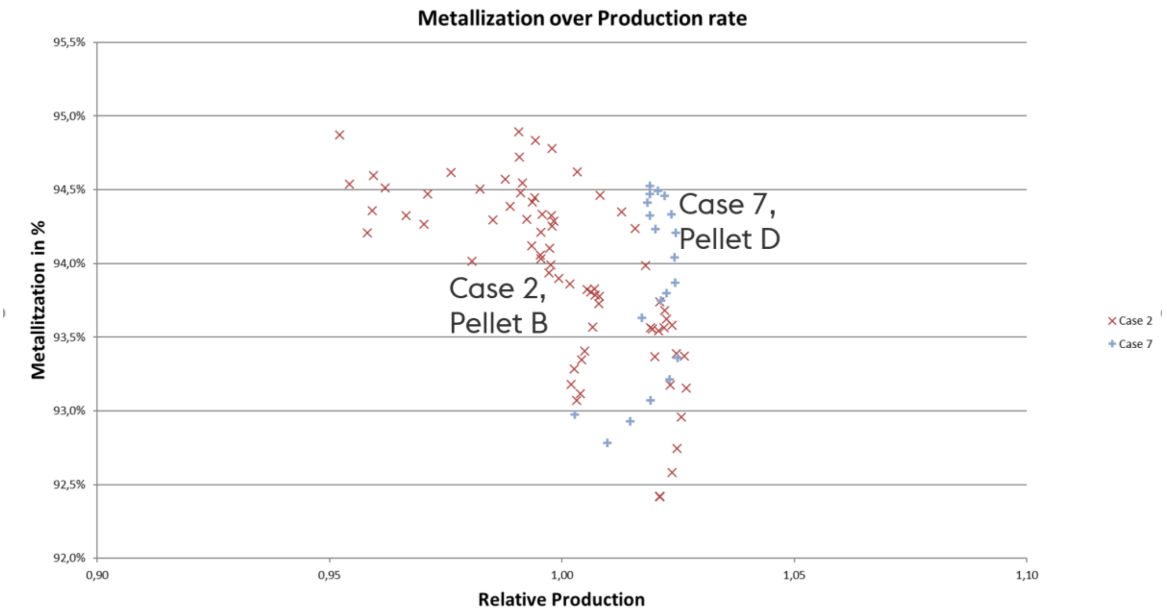

**Figure 34:** Metallization over relative production rate of cases 2 and 7

The resulting KPIs of this case are linearly extrapolated to predict 100 % pellet D feed, as seen in **Table 20**. Since the specific bustle gas flow and gas quality are very close to 1, this means that in this regard pellet D would perform quite similar to pellet B.

**Table 20:** KPIs of case 7 and pellet D prediction

| Pellet type | Metallization | rel. Production rate | rel. O-removal rate | rel. Specific BG flow | rel. Gas Utilization |
|---|---|---|---|---|---|
| D (17%) | 0.94 | 1.02 | 1.01 | 1.00 | 1.00 |
| D (Prediction) | 0.94 | 1.09 | 1.07 | 0.99 | 1.01 |

### 5.3.6 Pellet E (Case 8, 9 and 10)

Three cases containing pellet E are examined, the time periods of stable production being at least 22 hours or longer. Comparing the cases to each other and predicting the KPIs of 100 % pellet E feed, one case shows indications that the reducibility of the pellet is not the limiting factor during the period analyzed however. **Figure 35** shows how in case 9 the metallization is high, and no tendency is visible that the relative production decreases with increasing metallization as with the other cases. For this reason, case 9 is not used for predicting the performance of pellet E.

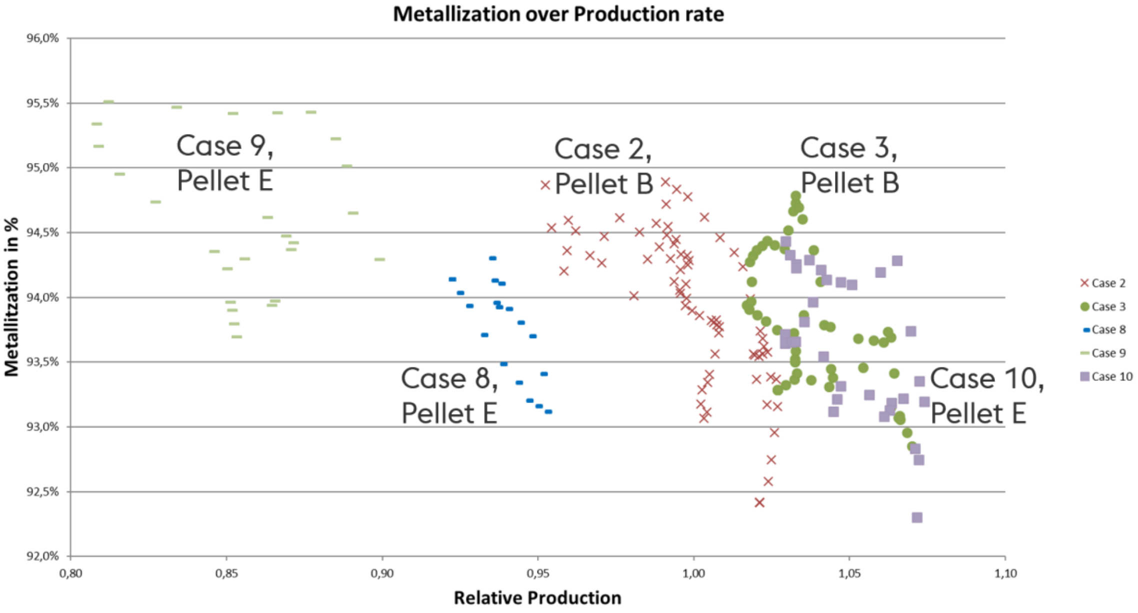

**Figure 35:** Metallization over relative production for cases 2,3,8,9 and 10

Based on Case 2, 8 and 10 the relative KPIs for pellet E are predicted. The same linear assumptions regarding pellets, and remet, influencing each other's KPIs as in chapter 5.3.4 are made. The resulting prediction of pellet E can be seen in **Table 21**.

**Table 21:** KPIs of pellet type E prediction

| Pellet type | Metallization | rel. Production rate | rel. O-removal rate | rel. Specific BG flow | rel. Gas Utilization |
|---|---|---|---|---|---|
| E (Prediction) | 0.94 | 0.88 | 0.88 | 1.07 | 0.96 |

### 5.3.7 Summary of Pellet Performances in the Furnace

**Table 22** shows a summary of the KPIs of all the pellets analyzed for this thesis. Assuming that the achieved metallization is roughly the same for all pellet types, which apart from pellet A is the case, the results can be ranked as follows.

- Production rate: D > B > F > E > A > C
- Oxygen removal rate: D > B > F > E > A > C
- Specific bustle gas flow: D > B > A > F > E > C
- Relative gas utilization: D > B > E > A > F > C

Overall, pellet D appears to be the best reducing pellet, followed by pellet B. From then on, the overall ranking depends on which KPI is considered most important. If all KPIs have equal weight, pellet F is the pellet with the third best reducibility, followed by pellet E and A. Pellet C has the lowest predicted KPIs regarding the reducibility in the furnace.

- Overall reducibility ranking: D > B > F > E > A > C

**Table 22:** Furnace performance KPIs of pellets A, B, C, D, E and F

| Pellet type | Metallization | rel. Production rate | rel. O-removal rate | rel. Specific BG flow | rel. Gas Utilization |
|---|---|---|---|---|---|
| A | 0.92 | 0.86 | 0.84 | 1.03 | 0.94 |
| B | 0.94 | 1.00 | 1.00 | 1.00 | 1.00 |
| C (Prediction) | 0.94 | 0.75 | 0.75 | 1.18 | 0.83 |
| D (Prediction) | 0.94 | 1.09 | 1.07 | 0.99 | 1.01 |
| E (Prediction) | 0.94 | 0.88 | 0.88 | 1.07 | 0.96 |
| F | 0.93 | 0.94 | 0.93 | 1.05 | 0.93 |

The ranked results help to draw trends which pellet may have a faster production rate and which pellet a higher gas consumption. However, the conclusion, especially regarding the predicted performances, that 100 % of any specific pellet type fed will always lead to the results calculated for this specific pellet type cannot be drawn. Because the values for pellets C, D and E are calculated from assuming a linear relation between the cases analyzed and the performance of pellet B, some uncertainty regarding these values exists. Other sources of uncertainty also influencing the results of pellets A, B and F, are that only very few periods, as few as one per pellet, are analyzed. In addition to this, the time periods being analyzed are very short, meaning a day or shorter, for some pellets. Lastly it is assumed, that the reducibility and quality of remet and different shipments are the same throughout the total period analyzed. While the influence remet on the results is limited because of the small amounts in the mix, the varying reducibility of shipments can have a big impact. All predictions for pellets not fed purely to the mix rely on the assumption that the reducibility of pellet B is always constant. Over the period analyzed, as many as 17 different shipments of pellet B were fed into the furnace. This obviously ads uncertainty to the resulting KPIs of pellet B, but also to the results of pellets C, D and E. Especially when evaluating the results of pellet C, it must be noted, that process engineers at the plant believe, that the performance of pellet B during this time was lower than for the pellet B cases analyzed. This would mean, that the KPIs of pellet C would be significantly better than they are now.

The specific gas consumption differs from case to case regarding the plant data. The cases analyzed represent constant production periods, during these periods a high but stable production was measured. Because the objective of the plant operator is to maximize the production, the total bustle gas flows for these cases are also high. The limiting factor concerning the gas flow is the capacity of the compressors. The specific bustle gas flow is defined as the gas flow per ton produced. For this reason, the specific bustle gas flows differ based on the production rate. This can be observed in **Table 22**. Cases in which the production rate is low, also show a high specific bustle gas flow and vice versa. It can be assumed, that when the specific bustle gas flow is kept constant for all cases, the resulting maximum production differs even more. This needs to be kept in mind in the following chapters, especially when drawing conclusions from the comparisons of maximum production values under industry conditions to the results of reduction tests.

## 5.4 Available Standardized Test Results

Two different types of test results for all pellets are available. Firstly ISO 11257 or Linder test results were made available by the industry partner. Secondly one ISO 11258 test per pellet type was performed at the chair for Ferrous Metallurgy. The available test results are compared to the maximum production under industry conditions. As mentioned in chapter 5.3.7 these maximum production values are influenced by the different specific bustle gas flows as well as the reducibility of the pellets.

### 5.4.1 ISO 11257 Results

Of each shipment a sample was taken and sent to an external laboratory, where the ISO 11257 test was performed. **Table 23** shows the average test results over all the shipments analyzed.

**Table 23:** Average ISO 11257 test results

| **Pellet** | A | B | C | D | E | F |
|---|---|---|---|---|---|---|
| **Avg Metallization %** | 89.6 | 93.5 | 92.1 | 92.9 | 90.8 | 93.0 |

Based on the results of the test, the pellets are ranked as follows: B > F > D > C > E > A.

The high standard deviation, especially for the pellets C and E, where only a few tests were performed, makes it difficult to evaluate a pellet without distinguishing between the shipments.

#### 5.4.1.1 Comparison to Plant Performance

To compare the ISO 11257 test results to the plant performance, the average test results are multiplied by the corresponding percentage of feed into the furnace. This is done for each case in which more than one pellet is fed into the furnace. The resulting values are then compared to the relative production rate of the 11 cases analyzed in chapter 5.2. **Figure 36** shows the resulting ISO 11257 reduction degrees over the relative maximum production of each previously analyzed case.

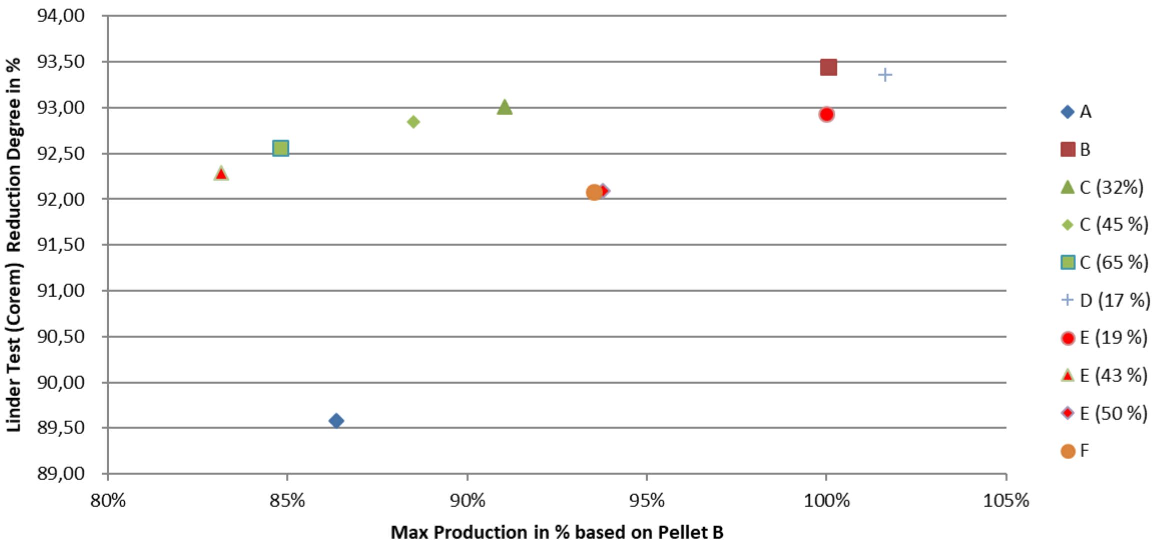

**Figure 36:** Plant performance compared to ISO 11257 results

For the cases in which only one pellet type was fed to the furnace (pellets A, B and F) the test results and maximum possible production seem to show a linear correlation. Similarly, this is true for the pellets D and two cases of pellet E. However, pellet C and the case containing 43 % of pellet E do not follow this trend.

### 5.4.2 ISO 11258 Results

One ISO 11258 test is performed per pellet type. The tests are conducted at the Chair for Ferrous Metallurgy as specified in chapter 3.3.3.1. The results regarding the final reduction degree, metallization, reducibility index and the reduction degree are calculated based on the sample weight before and after the test and can be seen in **Table 24**. The reducibility index at 90 % could not be calculated according to the specification, since not all pellets reached a reduction degree of 95 % necessary for the calculation.

According to the results of the test the pellet types are ranked as follows:

| | |
|---|---|
| Reduction Degree and Metallization: | A > E > C > D > B > F |
| Reducibility Index $dR/dt_{40}$: | E > C > B > A > F > D |

**Table 24:** Results of ISO 11258 test

| Pellet | A | B | C | D | E | F |
|---|---|---|---|---|---|---|
| **Reduction Degree %** | 94.1 | 91.7 | 93.1 | 91.7 | 94.0 | 90.4 |
| **Metallization %** | 91.3 | 87.6 | 89.8 | 87.8 | 91.2 | 85.8 |
| **$dR/dt_{40}$** | 1.5 | 1.5 | 1.6 | 1.2 | 1.6 | 1.4 |
| **Reduction Degree (wt. before test – wt. after test)** | 93.4 | 90.7 | 94.8 | 87.8 | 92.3 | 90,0 |

Compared to the ISO 11257 test, an advantage of the ISO 11258 test is that its results also include reduction curves in addition to the final reduction parameters. The reduction curves of the six analyzed pellets can be seen in **Figure 37**. Looking at the reduction curves, different behaviors can be identified. In approximately the first 45 minutes the pellets follow one of three different reduction rates. The fastest reducing pellet during this time is pellet E. Pellets A, B and C show a slightly lower reduction speed. Pellets D and F have the lowest reduction rates. In the second 45 minutes of the test, the differences between the pellets are smaller, pellets B, E and F reduce slightly slower during this time.

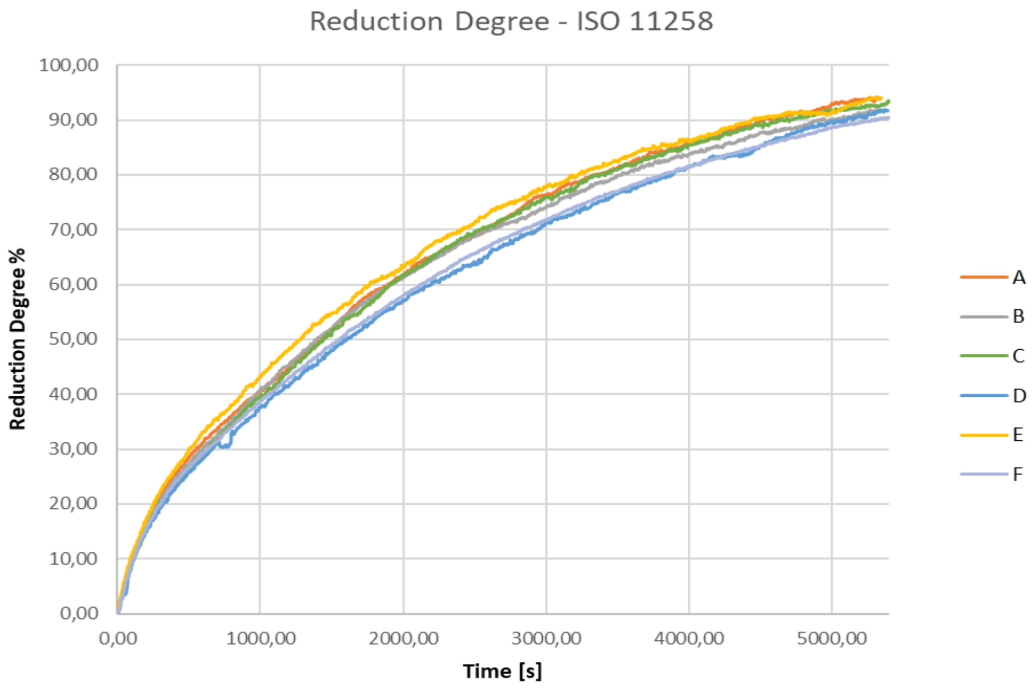

**Figure 37:** ISO 11258 reduction curve

#### 5.4.2.1 Comparison to Plant Performance

To compare the results of ISO 11258 to the plant performance, the same approach is taken as in chapter 5.4.1.1. The results can be seen in **Figure 38**. Unlike the ISO 1157 test, nearly no correlation exists. This may be due to the limited number of R90 tests done. With a higher amount of R90 tests, some correlation may have been detected. When comparing the reduction curves to the pellet performance in the furnace, no correlation is detected either. This indicates that the reduction behavior at a constant gas quality, as in the test, differs from the behavior at a varying quality, as occurring in the furnace.

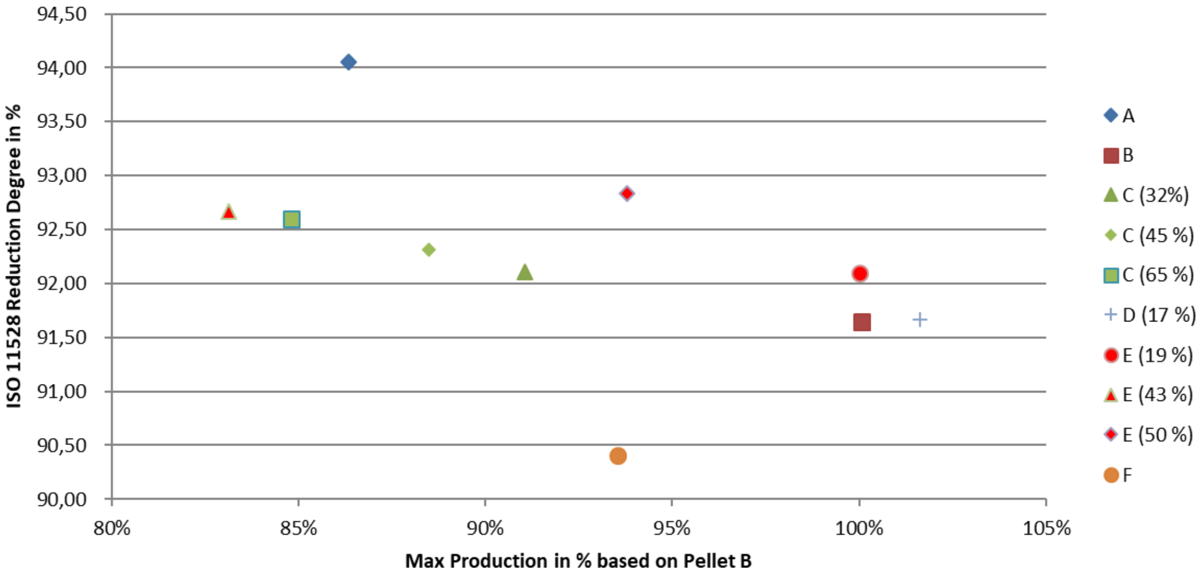

**Figure 38:** Plant performance compared to ISO 11258 results

# 6 Test selection

When selecting a test to classify pellets according to their reducibility and predicting their performance in the furnace, there are two options available. Firstly, the existing standardized tests most suitable are identified. Secondly a modified test based on the predicted furnace profiles is proposed.

## 6.1 Standardized Tests

To select a standardized test, a number of questions have to be considered. What is the objective of the test? How do the conditions of the test compare to the furnace? Are test results available? How do available test results compare to furnace performance? While these questions are answered in detail in the chapters 3.3.3, 4.4 and 5.4, no conclusion has been drawn to which test is most suitable.

The ISO 11257 test is the only test currently performed on a regular basis and test results of every shipment of pellets fed to the furnace are available. This shows that it is accepted by suppliers and plant operators as a quality indicator. Additionally, some limited correlation between the plant performance and the available test results exists. However, the temperature is constant and significantly lower than expected in the furnace. The gas quality is also constant and a lot higher than in the furnace. Moreover, there is no reduction curve, and therefore no information on how different pellets behave in the furnace, created during the test. Nevertheless, it is recommended, that the ISO 11257 is further employed to test incoming shipments and thereby continue building up comparable data.

To be able to understand the reduction behavior of the different pellets more in detail than with the ISO 11257, a test from which a reduction curve can be calculated is recommended. Both the ISO 11258 and the R180 include a reduction curve in their results. The ISO 11258 uses a gas quality and temperature close to furnace conditions. But, since both are constant, the resulting reduction curve does not resemble the reduction curve predicted for the furnace. The test results available also do not show any correlation to the performance of pellets in the furnace.

The R180 test uses three different gas compositions and temperatures to create profiles very similar to the profile calculated for the furnace. In addition to that, the literature research has shown that for Midrex plants the R180 test shows a much higher sensitivity and reproducibility than the ISO 11258 test [27]. Unfortunately, no results are available for this test. Nevertheless, if any additional standardized test is performed, this test would be recommended.

## 6.2 Modified Test

Another option to performing a standardized test is to create a testing procedure. The following test is based on the R180 test and is designed to resemble the conditions in the furnace even closer.

### 6.2.1 Test Parameters

The test setup and equipment are identical to the R180 and ISO 11258 tests. The test parameters are based on the ones of the R180 test. Changes to the R180 test are made regarding the temperature and the gas composition. The total reduction time, the number of gas composition and temperature steps and the reduction degrees triggering the next steps remain the same. **Figure 39** shows the temperature profile of the new suggested test and **Table 25** shows the different gas compositions of the three mixtures.

The test starts with Mix 1 and a total flow of 30 Nl/min at 400 °C. It is increased to 800 °C at a rate of 9 K/min. During the test the weight loss is measured, and at a reduction degree of 30 % the gas composition switches to Mix 2. Once a reduction degree of 70 % is reached the temperature is increased to 840 °C at a rate of 2 K/min. At a reduction degree of 80 %, the gas composition is changed to the final mix and is reduced until the total reduction time of 180 min is reached. The resulting reduction curve as well as final reduction degree is expected to be similar to those of the R180 test. Because the parameters are closer to industrial conditions, the results are expected to be even more representative of the furnace performance.

**Table 25:** Gas composition of the modified reduction test

| Gas Composition | Mix 1 | | Mix 2 | | Mix 3 | |
|---|---|---|---|---|---|---|
| | Nl/min | % | Nl/min | % | Nl/min | % |
| $N_2$ | 1.5 | 5.0% | 1.5 | 5.0% | 1.5 | 5.0% |
| $H_2$ | 13.2 | 44.0% | 14.73 | 49.1% | 17.07 | 56.9% |
| $H_2O$ | 5.19 | 17.3% | 3.95 | 13.2% | 1.59 | 5.3% |
| CO | 6.81 | 22.7% | 7.74 | 25.8% | 9.06 | 30.2% |
| $CO_2$ | 3.3 | 11.0% | 2.08 | 6.9% | 0.78 | 2.6% |
| Gas Quality | 2.36 | | 3.73 | | 11.03 | |

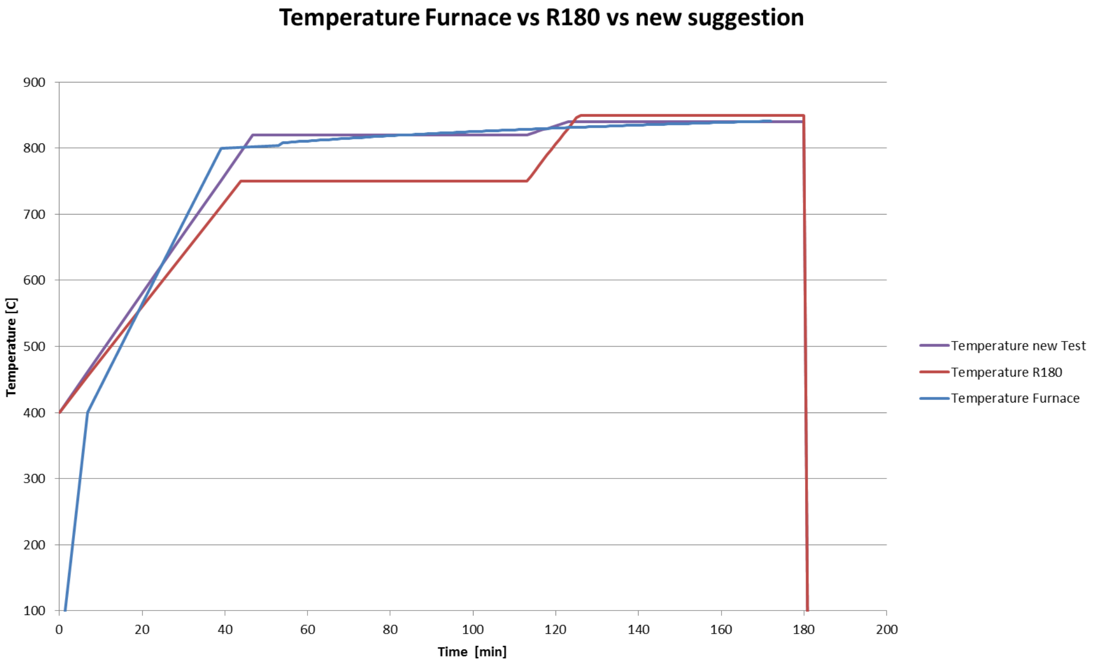

**Figure 39:** Temperature profile of the modified test

### 6.2.2 Test Results and Discussion

One modified test was performed per pellet type at the Chair of Ferrous Metallurgy. The final reduction degrees can be seen in **Table 26** and the full reduction curves of all pellet types are shown in **Figure 40**. Based on the final reduction degree the pellets in this test can be ranked as follows: D > E > A > B > F > C.

Pellet D shows an unexplainably high reduction degree of over 100 percent, which is clearly higher than the second highest reduction degree of pellet E. Interestingly, the reduction curves show that these two pellets are also the slowest to reach a reduction degree of 30 percent.

The pellets A, B and F show nearly identical final reduction degrees and also very similar reduction curves. Up to a reduction degree of approximately 70 percent, pellet C shows a very similar reduction curve to pellets A, B and F, from there on pellet C shows a significantly lower reducibility.

**Table 26:** Final Reduction Degrees of modified Test

| **Pellet** | A | B | C | D | E | F |
|---|---|---|---|---|---|---|
| **Reduction Degree %** | 96,7 | 96.5 | 93.4 | 100.4 | 97.7 | 96.3 |

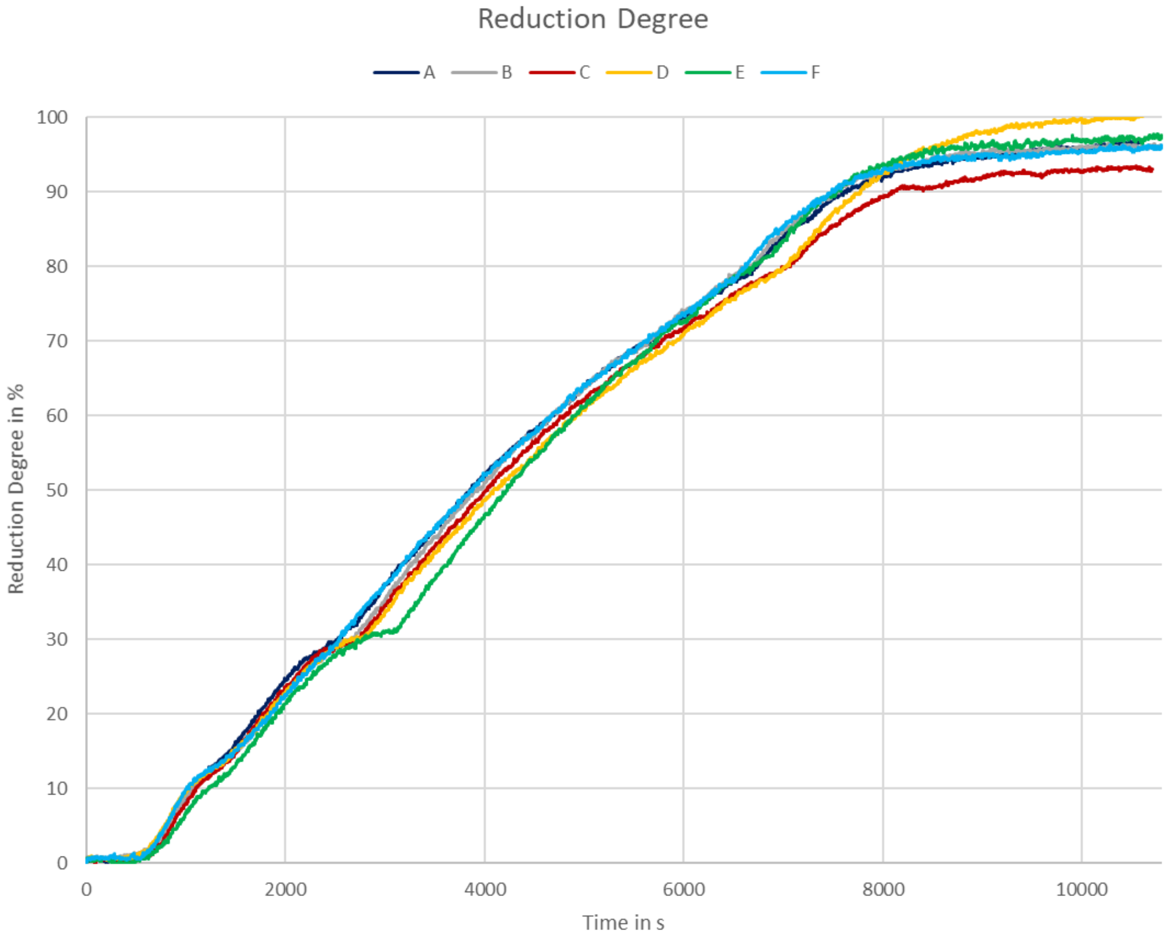

**Figure 40:** Reduction Curves of modified Test

Since the R180 test has proven that it can provide a higher sensibility than the ISO 11258 test [27], it was assumed that this modified version of the R180 test would also provide a higher sensibility. This can only partially be confirmed, while the pellets C and D show a very different behavior from the rest of the pellets, the other pellets are very close together, especially in the final half hour of the test. Nevertheless, compared to the ISO 11258 test the difference between the final reduction degrees is a lot higher, and also the difference in the reduction curves is higher. Possibly the lower temperature of the R180 test would have led to more pronounced results.

Compared to the performance in the furnace, this test shows a higher correlation than the ISO 11258 test, and about the same correlation as the ISO 11257 test. **Figure 41** shows the test results calculated for the eleven cases over the maximum production in the furnace. From this graph it can be seen, that pellets B, C, D and F show a correlation between the furnace performance and the test results, while pellets A and E do not.

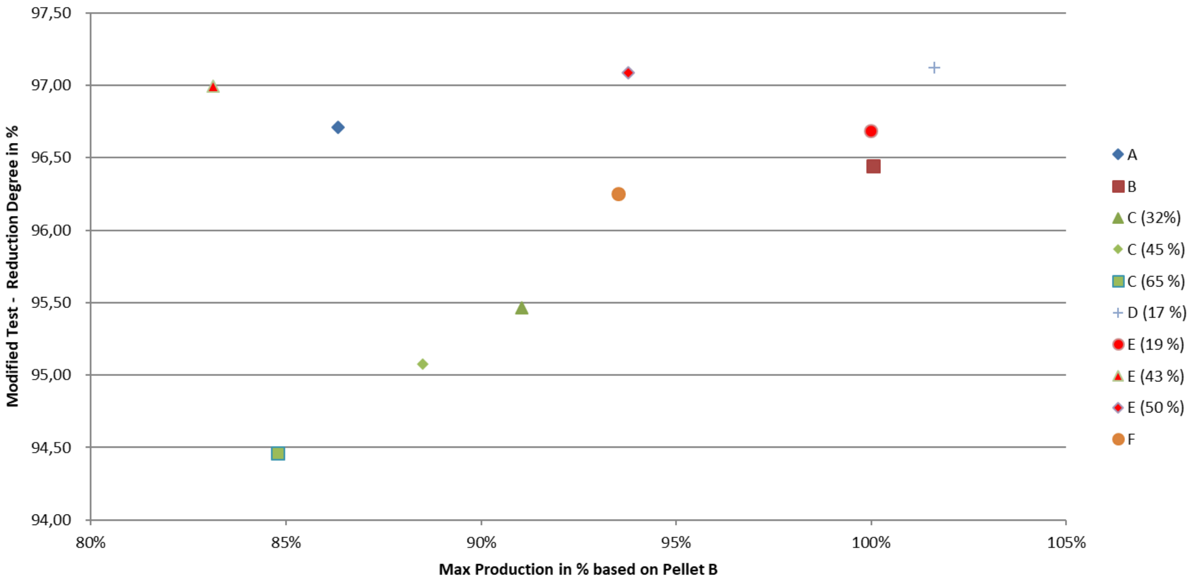

**Figure 41:** Modified Test Results compared to Plant Performance

This test was designed based on the idea of modifying the R180 test to better represent furnace conditions. Therefore, it is worth checking how the measured reduction degree and metallization during the test compare to the calculated furnace profiles of the pellet. **Figure 42** shows that the reduction degree (red) and the metallization (blue) of the test are similar to the calculated reduction degree (green) and metallization (purple). The main difference is that the reduction rate of the test is more linear than calculated over the first 100 minutes, and the metallization is steeper during this time. Towards the end of the test, the reduction rate and in consequence also the metallization rate is slower. For future improvements of the furnace profile calculations, this comparison delivers valuable information. When comparing these curves, it is necessary to keep in mind, that also the gas quality in the test differs from the one calculated in the furnace. To examine how big this difference is, the weight loss which equals the oxygen removed during the test is used to calculate the change in gas quality. While the gas quality going in to the test was given by the R180 test, the gas quality going out was calculated from the oxygen removed. From these two values an average gas quality can be calculated. **Figure 43** shows both gas qualities during the test, compared to the calculated gas quality in the furnace. Given that only three different incoming gas compositions were used, the average gas quality during this test resembles the gas quality in the furnace very closely.

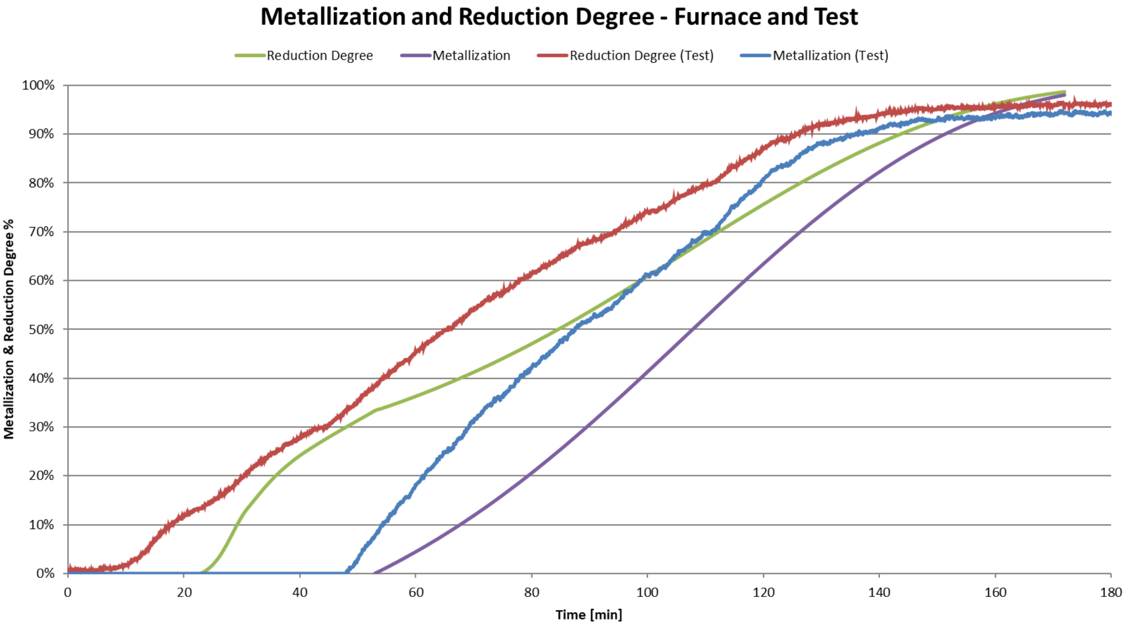

**Figure 42:** Reduction Degree and Metallization of modified test compared to calculated furnace profile

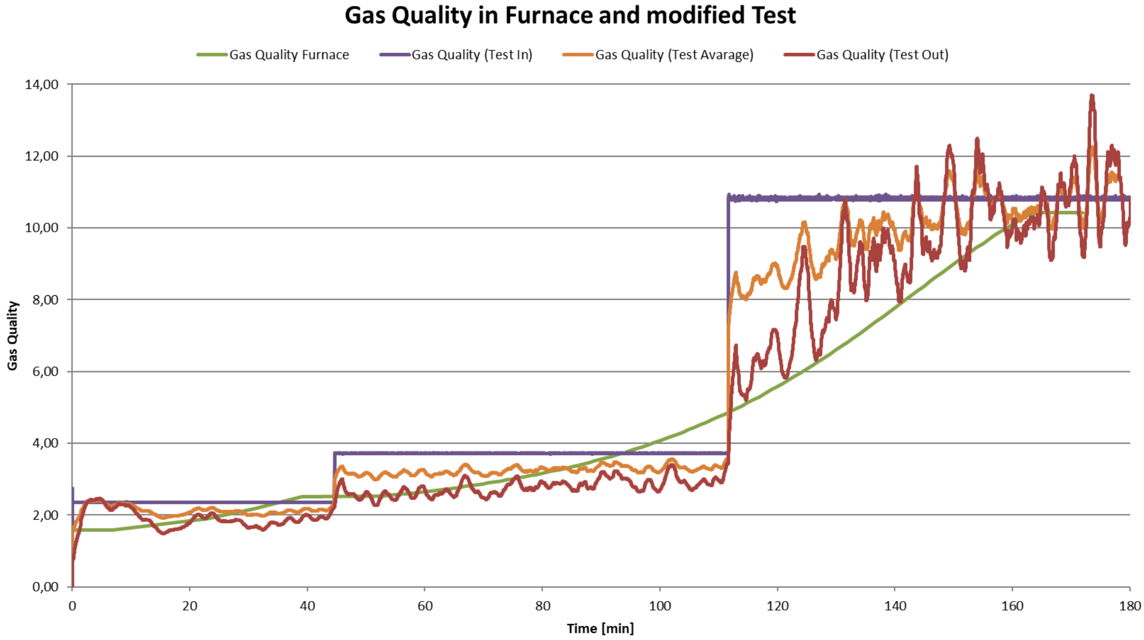

**Figure 43:** Gas Quality during modified test compared to calculated furnace profile

# 7 Summary and Conclusion

The objective of this thesis was to investigate the behavior of iron ore pellets under industrial conditions as well as in standardized tests in the laboratory. Six different pellet types (A through F) are analyzed in regard to their reduction behavior in the furnace, as well as in regard to their test results from two different reduction tests. Furthermore, a gas, temperature and reduction profile of the furnace was calculated based on industry data and then compared to the test parameters in detail. Finally, a suggestion was made on which reduction tests to adopt for future predictions of pellet performance.

Four key questions were investigated in detail and ultimately answered in this thesis. The following paragraphs sum up the results:

- How does the reduction behavior of six different pellet types compare in the shaft furnace?

To answer this question a series of key process and stability indicators are calculated from plant data. The most relevant indicators are the metallization, production rate, oxygen removal rate, specific gas flows and the gas utilization. Through a series of individual mass balances around the furnace, scrubber and reformer these indicators are calculated for hourly average values of plant data. From this information eleven different cases of stable production are identified, with at least one case per pellet type. Most pellets are fed to the furnace as part of mixes. Because of this, the key process indicators for each pellet type are calculated based on the assumption that they behave proportional to the ratio of pellets in the mix. Based on this, it is concluded that the performance of the six different pellet types in the furnace can be ranked as follows: D > B > F > E > A > C. It should be noted, that the pellets A, B and F are fed to the furnace exclusively, while the pellets C, D and E are only analyzed as part of mixes. Therefore, the ranking B > F > A can be made with more certainty than the ranking including all six pellets. Another limitation is the fact that all shipments of the same pellet type are assumed to behave the same. Insufficient data was analyzed to verify or discredit this assumption.

- What is the expected chemical and thermal profile these pellets experience under industrial conditions?

The thermal profile of the furnace is calculated based on temperature sensors inside the furnace and the temperature of the top gas leaving the furnace. The temperature increase from room temperature to top gas temperature, and from the top gas temperature to the first thermocouple temperature, is assumed to be linear. From the first thermocouple to the bottom of the furnace, a curve, based on the natural logarithm, is fitted to the plant data to predict the temperatures from there.

To calculate the chemical profile a relation needs to be established between the gas composition and the change rate in the pellet composition. For this reason, three reduction tests at different gas compositions are performed. Based on a reaction rate equation for the reduction from FeO to Fe, the constants in the equation are fitted to match the reduction curves. This reaction rate equation with the fitted constants is then used to calculate the gas composition as well as the pellet composition over the height of the furnace. The resulting final metallization calculated from different specific bustle gas flows is compared to plant data. By doing so the calculation model was verified.

Relating the profiles over the height of the furnace to a time was done by calculating the average material flow inside the furnace. Together with the inside geometry of the furnace a profile over time was calculated. In total the reduction time in the furnace is about 170 minutes.

- What pellet tests are available to date and how do their specified conditions compare to the industrial conditions in the shaft?

Six different pellet tests designed for evaluating the performance of DR-pellets are studied. The ISO 11258, the ISO 11257 (which is almost identical to the Linder test), the ISO 11258, the Midrex Hot Load test and the R180 all access the reducibility of iron ores in the direct reduction process. From a gas composition point of view, none of the tests include water vapor in their mix, as a result either the gas quality, or the H/C ratio differs from the one present in the furnace. Except for the ISO 11257 and the Hot Load test, the gas quality used in the tests is comparable to the one in the furnace at some point. But all tests except for the R180 use a constant gas composition, making them difficult to compare to the gas composition profile of the furnace. Regarding the temperature, again all except the R180 are isothermal, with temperatures between 760 °C and 850 °C depending on the test. The reduction times of most tests are either far too short, as in the case of the ISO 11258 with 90 minutes, or far too long, as the ISO 11257 with 300 minutes. Again, only the R180 with 180 minutes of test time seems to be closest to process conditions. A more detailed examination of this test reveals that also gas composition and temperature profiles fit the predicted furnace profiles very well. Furthermore, only the ISO 11258 and the R180 include reduction curves in their results. Because not only the prediction of pellet performance, but also the future optimization is of high importance to the industry partner, a test offering a reduction curve is preferred. Based on the conditions in the tests and the ones in the furnace, the R180 test must be the suggested test for this Midrex plant.

- Do any of the available test results correlate at all with the performance of the pellets in the shaft?

At the moment the Linder test (ISO 11257) is the only one performed on a regular basis for the incoming pellet shipments. Additionally, the ISO 11258 test is performed once per pellet type at the laboratories of the Chair of Ferrous Metallurgy. The results of both tests are compared to the industrial performance of the eleven cases analyzed. For all cases in which there is more than one pellet fed to the furnace, an artificial test result is calculated based on the mix of the pellets in the furnace. The ISO 11257 test shows a good correlation for the pellets fed exclusively and a limited correlation for the pellet mixes. The ranking based on the ISO 11257 result is the following: B > F > D > C > E > A. The ISO 11258 on the other hand does not show any correlation between its results and the furnace performance with its ranking being: A > E > C > D > B > F. Because only one test per pellet type is performed, the difference between the results is very small, a second test would likely to produce different results.

Overall the test recommendation is to keep performing the ISO 11258 test. Even though its test parameters are different from the profiles in the furnace, the test results indicate that it is predicting the plant performance correctly. Also, it appears that this test is widely recognized among pellet suppliers and consumers. It is also recommended to take up a second test for internal evaluation of different iron ore types and mixes. The test recommended is either the R180 test or a modified version of it. The modified version is introduced in the final chapter of this thesis and is based on the outcome of the previous findings. It includes water in the gas compositions and has a slightly different temperature profile in order to follow the predicted profile in the furnace even closer.

The results of this test show a higher correlation to the plant performance of the pellets than the ISO 11258. However, a high sensitivity is only given for two of the six pellets analyzed. To decide whether to further work towards creating a modified test based on the conditions in the plant, or to adopt the R180 test as an addition to the ISO 11257, it is recommended that the R180 is to be performed for the six pellets. In addition to that, it is recommended to perform the modified test as well as the ISO 11258 test more often to check for the reproducibility of the results.

# 8 References

[1] Meija, J.; Coplen, T. B.; Berglund, M.; Brand, W. A.; Bièvre, P. de; Gröning, M.; Holden, N. E.; Irrgeher, J.; Loss, R. D.; Walczyk, T.; Prohaska, T.: Atomic weights of the elements 2013 (IUPAC Technical Report), Pure and Applied Chemistry 88 (2016), Nr. 3, S. 695

[2] SPONGE IRON PRODUCTION BY DIRECT REDUCTION OF IRON OXIDE: Aphi - mit chatterjee, [S.l.]: PRENTICE-HALL OF INDIA, 2012

[3] Schenk, J.; Lüngen, H. B.: Potenziale der Direkt- und Schmelzreduktionsverfahren für eine effiziente Anwendunge in Europa, Stahl und Eisen 136 Nr. 6 (2016), S. 41–47

[4] Paris climate agreement: Beacon of hope, 1. Aufl., New York NY: Springer Science+Business Media, 2016

[5] Stephenson, R. L. (Hrsg.): Direct reduced iron: Technology and economics of production and use, Warrendale, Pa., 1980

[6] Anameric, B.; Kawatra, S. K.: PROPERTIES AND FEATURES OF DIRECT REDUCED IRON, Mineral Processing and Extractive Metallurgy Review 28 (2007), Nr. 1, S. 59–116

[7] Feinman, J.; Mac Rae, D. R. (eds.): Direct reduced iron: Technology and economics of production and use, Warrendale, Pa.: Iron & Steel Society ISS, 1999

[8] worldsteel: https://www.worldsteel.org/en/dam/jcr:4f060d8b-3602-4ffe-9e87-7e93e0659449/Word+Steel+in+Figures+2016.pdf

[9] Midrex, W. S. D.: http://www.midrex.com/news-literature/news-releases/world-dri-statistics

[10] Masaaki ATSUSHI, Hiroshi UEMURA, Takashi SAKAGUCHI: http://www.kobelco.co.jp/english/ktr/pdf/ktr_29/050-057.pdf

[11] Shams, A.; Moazeni, F.: Modeling and Simulation of the MIDREX Shaft Furnace: Reduction, Transition and Cooling Zones, JOM 67 (2015), Nr. 11, S. 2681–2689

[12] Bogdandy, L. v.; Engell, H.-J.: The reduction of iron ores: Scientific basis and technology, Berlin (u.a.): Springer-Vlg, 1971

[13] Eder, W.: investors-and-analysts-field-trip-corpus-christi, www.voestalpine.com/group/static/sites/group/.downloads/en/share/grouppresentation/2018-03-12-investors-and-analysts-field-trip-corpus-christi.pdf (04.06.2018)

[14] Hanel, M.: Characterization of ferrous burden material for use in ironmaking technologies, 2014

[15] Basdag, A.; Arol, A. I.: Coating of iron oxide pellets for direct reduction, Scandinavian Journal of Metallurgy 31 (2002), Nr. 3, S. 229–233

[16] Ball, D. F.: Agglomeration of iron ores, New York: American Elsevier Pub. Co, 1973

[17] Bohnet, M.: Einführung, in: Bohnet, M. (Hrsg.): Mechanische Verfahrenstechnik, D-69451 Weinheim, Germany: Wiley-VCH Verlag GmbH, 2003, S. 1–4

[18] Bohnet, M. (Hrsg.): Mechanische Verfahrenstechnik, D-69451 Weinheim, Germany: Wiley-VCH Verlag GmbH, 2003

[19] Turkdogan, E. T.: Fundamentals of steelmaking, 1. Aufl., Bd. 656, Book / The Institute of Materials, Leeds: Maney Publ, 2010

[20] Srivastava, U.; Kawatra, S. K.; Eisele, T. C.: Study of Organic and Inorganic Binders on Strength of Iron Oxide Pellets, Metallurgical and Materials Transactions B 44 (2013), Nr. 4, S. 1000–1009

[21] International Standard: ISO 11257: Iron ores for shaft direct-reduction feedstocks - Determination of the low temperature reduction-disintegration index and degree of metallization, 2007

[22] International Standard: ISO 11258: Determinatino of reducibility and metallization of feedstock for direct reduction by gas reforming, 2007

[23] Lu, L. (Hrsg.): Iron ore: Mineralogy, processing and environmental sustainability, Cambridge UK: Woodhead Publishing is an imprint of Elsevier, 2015. (Woodhead Publishing series in metals and surface engineering, number 66)

[24] Murat Özkan Aksit: REDUCIBILITY PROPERTIES OF ERDEMIR SAMPLES, 2004

[25] Lu, L.: Iron ore: Mineralogy, processing and environmental sustainability / edited by Liming Lu, Woodhead Publishing series in metals and surface engineering, Oxford: Woodhead Publishing, 2015

[26] METEC; ESTAD; European Steel Technology and Application Days: Proceedings / METEC & 2nd ESTAD 2015, European Steel Technology and Application Days: Düsseldorf, Germany, CCD Congress Center Düsseldorf, 15-19 June 2015, Aachen: TEMA Technologie Marketing AG, 2015

[27] Iron and Steel Society. Ironmaking Division: 58th Ironmaking conference proceedings, 1999

[28] Alhumaizi, K.; Ajbar, A.; Soliman, M.: Modelling the complex interactions between reformer and reduction furnace in a midrex-based iron plant, The Canadian Journal of Chemical Engineering 90 (2012), Nr. 5, S. 1120–1141

[29] Zuo, H.-b.; Wang, C.; Dong, J.-j.; Jiao, K.-x.; Xu, R.-s.: Reduction kinetics of iron oxide pellets with H2 and CO mixtures, International Journal of Minerals, Metallurgy, and Materials 22 (2015), Nr. 7, S. 688–696

[30] Takenaka, Y.; Kimura, Y.; Narita, K.; Kaneko, D.: Mathematical model of direct reduction shaft furnace and its application to actual operations of a model plant, Computers & Chemical Engineering 10 (1986), Nr. 1, S. 67–75

[31] Wang, G.; Zhang, J.; Zhang, G.; Wang, H.; Di Zhao: Experiments and Kinetic Modeling for Reduction of Ferric Oxide-biochar Composite Pellets, ISIJ International 57 (2017), Nr. 8, S. 1374–1383

[32] Shayegan, J.; Hashemi, M. M. Y. M.; Vakhshouri, K.: Operation of an industrial steam reformer under severe condition: A simulation study, The Canadian Journal of Chemical Engineering 86 (2008), Nr. 4, S. 747–755

[33] Sarkar, S.; Bhattacharya, R.; Roy, G. G.; Sen, P. K.: Modeling MIDREX Based Process Configurations for Energy and Emission Analysis, steel research international 89 (2018), Nr. 2, S. 1700248

[34] MIDREX TECHNOLOGIES, I.: METHODS AND SYSTEMS FOR INCREASING THE CARBON CONTENT OF SPONGE IRON IN A REDUCTION FURNACE